Technische Universität München
TUM School of Engineering and Design

Advanced Mission Simulation based Aircraft Design for UAVs

Ekaterina Skrobol

Vollständiger Abdruck der von der TUM School of Engineering and Design der Technischen Universität München zur Erlangung einer

Doktorin der Ingenieurwissenschaften (Dr.-Ing.)

genehmigten Dissertation.

Vorsitz: Prof. Dr.-Ing. Markus Ryll

Prüfer*innen der Dissertation:

1. Prof. Dr.-Ing. Mirko Hornung
2. Prof. Dr.-Ing. Peter Stütz

Die Dissertation wurde am 27.07.2022 bei der Technischen Universität München eingereicht und durch die TUM School of Engineering and Design am 03.02.2023 angenommen.

Kurzfassung

Unbemannte Flugzeugsysteme (UAS) werden zunehmend in zivilen Anwendungen eingesetzt. Je nach Missionsanforderungen kann ein unbemanntes Luftfahrzeug (UAV) mit einer Vielzahl von Sensoren und Kameras ausgerüstet werden, deren Leistungen für den Erfolg der Mission von größter Bedeutung sind. Dabei beeinflussen sich Bordkamera und Sensoren, Kommunikationssysteme und UAV-Design gegenseitig. Um eine effektive UAS-Lösung zu entwerfen, müssen neben dem Flugzeug somit auch die Bordsysteme in den Vorentwurfsphasen berücksichtigt werden.

Um dieses Problem zu lösen, wurde am Institut für Flugzeugentwurf eine missionsbasierte Entwurfsumgebung für UAS entwickelt. Im Rahmen dieser Arbeit wurde die bestehende Simulationsumgebung um wichtige verschiedenste Funktionen erweitert:

- Eine Visualisierung der Einsatzumgebung, um Leistungsbewertungen von Bordkameras und Kommunikationssystemen unter Berücksichtigung der Geländeform im Einsatzgebiet zu ermöglichen.
- Eine Missionsleistungsanalyse, um den Missionserfolg verschiedener UAS-Designs zu vergleichen. Die Analyse basiert auf dem Gewichtungssummenansatz, der die wichtigsten Leistungsparameter wie Flächenabdeckungsrate, Wahrscheinlichkeit der Objekterkennung, Missionszeit, Energieverbrauch, Kommunikationsleistung und Benutzerbedienung umfasst;
- Einem Flugplan-Optimierungsalgorithmus, der den Flugplan des UAV entsprechend der erforderlichen Bildauflösung der Kamerasysteme und der Geländelandschaft optimiert. Ziel ist es, starke Flughöhenunterschiede im Gebirgsgelände zu reduzieren, um so den Energieverbrauch und die Anforderungen an das Antriebssystem zu minimieren;
- Zusammenführung aller Teile zu einem multidisziplinären Design-Loop-Algorithmus, der das UAS optimiert, um so den Erfolg einer bestimmten Mission zu maximieren. Entwurfsparameter dabei sind Flügelfläche, Streckung, Fluggeschwindigkeit und Art der Kamera.

Zur Validierung der Machbarkeit des vorgestellten Design-Ansatzes, wurden zwei Anwendungsstudien für die zivile Nutzung unter Berücksichtigung der Leistungen der Sensor- und Kommunikationssysteme durchgeführt. Die erste Studie demonstriert die Konvergenz und Genauigkeit des Optimierungsalgorithmus. In der zweiten Studie, einer Such- und Rettungsmission, zeigt sich der Vorteil der visualisierten Einsatzumgebung während der Missionssimulation speziell für signifikant verändernde Geländeformen. Die durchgeführten Anwendungsstudien haben die Machbarkeit und die Leistungsfähigkeit des vorgestellten Ansatzes vollständig bewiesen.

Abstract

Unmanned Aircraft Systems (UAS) are increasingly used in civil applications. Depending on the mission requirements, an Unmanned Aerial Vehicle (UAV) can be equipped with a variety of sensors and cameras. Since an UAS interacts with the environment primarily via these integrated sensors, its performance is of utmost importance for the success of the mission. Thereby, onboard camera and sensors, communication systems and UAV design influence each other. In order to design an effective UAS solution, beside the aircraft also the onboard systems have to be taken into account during the conceptual and preliminary design stages.

In order to address this issue, an UAS mission based design environment was developed at the Institute of Aircraft Design. Within this thesis the existing simulation environment was extended by various important features:

- A visualization of the operation environment in order to address performance evaluations of onboard cameras and communication systems taking into account the terrain land shape in the mission area. The visualization environment is based on the osgVisual toolkit and was adapted to the requirements for the UAS mission simulation.
- A mission performance analysis, yielding a scalar Mission Performance Index (MPI) in order to compare the mission success of various UAS designs. The MPI is based on the weighting sum approach including the main key performance parameters as area coverage rate, probability of object detection, mission time, energy consumption, communication performance and user operating issues.
- A flight path optimization algorithm, which optimizes the flight path of the UAV according to the required image resolution of the camera systems and the terrain landscape. The goal is to reduce strong flight altitude differences in mountain terrain, in order to minimize energy consumption and requirements on the propulsion system while maintaining the desired image quality.
- Bringing together all parts into a multidisciplinary design loop algorithm, which optimizes the UAS in order to maximize the success of a specific mission in a form of the introduced MPI. Design parameters are wing area, aspect ratio, flight speed and type of camera.

In order to validate the feasibility of the UAS design approach presented in this thesis, two application studies for civil usage were carried out. Here, within the design process the sensor and communication performances are taken into account. The first study demonstrates the convergence and accuracy of the optimization algorithm. In the second study presented by, a search and rescue mission, advantages of the visualized operational environment during the mission simulation are shown. It allows to obtain additional performance evaluation data where the landscape shape changes are significant. The conducted application studies fully proved the feasibility and performance of the presented approach.

Acknowledgements

The presented work was created during my scientific work at the Institute of Aircraft Design at the Technical University of Munich from December 2013 to November 2019. There were a large number of people who supported me during this intensive and exciting time and made a significant contribution to the successful completion of this work.

First of all, I would like to thank Prof. Dr.-Ing. Mirko Hornung for giving me the opportunity and trust to write a thesis at his chair and for supporting me in the preparation of this work. As a doctoral supervisor, he gave me the freedom to realize my own ideas and concepts in the development and processing of many topics and was always available with advice and expertise.

The time of the work at the institute will remain in my memory as pleasant and unforgettable as exemplary and extremely friendly colleagues and friends surrounded me there. Very big thanks goes to Jens Feger for stimulating technical discussions, useful ideas, brainstorming and nice coffee breaks. Thank you, Philip Stahl, Johannes Michelmann, Gilbert Tay, Felix Will and Thomas Lampl for the good and profitable collaboration as well as for the wonderful moments and easy atmosphere at the institute. A great thank to Moritz Thiel for his technical support during my time at the chair as well as after. Special thanks go to my office colleague Joachim Sturm for his willingness to discuss all my questions and his easy way of taking things. I was also very happy to get to know Anna Scholz at the Institute and to get a female colleague as well as a friend.

Very big thanks to Hannes Ross for the very interesting discussions, useful tips, interest in my work and Russian culture. John Lewis for his experienced and wise advice and readiness to show something new. Also not to be forgotten is Natalie, the good soul of the chair, who was a great help to me in all administrative matters and simply contributed to a relaxed working atmosphere!

I would also like to thank all students who supported my research with their studies or theses. Special thanks go to Bernardo de Serpa Marques, who played a key role in driving the development forward.

The biggest thanks go to my family: my parents, who have always supported me without reservation and have always encouraged me in my decisions, especially in moving to Munich; my parents-in-laws who support me wherever they can and especially for taking care of our little Sophia; and my wonderful husband Christoph, who is always there for me and does everything he can, I wouldn't be able to do it without your support. And of course a big thank you to our little lovely Sophia, who slept well during the final work on this thesis.

Dedicated to my family.

Contents

List of Figures

List of Tables

Symbols and Acronyms

Abbreviations

AHP	Analytic Hierarchy Process
BLOS	Beyond Line-Of-Sight
FCM	Flight Control Model
GAME	Genetic Algorithm for Multi-criteria Engineering
GPS	Global Positioning System
HALE	High-Altitude Long Endurance
KPP	Key Performance Parameters
LOS	Line-Of-Sight
MAPPAC	Multi-criterion Analysis of Preferences by means of Pairwise Actions and Criterion comparisons
MCDA	Multi-Criteria Decision Analysis
MMM	Mission Management Model
MSL	Mean Sea Level
MPI	Mission Performance Index
RGB	Red, Green and Blue colors
RF	Radio-Frequency communication
RPV	Remotely Piloted Vehicle
PSM	Payload Sensor Model
SATCOM	Satellite Communication
SWAP	System size, Weight and Power
UAS	Unmanned Aerial System
UAV	Unmanned Aerial Vehicle
VLOS	Visible Line-Of-Sight
WGS84	World Geodetic System
WSM	Weighted Sum Model

Greek symbols

α	angle of attack	[deg]
β	sideslip angle	[deg]
δ_T	thrust level setting	[-]
Υ	kinematic climb angle	[deg]
$\dot{\Upsilon}$	kinematic climb rate	[deg/s]
Θ	pitch angle	[deg]
θ_{Look}	look angle	[deg]
λ	geodetic latitude	[-]
μ	kinematic bank angle	[deg]
η_h	trim surface deflection	[deg]
η_V	coefficient for airspeed influence on thrust	[-]
η_ρ	coefficient for altitude influence on thrust	[-]
ρ	air density	[kg/m^3]
Φ	roll angle	[deg]
φ	geodetic longitude	[-]
χ	course angle	[deg]
$\dot{\chi}$	kinematic azimuth rate	[deg/s]
Ψ	yaw angle	[deg]
$\alpha, \beta, \gamma, \delta, \varepsilon, \zeta$	weighting coefficients	[-]

Latin symbols

a	length of the reference ellipsoids semi major axis	[m]
ACR	area coverage rate	[m^2/s]
ACR_{ref}	reference area coverage rate	[m^2/s]
alt_{max}	maximum flight altitude defined by GSD_{inacc}	[m]
alt_{min}	minimum flight altitude defined by GSD_{req}	[m]
alt_{WP}	flight altitude based on a waypoint	[m]

b	length of the reference ellipsoids semi minor axis	[m]
B	distance between centers of two images	[m]
C_D	drag coefficient	[-]
C_L	lift coefficient	[-]
C_M	pitch moment coefficient	[-]
CA	communication abilities	[s]
CA_{ref}	reference communication abilities	[s]
D	aerodynamic drag force	[N]
dc	object characteristic dimension	[m]
E	required energy	[J]
E_{ref}	reference required energy	[J]
f	focal length of the camera	[m]
f_d	detection factor	[-]
f_{rate}	frame rate of the camera	[Hz]
$f_{rate\ max}$	maximum frame rate of the camera	[Hz]
F	required thrust	[N]
FOV	Field Of View	[deg]
G	covered distance on the ground by an image	[m]
GSD	Ground Sample Distance	[m/pix]
GSD_H	Ground Sample Distance in horizontal plane	[m/pix]
GSD_V	Ground Sample Distance in vertical plane	[m/pix]
GSD_{avg}	average Ground Sample Distance	[m/pix]
h	flight altitude	[m]
im_s	image storage per band	[Mb]
H	object height	[m]

HFOV	horizontal field of view	[deg]
$HFOV_{max}$	maximum horizontal field of view	[deg]
H_{res}	number of pixels in horizontal plane	[pix]
L	aerodynamic lift force	[N]
n_b	amount of bytes for a pixel per band	[byte]
N	number of line pairs (cycles)	[-]
N_{50}	number of cycles, which gives an observer 50% probability discriminating an object to the specified level	[-]
N_{im}	number of images	[-]
m	amount of bands	[-]
$overlap_V$	forward overlap	[%]
$overlap_S$	side overlap	[%]
P	distance between two pixels on the camera chip	[µm]
P	power	[W]
P(N)	Johnson criteria	[%]
P_{det}	detection probability	[%]
$P_{det\ ref}$	reference detection probability	[%]
R	distance from the camera to the ground	[m]
S_{total}	total storage requirements	[Mb]
SP	line spacing	[m]
SW, G	sensor ground swath width	[m]
SW_{req}	required sensor ground swath width	[m]
T	propulsive thrust	[N]
T_{cl}	time during the UAS was not within the VLOS	[s]
T_{rate}	transfer rate	[Mb/s]

T_m	mission duration	[s]
$T_{m\,ref}$	reference mission duration	[s]
t	time	[s]
t_{det}	detection time, e.g. object of interest is in the FOV of the camera	[s]
UOI	User Operating Issue	[-]
UOI_{ref}	reference User Operating Issue	[-]
V	kinematic velocity /flight speed	[m/s]
V_{max}	maximum flight speed	[m/s]
$\dot{V}$	kinematic acceleration	[m/s^2]
V_{res}	number of pixels in vertical plane	[pix]
V_{stall}	stall speed	[m/s]
VFOV	vertical field of view	[deg]
W	object width	[m]

1 Introduction

The term Unmanned Aerial Vehicle (UAV) refers to an aircraft without human onboard or to a remotely piloted vehicle (RPV). The first mention of an UAV usage dates back to the mid-19th century where it was used for warfighting as a balloon carrier (Buckley 2006). With the development of new technologies, UAVs became more comprehensive and have been widely used for military purposes in the 20th century. The late 1980s and early 1990s enabled technical innovations such as digital electronics, global positioning system (GPS), digital data links and satellite communications, strongly influencing the development of UAV systems (Gundlach 2012). However, a UAV system is more than just the unmanned aircraft. Key elements of it include the UAV, payload, communication systems and ground station as well as launch and support equipment. For the successful functioning of the system, it is necessary that performances, weights, size and requirements of the elements matched to each other. Therefore, in order to emphasize this, the term Unmanned Aerial System (UAS) was introduced.

Further developments of technologies made it possible to produce UAVs cheaper and faster compared to manned aircraft vehicles. Nowadays favorable attributes of unmanned aircraft include the following (Gundlach 2012):

- Better transportability due to smaller size;
- Lower cost expectations, except very large UASs such as high-altitude long endurance (HALE);
- Fast prototyping and bringing into operations.

As there is no pilot onboard, UASs are used for missions, which are unacceptable or less effective with manned aircraft. These missions are often characterized as “dull, dirty, and dangerous”. For example, it can be missions with long-duration target coverage, with flights through contaminated air that would be harmful to humans or missions which put human lives at risk.

All these factors drive the usage of UAV systems in the civil area as well. The scope of UASs for civilian applications is extremely broad – from crop surveys, inspection of power lines, land monitoring to border control and search and rescue type of missions and many more. Depending on the mission requirements, a UAV can be equipped with a variety of sensors such as multispectral and magnetic fields sensors, thermal imagers, metal detectors and etc. Since a UAS interacts mainly with the environment with the onboard sensors, their performance is of utmost importance for the success of a mission. Therefore, in order to design an effective UAS solution, besides the aircraft, the onboard systems as well have to be taken into account during the conceptual and preliminary design.

Mission application or mission requirements define performance demands to the overall UAS design and to its elements individually. Onboard camera, communication systems and UAV design have a huge impact on mission success and influence each other. In addition, despite the fact that the mission planning part is not an UAS element, it has an influence on the mission fulfilment grade as well and is driven by the UAV, camera and communication parameters.

Figure 1.1 presents the interrelation of UAV, sensors, communication and mission fulfilment grade. The UAV design is strongly driven by the mission requirements such as endurance and flight performance, which the UAV has to fulfil. The mission requirements define demands to the onboard camera and communication system, whose weight, size and power consumption influence the UAV design. All of these define the final geometry, size and propulsion system of the UAV, which determine the UAV available performance. At the same time, efficiency of the onboard camera is driven by the UAV and communication system performances, which influences the mission fulfilment grade. Camera characteristics such as field of view and resolution together with the flight altitude define the resolution of the sensor ground footprint. The lower the flight altitude is, the narrower the sensor ground swath width of the camera and the higher the resolution of collected images is. However, flights at higher altitudes lead to larger sensor ground swath width yielding a larger area coverage. Together with high airspeed, it allows a shorter mission time.

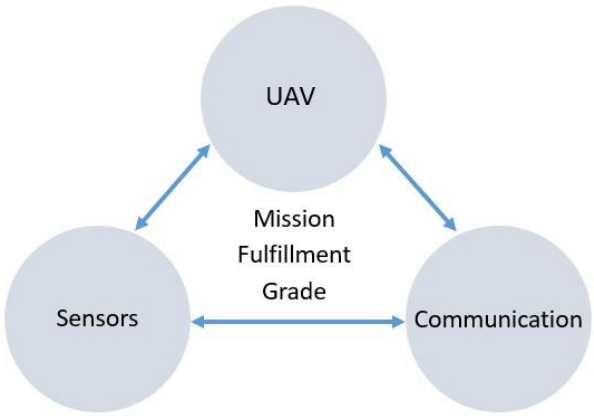

Figure 1.1: Interrelation of UAV, sensors, communication and mission fulfilment grade (Fokina et al. 2018b)

The challenges discussed above in UAS design can be divided into several topics:

- Problem of matching sensor and UAV platforms;
- Aircraft concept selection and evaluation;
- Sensor and communication system performance evaluation.

The problem of matching sensor and UAV platforms to specific mission requirements has already been considered by different research groups. For example, Preece (Preece et al. 2008) and Gomez (Gomez et al.) presented the methodological approach which solves the sensor-mission matching problem by means of collecting interlinked knowledge bases in form of ontologies, where the capabilities required by a mission are compared with sensor‘s capabilities.

An approach for aircraft concept selection and evaluation based on creating the inclusive overall evaluation criteria is developed at the Georgia Tech´s Aerospace Systems Design Laboratory (Mavris, DeLaurentis 1995). This criteria contain information about affordability, mission capability, operational safety, operational readiness and survivability.

Another way of selecting an appropriate UAS design for a specified mission is presented by Morawietz (Morawietz et al. 2018, 2019), where the same aspects are considered. The approach is based on the House of Quality method and is called House of Metrics. In this approach “the method for supporting a holistic evaluation process through the derivation of a descriptive metric structure in combination with relevant decision parameters is presented” (Morawietz et al. 2018).

However, the last two approaches have been developed for military aircraft concept evaluation taking into account parameters, which are not feasible for civil UASs.

At the Australian Centre for Field Robotics an environment for UAS mission simulation together with the onboard camera visual representation is developed. Sensor capabilities can be assessed and used in order to find the best relation between the missions and onboard sensors (Göktogan et al. 2005).

Furthermore, there is commercial software available for sensor and communication performance evaluation in the visualized operational environment, for example, UgCS software developed by SPH Engineering (SPH Engineering 2020). It uses elevation based terrain landscape for mission planning and UAS performance evaluation with the possibility to:

- automatically calculate key variables such as the course heading and track spacing necessary to provide the prescribed coverage area for a search target based on the initial flight altitude;
- create a user defined search area with selected camera's profile and flight altitude;
- calculate and visualize different flight paths that cover the specified area with no gaps and a specified camera footprint.

However, this very powerful visualization software is developed for UAS mission planning and not for UAS design as it considers an UAS is already designed.

Thus, research groups have already considered the UAS challenging topics from different sides. However, according to our knowledge, no research has been conducted where the goal was to involve the sensor and communication performances assessed in the operational environment into the multidisciplinary UAS design loop.

Therefore, future unmanned aerial vehicle applications require the development of new advanced design environments. To get an effective UAS solution, it is necessary to take into account all elements of the system, e.g., to bring together aircraft design, payload, communication and other elements into one multidisciplinary design process. In the classical aircraft design, the performances of onboard sensors are not considered during the conceptual design stage and only during the operational analysis, when the overall architecture is already defined. In order to take into account the sensor and communication requirements early enough, an operational environment has to be simulated and implemented into the UAS design loop. Furthermore, this allows considering specific mission requirements such as high gradients of the terrain elevation of the mission area and therefore additional requirements to the UAS elements performances.

1.1 Objectives

Different kinds of applications for UASs are driven by a variety of sensors and payloads. Compared to manned aircrafts, a UAV interacts with the environment through the onboard sensors only and therefore sensor and communication performances are especially important for the mission fulfilment. Thus, the UAS design requires an approach, which takes onboard sensor requirements and performances into the overall design loop already at the conceptual stage. Furthermore, in real mission applications the shape of the landscape puts limitations on sensors and communication performances, which should be considered as well.

Therefore, the overall goal of the thesis is to present an approach, which focuses on several objectives:

1. The first objective of the approach is to develop a visualized operational environment where the performances of onboard cameras and communication systems can be simulated and evaluated taking into account the shape of landscape in the mission area.
2. The second objective is to present a methodology allowing to assess a mission success by a designed UAS and to compare different UAS configurations based on several key mission evaluation parameters.
3. The third objective is to present a UAS design loop taking into account sensors and communication performances in order to obtain a feasible design tailored to mission requirements.

1.2 Structure of the thesis

The goal of this thesis is to present the methodological framework for advanced mission simulation based aircraft design for UAVs. Therefore, the thesis consists of three main parts: theoretical background for UASs, the description of the modelling environment and the demonstration of two application studies.

The theoretical background for UAS mission simulation and evaluation based design is presented in Section 2. It starts with the overall description of a UAS and its elements with the focus on sensor and communication systems performances. Then, the general design aspects for fixed-wing UASs are considered. As the focus of the thesis lies on the UAS design for civil applications, the overall description of possible examples of UAS usage in civil areas with its key performance parameters is presented. In order to assess a UAS design for a certain mission and to compare different designs a Mission Performance Index (MPI) based on key performance parameters is introduced. For a mission performance of a designed system simulation and evaluation a mission flight planning with the following aspects is taken into account: equations of motion, flight patterns, flight altitude definition and mission definition. In order to find an optimum UAS design for a required mission an optimization process is presented.

The developed environment for the mission based UAS design, simulation and evaluation is presented in Section 3. The main focus of this section lies on the presentation of the visualized operational environment and description of the main features for the sensor and communication performances analysis.

For the feasibility validation of the presented UAS design approach, two application studies are presented in Section 4. The first application study is an agriculture mission with the focus on a general validation of the presented approach which takes the sensor and communication performances analysis into account during the UAS design process. The second application study is a search and rescue mission. It highlights the usage and advantage of the visualized operational environment during the mission simulation, as it allows to obtain additional performance evaluation data, where the landscape shape changes significantly.

Section 5 describes the summary of the work presented in this thesis and gives an outlook of possible future improvements.

In Appendix A, figures and data describing the UAS mission simulation and evaluation environment are presented. Appendix B contains additional figures and data for the application studies.

2 UAS system and elements

According to Gundlach (Gundlach 2012) the design of unmanned aircraft offers more configuration freedom compared to the design of manned aircraft. Furthermore, an UAS interacts with the environment through the onboard sensors, only. Therefore, the UAS configuration should be influenced by the design requirements to enable a compliant system as there are many additional drivers such as sensor field of regard, payload flexibility, satellite communications, transportability, maintainability and launch and recovery provisions.

The UAV is the most visible segment of the system, however its successful performance is highly dependent on all segments. Classical aircraft design takes payload weights into the design loop, but not its performance which influences the mission success at the end. Therefore, for a UAS design it is important to implement the dependencies of all sub-systems into the design loop. For that, a simulation environment is necessary which allows assessing the camera and communication performances, to simulate the performance of UAS elements together and to include it into the UAS design process.

In this Section a generic UAS and main parameters of its elements used for the theoretical background for the mission simulation and evaluation based UAS design approach are described. It consists of an overview of civil UAS applications, general fixed-wing UAV design aspects, sensor and communication system performance parameters analysis. Elements of the mission flight path planning such as flight altitude definition, flight patterns and its optimization are considered as well. A Mission Performance Index (MPI) is introduced in order to asses a UAS design for a specific mission and to compare different designs.

2.1 Generic UAS system

According to the International Civil Aviation Organization (ICAO) “An unmanned aerial vehicle is a pilotless aircraft, which is flown without a pilot-in-command on-board and is remotely or fully controlled from another place (ground, another aircraft, space) or programmed and fully autonomous”. In order to emphasized the importance of the elements other than the aircraft the term UAS was introduced by the United States Department of Defense (DoD) and the United States Federal Aviation Administration (FAA) in 2005 followed by the ICAO and the European Aviation Safety Agency (EASA):

> An Unmanned Aircraft System (UAS) comprises individual system elements consisting of an “unmanned aircraft”, the “control station” and any other system elements necessary to enable flight, i.e. “command and control link” and “launch and recovery elements”. There may be multiple control stations, command & control links and launch and recovery elements within a UAS (European Aviation Safety Agency 2009).

The generic UAS is depicted in Figure 2.1. It includes the UAV, payload, communication element, control element and support equipment. The UAV element is the most visible element of the system. It can be represented by different aircraft types such as conventional fixed wing, VTOLs, UCAV,

helicopter, quadro- or multicopter. Depending on mission requirements and therefore required payload on board the UAV will have different type, weight and size. In the mission based UAS design approach presented in this work the conventional fixed wing is considered.

Payload element means the equipment for which the UAV provides a platform and transportation which is added to the UAV for the purpose of performing missions. It includes sensors, emitters and excludes flight avionics, data link and fuel (Fahlstrom, Gleason 2012). Depending on mission requirements different sensor systems can be added on board: EO/IR or multispectral cameras, SARs, LiDARs and etc. Sensors on board provide interaction between the UAV and the operational environment and therefore play a key role for the mission success. In the presented approach in this work an EO/IR camera is considered. Its parameters influencing the UAS design and mission success are presented in the next section.

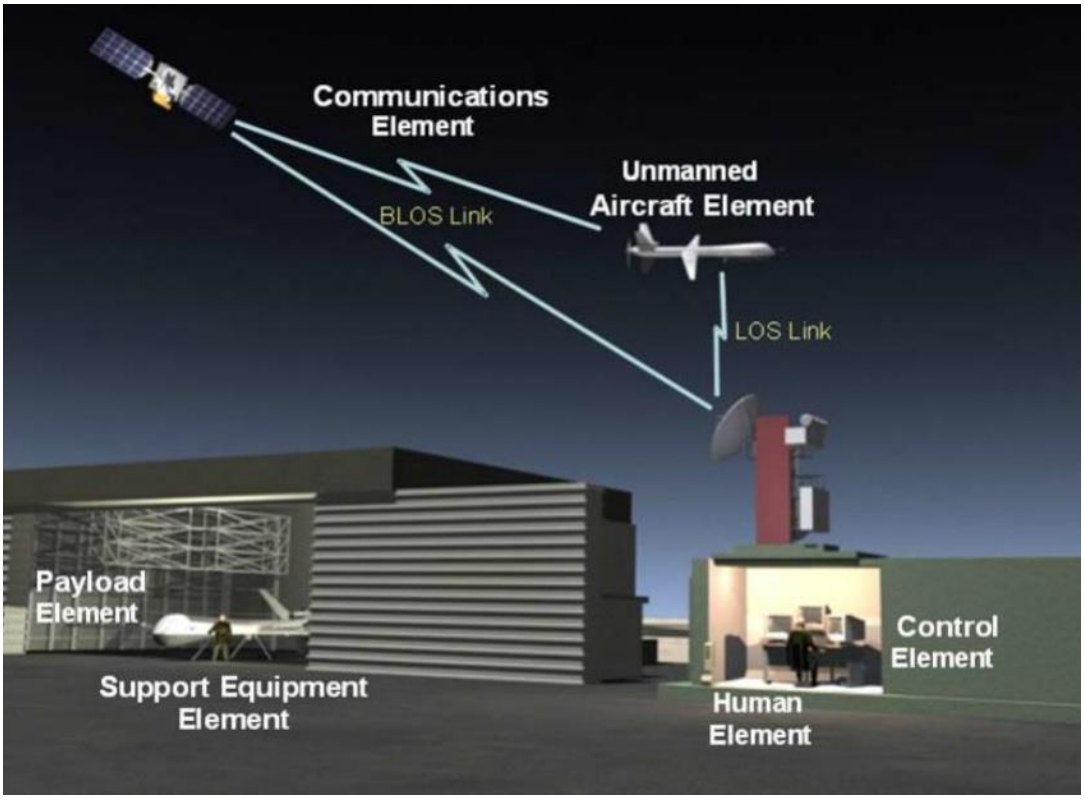

Figure 2.1 Components of an Unmanned Aerial System (Hornung 2020)

The communication element distributes data between system elements and to external entities. The main way to transmit data uses radio-frequency (RF) communication. For that direct line-of-sight communication between the UAV and ground control station is required. It transmits the commands from ground control operators to the UAV. Payload data as well as UAV flight status information are transmitted back to the ground for processing. Indirect beyond line-of-sight communications take place with satellite communication (SATCOM) or airborne relays.

Control element is presented by a ground control station. The duties of it are divided into 2 groups: flight management and mission management. The first one concerns navigation, flight path planning,

flight status monitoring. Mission management covers payload image processing, display, storage and dissemination (Hornung 2020).

The support equipment covers launch and recovery, datalink antenna, transport and maintenance equipment. The ground infrastructure also depends on the UA size, onboard systems, and mission capabilities (Gundlach 2012).

2.2 Sensor and communication systems

In the presented UAS mission based design approach, performances of the sensor and communication elements are taken into account into the design loop. This subsection describes the key performance parameters for these elements.

2.2.1 Sensor performance

Mission requirements drive the payload systems. An UAS interacts with the environment through sensors on board, therefore sensor performance is one of the most important parameters for the UAS mission assessment. For civil applications, the most commonly used are electro-optical systems which range from simple monochrome or color single-frame cameras through color TV systems, thermal imaging video systems to multi-spectral systems (Austin 2010).

Such a mission sensor is usually characterized by its vertical and horizontal resolution and a frame rate. With these parameters, the actual ground sample distance (GSD), image overlaps for the flight path, flight altitude and the maximum speed can be calculated for a desired mission result. These parameters allow to assess the mission success from the sensor performance point of view. In order to assess the probability of object detection by a certain sensor onboard the Johnson Criteria is used.

2.2.1.1 Ground sample distance

In order to measure an achievable resolution of the collected data, a parameter called Ground Sample Distance (GSD) is used. GSD is a function of the camera focal plane array, optics and collection geometry (see Figure 2.2). In other words, the GSD represents the distance between the pixels projected on the ground at slant range (Gundlach 2012). The horizontal GSD at the center of the image is derived as:

$$GSD_H = \frac{P}{f} \cdot R \tag{2.1}$$

Where P is the distance between two pixels on the camera chip, f the focal length of the objective and R is the slant range, which is the distance from the camera to the target on the ground. *D* on the Figure 2.2 means the lens diameter.

The vertical GSD at the center of the image considers the look angle θ_{Look} and is derived as:

$$GSD_V = \frac{P}{f \cdot \cos(\theta_{Look})} \cdot R \tag{2.2}$$

The look angle θ_{Look} is the angle between vertical line perpendicular towards the ground and the line between the sensor and the target.

By representing the focal plane array by pixels in horizontal (H_{res}) and vertical (V_{res}) planes format and taking field of view angle (FOV) of the camera into consideration, the GSD equations are:

$$GSD_H = 2 \cdot tan\left(\frac{FOV_H}{2 \cdot H_{res}}\right) \cdot R \tag{2.3}$$

$$GSD_V = \frac{2 \cdot tan(FOV_V/2 \cdot V_{res})}{\cos(\theta_{Look})} \cdot R \tag{2.4}$$

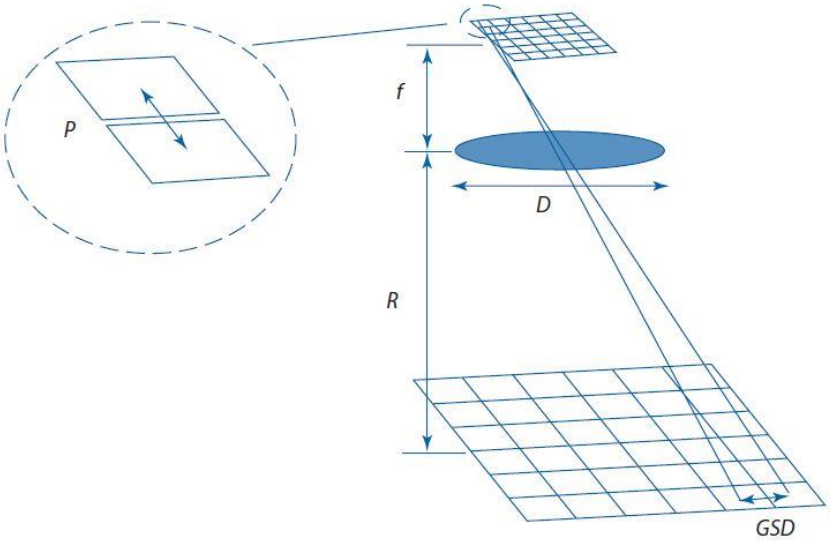

Figure 2.2: Optics geometry (Gundlach 2012)

Sensor camera characteristics and required image quality drives the flight altitude, overlap between flight paths and airspeed of the aircraft during the mission. The flight altitude is a function of image ground coverage size and camera resolution and is defined as (Fokina et al. 2018b):

$$alt_{WP} = \frac{SW_{req}}{2 \cdot tan \cdot \left(\frac{HFOV_{max}}{2}\right)} \tag{2.5}$$

where $HFOV_{max}$ is the maximal horizontal field of view of the camera. The required sensor ground swath width SW_{req} is determined as a product of number of pixels in the horizontal plane H_{res} and required GSD_{req}:

$$SW_{req} = H_{res} \cdot GSD_{req} \tag{2.6}$$

2.2.1.2 Images overlap and camera frame rate

In the process of collecting photographic images, two types of overlapping are distinguished: forward overlap and side overlap.

Forward overlap, which is also called endlap, describes the amount of image overlap introduced between consecutive photos along a flight line. Figure 2.3 illustrates an aircraft equipped with a mapping camera taking two overlapping images, where *B* is the distance between the centers of two images called airbase and *G* is the covered distance on the ground by an image (Wolf et al. 2014). Usually the forward overlap is defined as a percentage of the total image coverage and depends on the required image type and surrounding terrain. For example, for a stereoscopic coverage of an area forward overlap is taken usually approximately 60%.

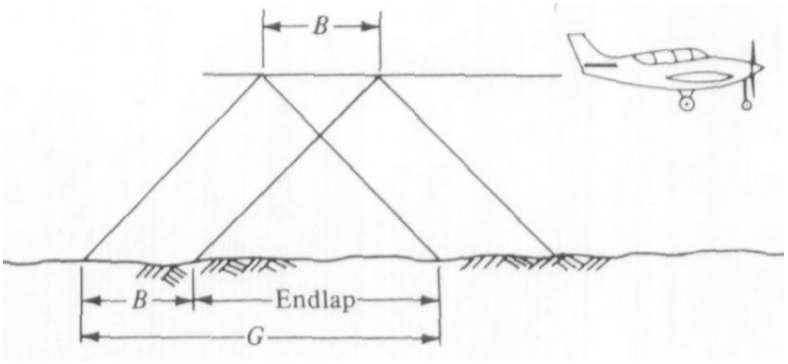

Figure 2.3: Imagery forward overlap (Wolf et al. 2014)

For creating a stereoscopic or non-stereoscopic image coverage of larger areas a well-planned flight line pattern is desirable. It is a sophisticated combination of flying height, flight speed, image size, focal length and exposure interval of the sensor. The tradeoff study of the flight pattern definition based on sensor parameters is to define which variables are dependent and which are independent. For a given aircraft and a camera, the most easily adoptable variable is the flying height. At the same time, the flying height defines collected image size and GSD. This leaves the exposure interval of the mission sensor as potentially the most independent variable (Aber et al. 2019). In addition, according to Qassim A. Abdullah for maintaining the necessary forward or endlap expected for the imagery the aircraft speed has to be controlled. An increase in speed reduces the expected overlap, which makes imagery processing or image stereo viewing difficult. Thus, for image analysis the following method is proposed (Aber et al.):

- Calculate flying height and ground image size based on sensor properties and desired GSD
- The airbase or the distance between two consecutive images B along one flight line for the desired endlap is calculated as:

$$B = G \cdot \left(\frac{100 - Endlap}{100}\right) \tag{2.7}$$

- Once the airbase is determined and the aircraft speed is set up, the time t between two consecutive images or time interval between exposures is obtained as:

$$t = \frac{B}{V} \tag{2.8}$$

For mission planning it is important to check whether the required calculated exposure interval of the sensor is not bigger than the maximum defined in the camera specifications. At the same time based on the specified camera frame rate and a calculated airbase the maximum possible airspeed V_{max} for good and equal images quality can be assessed.

Side overlap describes the amount of overlap between images from neighboring flight lines. Figure 2.4 illustrates an aircraft equipped with a mapping camera taking two overlapping images from neighboring flight lines, where *W* is the distance between the centers of two flight lines, called lines spacing. *G* is the covered distance on the ground by an image that is different to the one used for forward overlap calculation as both are calculated based on HFOV and VFOV respectively. The side overlap is defined in percentage of the total image coverage and is required in order to avoid gaps in the area coverage (Wolf et al. 2014). Line spacing SP is obtained as:

$$SP = G \cdot \left(\frac{100 - Sidelap}{100}\right) \tag{2.9}$$

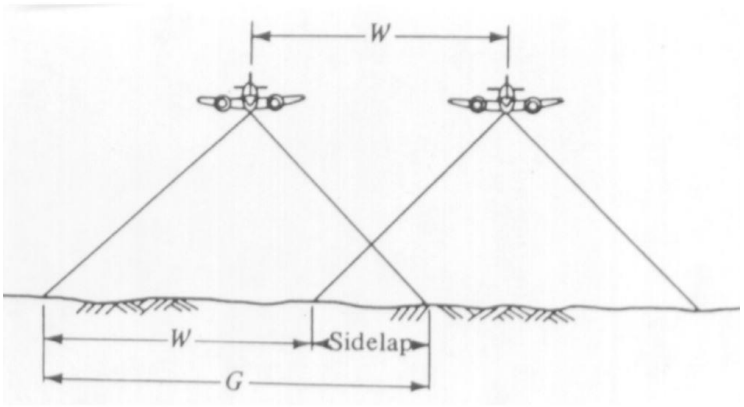

Figure 2.4: Imagery side overlap (Wolf et al. 2014)

2.2.1.3 Johnson Criteria

Johnson Criteria is a method for determining the probability of detection, recognition and identification of an object based on the sensor's resolution. Therefore, it is used to predict the quality of the gathered imagery. This method was first introduced in 1958 by John Johnson (Johnson 1958) and is known as Johnson Criteria, *P(N)*. According to it, an object is replaced by *N* line pairs, one of each is called a cycle and corresponds to two pixels, of the sensor on the ground, see an example in Figure 2.5 .

The mathematical representation of it is:

$$P(N) = \frac{\left(N/N_{50}\right)^{2.7+0.7\cdot(N/N_{50})}}{1+\left(N/N_{50}\right)^{2.7+0.7\cdot\left(N/N_{50}\right)}} \tag{2.10}$$

Where N_{50} is a number of cycles, which gives an observer probability of 50% discriminating an object to the specified level. It is assumed in this method that:

- N_{50} = 0.75 for detection task, an object of general group is present
- N_{50} = 3.0 for recognition task, the object type is discerned
- N_{50} = 6.0 for identification task, i.e. object discrimination

The number of line pairs is defined as relation of the object characteristic dimension d_c to the average ground sample distance GSD_{avg}:

$$N = \frac{d_c}{2 \cdot GSD_{avg}} \tag{2.11}$$

The object characteristic dimension d_c is obtained as square root of the product of the object height, H, and width, *W*.

$$d_c = \sqrt{W \cdot H} \tag{2.12}$$

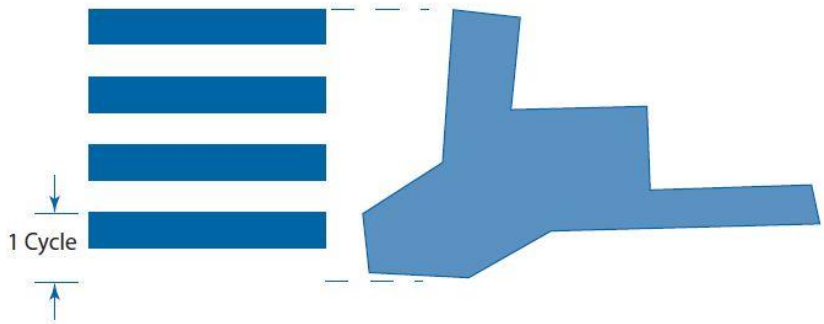

Figure 2.5: Four-cycle representation of a target for Johnson Criteria (Gundlach 2012)

In order to determine the appropriate values of GSD based on the given object size Eq. (2.11) and Figure 2.6 are used. According to it, the minimum amount of cycles has to be 3 in order to be able to detect the object with the probability of 100%. Detection means that it will be possible to notice a target, but difficult to classify it. Recognition means that it will be possible to recognize an object class, for example human or a car. Identification means that it will be possible to differentiate between objects, for example to identify the type of vehicle. In order to improve the probabilities of recognition and identification, the number of cycles has to be increased. 15 cycles give a 100% probability for all three levels: detection, recognition and identification. However, it requires a small GSD and therefore a lower altitude, a camera with a higher resolution and a smaller field of view, which increases the mission time.

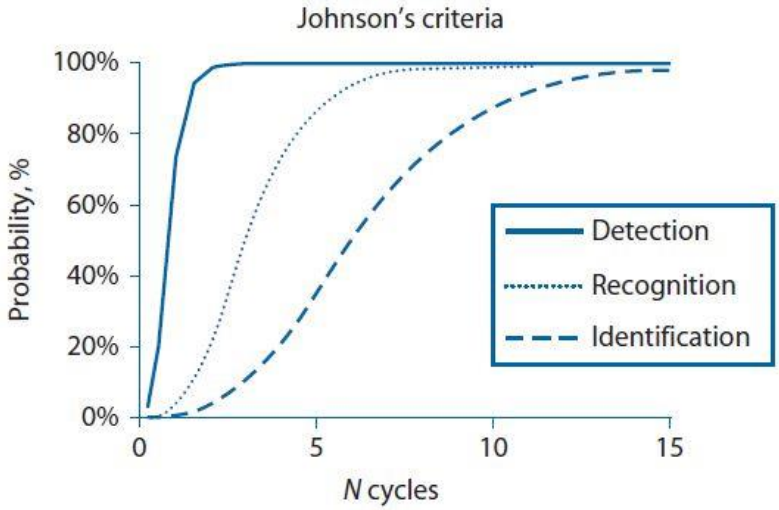

Figure 2.6: Johnson criteria plot (Gundlach 2012)

2.2.2 Communication performance

Under the communication performance in this work, two issues are considered:

1. Losses during the line-of-sight (LOS) communication:

   Defines if the LOS was interrupted by a terrain during the mission and for how long the communication losses took place.

2. Data link capacity:

   Describes if the data link capacity is enough to transmit the collected image data back to the ground control station.

Communication systems provide interaction between system elements and external entities. The main way to transmit data is the usage of radio frequency (RF) communication for which a direct line-of-sight communication between the UAV and ground control station is required. BLOS communication occurs when there is no direct line of sight between the transmitter and receiver due to physical blockage caused by terrain or the Earth's curvature. To complete the link BLOS communication requires satellite communications (SATCOM) or airborne relay to retransmit the signal. Other UASs, airships, tethered balloons, or fixed-wing manned aircraft can be used as relay airborne. SATCOM offers relaying information over very large distances, but compared to LOS communication it requires higher operating altitudes and maintenance costs.

Loss of communication during the mission may result from (Austin 2010):

- failure of all or parts of the system due to lack of reliability;
- loss of line-of-sight due to geographic features blocking the signals;

- weakening of received power due to the distance from the UAV to the control station becoming too huge;
- intentional or inadvertent jamming of the signals.

In this work, the losses due to geographic features blocking the signal are simulated and evaluated during the UAS mission simulation in the visualized operational environment. The details of it are describes later in Section 3.2.4.

Communication between the UAV and the control station consists primarily of an uplink and a downlink data link, see Figure 2.7. An uplink (or command link) has a bandwidth of a few kHz and transmits from the ground station control signals to the UAV and its payload. Usually, the downlink has two channels, which may be also integrated into a single-data stream (Fahlstrom, Gleason 2012):

1. A status (or telemetry) channel with a low data-rate bandwidth to acknowledge commands and transmit status information about the air vehicle to the ground control station.
2. A high data-rate channel transmits sensor data. It requires a bandwidth sufficient to transmit the amount of data produced by the sensors, usually from 300 kHz to 10 MHz. This data link is also called payload datalink and is usually mission critical as it influences the mission success, however it is not flight critical. Normally the downlink operates continuously, but in case of data link losses or delayed transmission the data can be temporary recorded onboard.

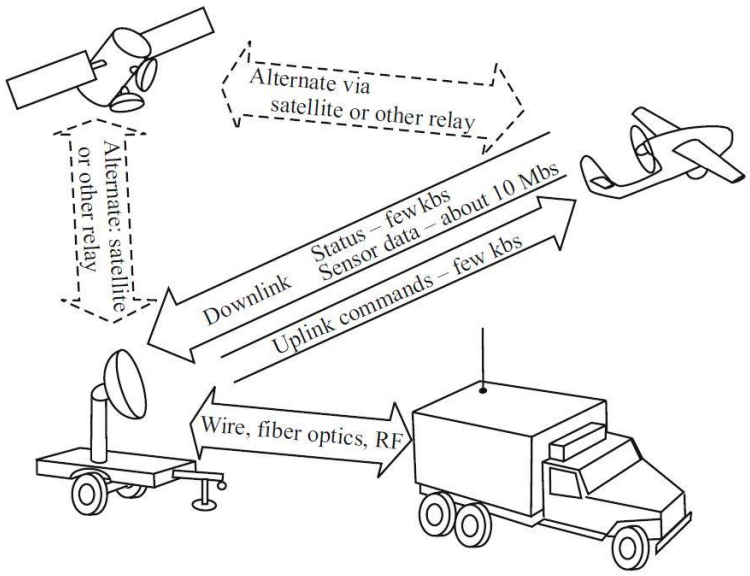

Figure 2.7: Basic functions of UAS data link (Fahlstrom, Gleason 2012)

The data link has to meet UAV size, weight, cost constraints and needs to have enough capacity to transmit the required data rate. Especially, it concerns payload data, which can generate vast quantities of data that can exceed the capabilities of other system elements. The payload data onboard the UAV must be sent to the communication downlink, compressed, stored, or deleted (Gundlach 2012). Restrictions on the sensor downlink data rate may influence the rest of the system.

The size of the survey area and the image size determine the amount of collected data, which has to be transmitted to the ground station or stored on board. In case of a direct data transfer from the UAV to the ground station, the actual frame rate defined by the airspeed and amount of overlap should not exceed the communication transfer rate. Otherwise, the collected data should be stored on board during the whole mission time.

The camera resolution in horizontal H_{res} and vertical V_{res} directions and the amount of bytes for a pixel per band, n_b define the necessary storage requirement for an image. Furthermore, the compression rate of the used file format plays a role. For example, for a .tiff file format with 8 bits per band each pixel requires 1 byte. For a natural color image three (R, G, B) bands and therefore 24 bits are required. The image storage per band im_s is determined then as:

$$im_s = H_{res} \cdot V_{res} \cdot n_b \tag{2.13}$$

Knowing the image size im_s and camera frame rate for a live transfer, see Eq. (2.8) one can determine the required data transfer rate T_{rate} as:

$$T_{rate} = im_s \cdot f_{rate} \cdot m \tag{2.14}$$

The required transfer rate should not exceed the maximum possible transfer rate defined by the communication system. The required transfer rate can be decreased by reducing the image size, UAV airspeed or overlap between images. Another option is to save the images onboard. For that, the necessary storage size has to be defined and implemented on the platform, which can lead to an increase in the weight of the system.

Thus, the total storage requirement S_{total} depends on the number of images N_{im} needed to cover the whole area of interest and the amount of bands m:

$$S_{total} = N_{im} \cdot m \cdot im_s \tag{2.15}$$

2.3 UAS design loop

In this Section the background and methods used for the UAS mission based design loop presented in this work are described. At the beginning mission definition and general UAS design aspects are considered. Then the UAS design loop and its challenges based on an example of a search and rescue mission in a region with high gradient terrain are discussed. At the end, the optimization method used in the design loop is presented.

2.3.1 Mission definition and key performance parameters

The UAS design process starts with the definition of requirements for a certain mission or for a set of missions. The UAS mission is a task, which has to be fulfilled during the flight with the help of onboard sensors. Initial mission requirements define UAV type, sensors onboard, mission area, desired GSD, flight pattern and set requirements to the flight path planning for a successful mission. The following

parameters have to be defined by a user for the UAS mission simulation according to the approach presented in this work:

- Mission area;
- Start and end points for the mission flight path;
- Type of flight pattern (lane, spiral, sector);
- Waypoints for a desired flight pattern;
- UAV airspeed;
- Overlaps between passes of the flight path in %;
- Required GSD and inacceptable GSD;
- Position of the ground control station in order to prove LOS availability;
- Image requirements;
- Definition of key mission performance parameters for a mission performance assessment.

Key performance parameters (KPP) are quantifying or describing the system performance. A system requirements document can contain hundreds or thousands of parameters that have to be met for a compliance. Therefore, the user has to choose the most relevant KPPs for his mission, which should be taken into account in the UAS design loop. The following KPP can be obtained or assessed in the presented design approach:

- Total endurance;
- Energy consumption;
- Mission time;
- Time to target;
- Target detection;
- LOS availability;
- Sensor performance;
- Area coverage;
- Communications range.

Some of these key performance parameters can be assessed only during the operational analysis, which represents the systems simulation in a geospatial simulation environment. These parameters are: target detection, sensor effectiveness in operational environment, LOS communication and gaps in area coverage.

2.3.2 General design aspects

The mission requirements place demands upon the UAS. They determine the shape, size, performance and costs of the air vehicle and put demands to the overall UAS architecture. The payload size, weight and power supplies are often the premier determinant of the layout of the aircraft. Imaging payloads may require in addition a full hemispheric field of view. The required speed range defines the configuration and propulsion power of the UAV. The radius of action is preset by the amount of fuel or power on board and communication links. The data rate requirements of the payload effect the electrical power, frequency range needed for the radio-links and quality of the transmitted data to the ground station. The UAV launch and recovery is driven by the mission role and determine the aircraft configuration (Austin 2010). The UAS design process starts with the definition of requirements, where the information presented in Table 2.1 is the starting point in the presented approach in this work. Depending of the UAS class, different orders of design methods, constraints and assumptions are applicable.

Table 2.1: UAS initial design information

Geometry	• General configuration • Wing geometry • Geometry rules (for tail sizing)
Mass properties	• Avionics and communication system size, weight and power • Sensor size, weight and power
Propulsion	• Propulsion type • Specific engine • Number of engines • Estimated propulsion system requirements
Performance	• Mission profile • Performance requirements
Aerodynamics	• Airfoil families
Mission effectiveness	• Sensor field-of-regard requirements • Desired image quality • Probability of objects detection

The UAS design is a closed-loop optimization process in which the design variables and boundary conditions must be selected in such a way that they should be present in a small number and with high impact. The following parameters can be chosen as design variables in a UAS design process:

- Geometry parameters: span, wing area, aspect ratio, fuselage length and shape;
- Mass properties: fuel weight or fuel mass fraction;
- Propulsion properties: thrust, thrust-to-weight or power-to-weight ratios, propeller diameter;
- Payload requirements: camera type, communication system;
- Mission requirements: design speed.

In the presented approach the wing geometry parameters such as wing area and aspect ratio, design speed and camera type are used as design variables.

As constraints in the UA design, the following parameters can be used:

- Performance: stall speed, climb angle, rate of climb, range;
- Weight: maximum weight, weight convergence;
- Geometry: dimension, storage constraints;
- Systems: fuel volume, avionics and payload power requirements, field-of-regard requirements, communication requirements;
- Propulsion: required thrust, power limits.

The stall speed is used as constraint parameters for the presented UAS design process.

At the next step the objective function has to be defined, which emphasize the most important system characteristics and performances, for example:

- Minimum weight;
- Minimum size;
- Minimum fuel burn;
- Minimum cost (acquisition, operations or life cycle);
- Mission effectiveness (area coverage, time on station, target access);
- Compound objective function.

In case of the compound objective function, several attributes are used where each attribute is scaled and weighted to ensure the appropriate balance. This is the case in the UAS mission based design environment presented in this work. For the objective function definition, a Mission Performance

Index (MPI) is introduced in order to take into account several performance attributes. In details, it is discussed later in Section 2.4.2.

The difference of the UAS design process compared to the classical aircraft design process, is the necessity of having the operational analysis stage within the design loop. On the operational analysis stage, an isolated element of the system is assessed or the whole system is simulated in a geospatial environment and the results are incorporated into the objective function. The operations analysis tasks can include the following (Gundlach 2012):

- Target coverage;
- Survivability analysis;
- Payload effectiveness in operational environment;
- Communications analysis;
- Fleet sizing.

In the presented approach target coverage, payload and communication effectiveness simulated and evaluated in the visualized operational environment are considered.

2.3.3 UAS design challenges

In the presented work, a design loop for a fixed-wing UAS is introduced. The fixed-wing UAV can be used for many applications as it can carry onboard different payload types and can vary in size. The UAV design is then similar to a conventional aircraft design and therefore, already known methods and theoretical aspects for a manned aircraft design can be taken over.

After the definition of the initial requirements, objective function and constraints, the geometry of the aircraft is calculated. Usually it is highly parametrized, but with relatively few geometry terms. For example with the aspect ratio and wing area, the complete configuration is defined. This process contains also tails sizing, calculation of fuselage geometry, spaces available for payloads, avionics and other components of the UAS. The next step is the mass calculation, which should include an internal weight convergence procedure. Then propulsion as well as aerodynamics calculations are performed. After that, a flight performance analysis can be fulfilled. The fuselage is designed in a way for housing an arbitrary number of system components as well as a sensor payload and propulsion system components, while maintaining a minimal surface area to minimize structural weight and drag. Electro-optical sensor payload is placed with an acceptable level of obscuration of its field of view by structural components of the UAV like wings and tail surfaces, which is defined by the user. More about wing weight estimation, payload placement, fuselage lofting, electrical propulsion system layout and tail sizing can be found in (Feger et al. 2018).

The goal of the UAS usage is to fulfil the mission with the desired results. The mission fulfilment grade is driven by the UAV performance as well as performances of other UAS elements, especially by the mission sensor and communication system. Furthermore, mission planning is also driven by the UAS

elements performances and influences the mission success. The UAS elements considered in the design process in this work and its key parameters influencing each other are presented in Figure 2.8. The matching of UAS elements and its parameters to each other defines tradeoffs in UAS mission based design.

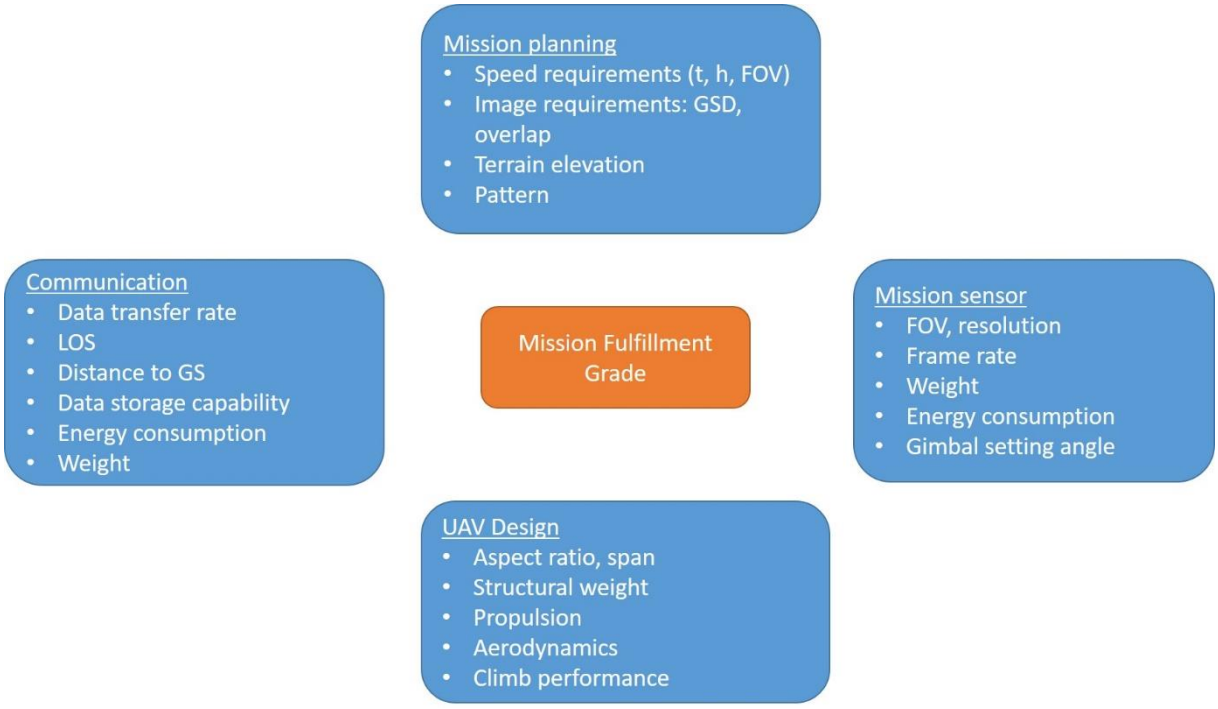

Figure 2.8: Tradeoffs in UAS mission based design

Each type of sensor has certain requirements for integration in the UAV, for example with regard to freedom from shadowing, structural fastening, thermal management, and energy consumption or vibration level. Weight and energy consumption parameters of onboard systems put limitations on the UAV performance. Thus the heavier the UAV the higher propulsion performance is required. At the same time the heavier mission sensor might has better performance parameters, which can significantly improve the mission result.

Mission sensor performance is defined by its resolution, field of view and frame rate. Its influence on mission success is closely interacted with mission planning parameters such as flight altitude, speed and flight path. The desired image quality on the ground defines the maximum flight altitude. With a decrease in altitude the sensor ground swath width decreases as well, but the resolution of collected images increases. On the other side, higher flight altitudes provide larger coverage area and together with higher speed the mission time is reduced.

Communication system performance is considered by its capabilities to transfer data within the LOS back to the ground control station, which influences the mission fulfilment grade as well. The transfer rate has to be either large enough in order to fully transmit collected data, defined by the camera properties, from the UAV to the ground station or a buffer storage is required onboard, which gives additional weight to the UAS.

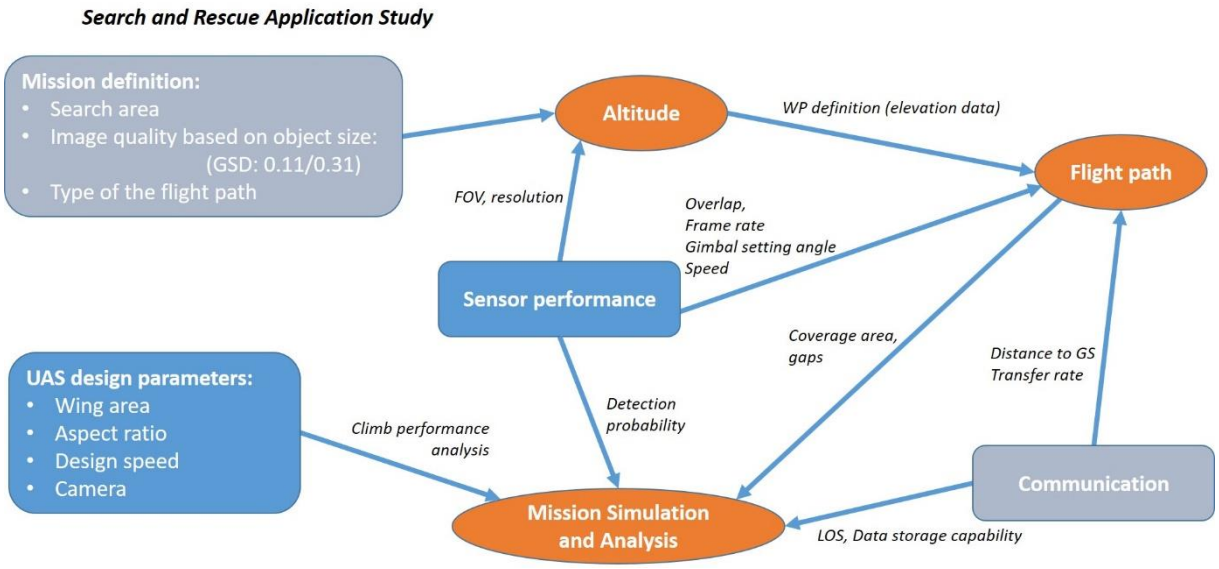

Figure 2.9: UAS design challenges for Search and Rescue mission

An example of interactions between the system elements and its parameters for a UAS design for a search and rescue mission is presented in Figure 2.9. One of the key issues in this work is to include sensor performance parameters into the UAS design loop. For that, it is necessary to know the influence of its parameters on other elements of the system. In this mission example the initial mission requirements for the desired image quality are defined by an acceptable and an inacceptable GSDs. Together with the sensor FOV and resolution it defines the desired flight altitude range. The last one and other sensor parameters as frame rate, gimbal angle setting are used for flight path calculation. The parameters of the flight path together with the UAS mission simulation in the terrain based visualized operational environment give information about gaps in the coverage area, losses in communication and actual values of GSD. During the mission planning calculations, it also has to be verified if the UAV propulsion and climb performances are capable to fulfil the flight path. Thus, one can see how the UAS mission effectiveness depends on the performance capabilities of the system elements. A change of sensor camera, flight altitude, speed, communication system will influence mission time, energy consumption, area coverage rate and other performance parameters.

2.3.4 UAS optimization

According to Torenbeek (Torenbeek 2013) “In today’s state of practice, the methodology of multidisciplinary analysis and optimization coherently exploits the synergism of mutually interacting computational domains to improve the design of complex engineering system”. The goal of the UAS optimization process is to tailor an UAS to certain mission requirements so that the best possible mission fulfilment is achieved. For that an optimization method called GAME (Genetic Algorithm for Multi-criteria Engineering) developed at the Institute of Lightweight Structures at the Technical University of Munich (Langer 2005) is implemented into the UAS design loop. Although it was developed mainly for general design issues it perfectly fulfils all requirements for the conceptual aircraft design task (Rößler 2012). This optimization method was chosen due to its ability to handle discrete and continuous design variables simultaneously and the usage of integer and Boolean number

types. Thus, the optimizer permits the flexibility of selecting the system architecture and system characteristics as integer design variables like number of engines, propulsion type, and camera type or configuration selection. In the case of UAS optimization, the camera type is defined as an integer design variable.

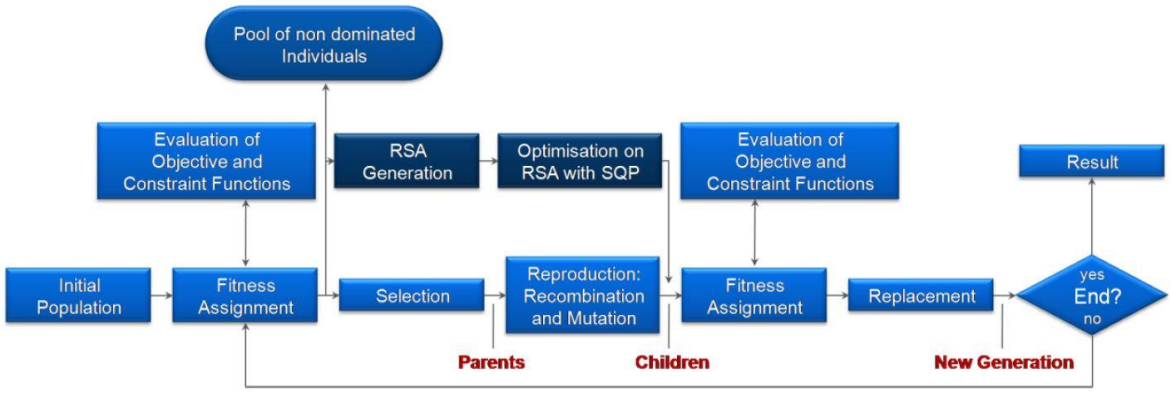

Figure 2.10: Flow chart of GAME (Rößler 2012)

The flow chart of GAME is presented in Figure 2.10. The UAS optimization starts by generating an initial population of individuals from randomized values of the design variables. A generation consists of a number of individuals, where each individual has a collection of genes called genotype. Each gene corresponds to a design variable. All individuals get a fitness value based on the objective and constraint functions. This is the basis for the selections as a parent. By analogy with genetics in order to produce a children generation three main operations are used: reproduction, recombination and mutation. Reproduction brings forward individuals with the best fitness value to the next generation. Recombination means that two randomly selected individuals exchange parts of their genotype. The switching of a single value within a genotype is called mutation. Fitness value is also assigned for the children generation. Based on a replacement scheme, which controls which individuals of the last generation will survive and which will be replaced by the offspring the next generation is then set up. This optimization process is repeated until the termination criterion is met (Rößler 2012).

In the presented work the objective function of the UAS optimization process is to maximize the scalar MPI value by varying aircraft geometry and payload sensor parameters while not exceeding a specified stall speed. For each individual the aircraft sizing process, modelling in the visualized operation environment and mission performance evaluation process are executed.

The objective function is called the fitness function in Genetic Algorithm term, by biological analogy of the survival of the fittest. The Pareto-dominance ranking approach based on the so called — goals and priorities approach is used in GAME to consider multi objectives as well as constraints (Fonseca, Fleming 1993). Each objective and constraint has a goal and a priority assigned. In this approach constraints get higher priority while the objectives get the lowest priority. The ranking scheme of GAME compares designs on the highest priority level first, i.e. constraints functions. The design, which fulfils all goals on this priority level, is considered better. In case when two designs fulfil all goals on this priority level, the decision is shifted to the next lower priority level. On the lowest level a ranking

according to Pareto is carried out, where all designs on the Pareto-frontier have the rank 0. (Rößler 2012).

An example of the ranking approach is presented in Figure 2.11. The objective function is located along the horizontal axis and the constraint along the vertical axis. The individuals ranked with “0” and “1” fulfil the constraint limit. However, individual “0” has a higher MPI and therefore it has the highest priority. Thus, the presented individuals are ranked from 0 to 6, where 0 is the highest priority.

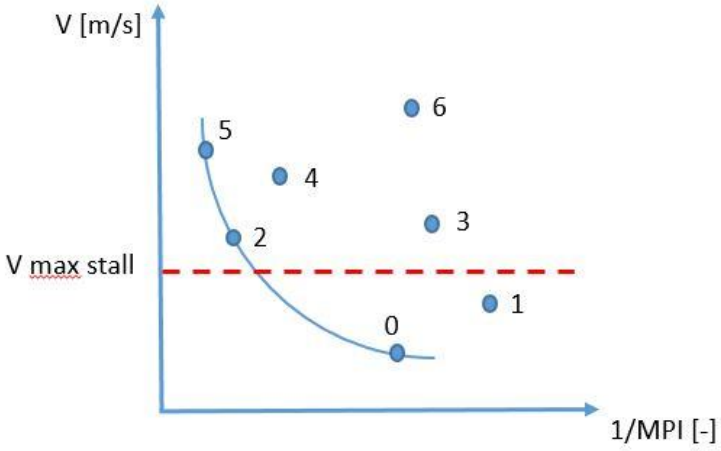

Figure 2.11: Ranking method with objective function and constrain

2.4 UAS design assessment

There are currently no corresponding metrics for evaluating mission performance for civil UAS applications. So far, no methods are known by means of which, for example, the reconnaissance performance of an aircraft can be quantified, compared and thus evaluated using a specific sensor selection. In addition, different types of missions such as reconnaissance missions, transport missions, relay missions or monitoring missions have fundamentally different assessment parameters. As a result, there is no quantitative basis to be able to compare different aircraft or design concepts. It is therefore important to identify measurable assessment parameters for different mission classes and to transfer them to a corresponding scale.

2.4.1 UAS civil applications and mission requirements

The entire reason for the existence of a UAS is its mission with the main goal to effectively perform the mission of interest (Gundlach 2016, 2012). Despite the fact that UAVs were originally developed for military purposes, currently there are two major divisions of missions for UAVs: civilian and military. Reconnaissance and surveillance missions represent an overlap between these two, where for civilian missions it is called search and surveillance or observation. To date, it is the largest single application of UAVs in both the civilian and military worlds and its sensors and data-links are the focus of most of today’s development (Fahlstrom, Gleason 2012).

Most commonly used for civilian missions are 2 types of UAVs: fixed wing and copter UAVs. A fixed wing UAV suits best for monitoring large areas as it has high aerodynamic performance. However, this type of UAV cannot hover over objects. Copter UAVs allow a hover mode for spot shooting and monitoring small areas. This type of platform is simple in design and flight stable. However, it flies with a low speed and has a limited flight time due to which the radius of action is less than that of a fixed wing type. In the methodology presented in this work, the fixed wing type for UAS design is used.

This work is focused on civil UAS mission applications and its key performance parameters evaluation. Military missions have different key performance evaluation parameters (Mavris, DeLaurentis 1995) and are not included in this study. The non-military UAS applications can be classified in many different ways as it is presented by Gundlach and by Valavanis Vachtsevanos. In this work, civil applications of UASs are classified according to their key mission performance parameters. For that, a following classification presented in Figure 2.12 is proposed. The goal of such classification is to show that different mission types have different assessment criteria, which drive the UAS design. The basic civil applications of UASs are divided into 3 groups based on their main tasks: surveying areas, delivery or transport and search and tracking missions.

For the first group the main task is to explore a big area and to gather data with a desired image quality. Key performance parameters are area coverage, endurance, data quality and costs. Mission time is not a critical parameter and in a tradeoff with costs, it is more important to have a lower fuel consumption than a short mission time.

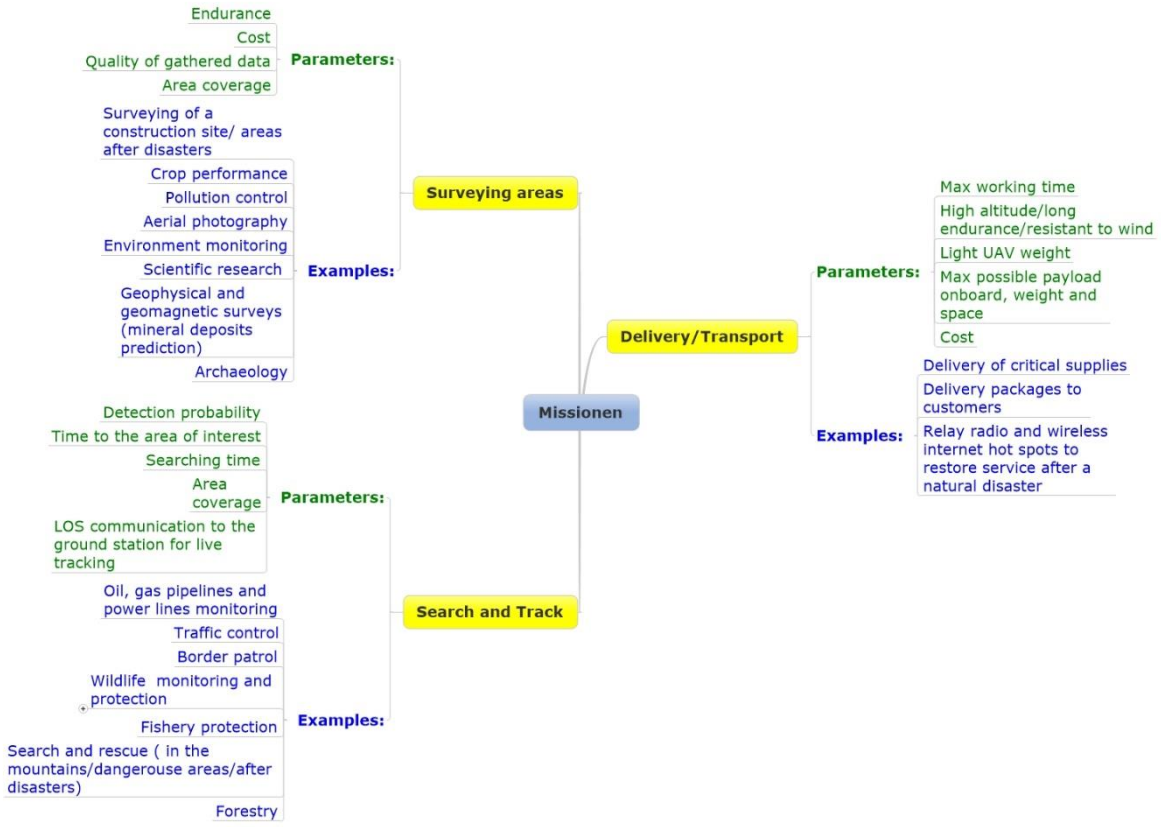

Figure 2.12: UAS mission types based on mission key performance parameters

For the missions from the group Delivery and Transport it is important that a UAV has enough space onboard and performance for a payload transportation. Endurance, UAV performance and costs are the key performance parameters in this case.

Object detection, time to the area of interest and mission time are important criteria for missions from the group Search and Track. During these missions, it is important either to track or to search for something. The state of the objects of interest are changing with the time during the mission and therefore mission time is one of the critical parameters.

Thus, mission type and its requirements define key mission evaluation parameters. In order to assess a mission success fulfilled by a certain UAS, taking into account different key evaluation parameters, a metric based on a Mission Performance Index is introduced and presented further down in details.

2.4.2 Mission performance index

As a rule, aircraft or unmanned systems are not developed exclusively for one mission, but must be able to fulfil a large number of types of missions, some of which have contradicting requirements and different sensor packages. This may require that performance losses be accepted for individual missions in order to develop an overall more powerful and versatile system. Evaluation methods are lacking for evaluating either a design concept or for comparing different existing aircraft with regard to different types of missions and must therefore be developed.

Classic system evaluation and optimization methods concentrate on one or two system attributes independently (Gundlach 2012). The design of an UAS requires evaluation of the system as a whole. In order to take into account different mission performance contributing factors and to assess different UAS system architectures or different sensor packages onboard a Mission Performance Index (MPI) in form of a scalar value is introduced (Feger et al. 2018). It takes into consideration the correlation between the performance capabilities of the system elements, air vehicle design and mission requirements. Thus, the MPI assesses a UAS mission success and allows comparing different UAS architectures with each other.

The most commonly used multi-criteria decision analysis (MCDA) method to handle more than one decision criteria and which allows to derive an overall performance score is the Weighted Sum Model (WSM). This approach is used for the MPI definition where each key evaluation parameter is multiplied with a weighting factor α_i, β_j and summed together:

$$MPI = \sum_i \alpha_i \cdot \frac{Effectivity_i}{Effectivity_{ref,i}} + \sum_j \beta_j \cdot \frac{Effort_{ref,j}}{Effort_j} \tag{2.16}$$

The parameters positively influencing the mission performance such as area coverage rate and detection probability are called effectivity parameters. Effort parameters quantify resources needed to fulfil the mission, such as mission time or fuel. This way of MPI representation allows to consider any number of mission evaluation parameters.

To implement a mission evaluation index into a multidisciplinary design process, the following requirements have to be fulfilled:

- Quantification of the MPI in form of a scalar value, which is then used as a result of an objective function for a numerical optimization;
- Normalization of contributing attributes by a referenced value with the same physical unit for comparability between mission evaluation metrics;
- Sum of the weighting coefficients of all the attributes have to sum to unity.

According to the main key performance parameters for civil UAS missions described in Sections 2.3.1 and 2.4.1 the MPI is defined in the presented work as (Fokina et al. 2018c):

$$MPI = \alpha \cdot \frac{ACR}{ACR_{ref}} + \beta \cdot \frac{E_{ref}}{E} + \gamma \cdot \frac{P_d}{P_{d_{ref}}} + \tag{2.17}$$

$$+\delta \cdot \frac{T_{m\_ref}}{T_{\mathrm{m}}} + \varepsilon \cdot \frac{CA}{CA_{ref}} + \zeta \cdot \frac{UOI}{UOI_{ref}}$$

where α, β, γ, δ, ε, ζ are weighting coefficients of each attribute. ACR_{ref}, E_{ref}, $P_{d_{ref}}$, T_{m_ref}, CA_{ref}, UOI_{ref} are the reference values for the parameters presented further.

ACR: Area Coverage Rate

Since the sensor swath width on the ground SW and airspeed V depend on the flight path and are variables in time, the area coverage rate (ACR) is determined as integration of the covered area over the mission duration T:

$$ACR = \frac{1}{T} \cdot \int_0^T SW(t) \cdot V(t) dt \tag{2.18}$$

In the presented method, the ACR is only determined in the actual reconnaissance phases of the mission, thus during arrival and departure to the target area the value is set to 0.

E: required Energy

Often for mission evaluation, the used energy is evaluated together with ACR, where the latter one is divided by the required energy E. Thus UAS parameters such as camera resolution, propulsion, speed and flight altitude can be evaluated together and give a mission performance assessment. Another approach presented in this work is to introduce E and ACR into the metric separately from each other. The reason for that is the possibility to give the energy factor a separate importance weight for those type of UAS civil missions where it is necessary. In its physical form the energy is calculated as:

$$E = P \cdot t = F \cdot V \cdot t \tag{2.19}$$

where P is the power in [W], which can be determined as multiplication of required thrust F in [N] and velocity in [m/s]. Since F and V are variables of time the required energy for a mission is determined as:

$$E = \int_0^T F(t) \cdot V(t) dt \tag{2.20}$$

Here, the efficiency of thrust generators (propellers, turbines) or other drive components (motors, silencers, power electronics) are not taken into account for reasons of simplicity. In the presented work, a simple rubber method for propulsion sizing of a combustion engine is used. The required energy in this case is measured as used fuel. In the model a simple method for electric motor calculation is implemented as well. In this case the required energy for a mission is measured as a electrical power. Thus, different drive concepts such as electrical versus combustion engines or different sized aircraft can be compared directly.

Pd: Probability of object detection

Probability of object detection P_d is calculated according to the Johnson Criteria $P(N)$, see Eq. (2.10), and the detection factor f_d:

$$P_d = P(N) \cdot f_d(t_{det}) \tag{2.21}$$

where t_{det} is the time the object was in the camera's field of view. The detection factor defines the probability that an objects can be detected by an operator based on the time being in the field of view. Considering that in average a human needs 0.25 s to notice visual changes (Jain et al. 2015), it is assumed that to detect and identify an object of interest on the screen an operator needs 2 seconds. It is further assumed that in the range between 0 and 2 seconds the probability rises linearly and after being for 2 seconds in the field of view the operator will detect an object with the probability of 70%. Afterwards it is rising further linearly and achieves 100% at a time of 10 s. The dependence of detection factor and detection time is depicted in Figure 2.13.

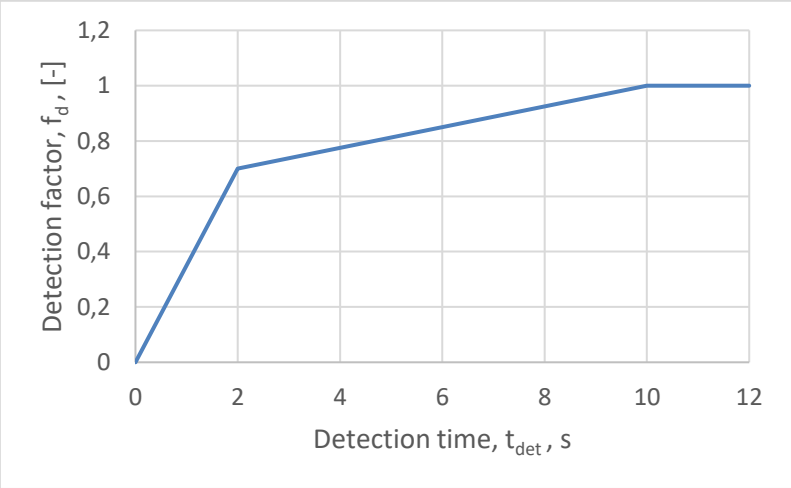

Figure 2.13: Dependence of detection factor and detection time (Fokina et al. 2018c)

CA: Communication Abilities

The introduced Communication Abilities (CA) parameter provides the information about time of communication losses:

$$CA = \frac{Tm - Tcl}{Tm} \tag{2.22}$$

where Tm is the mission time and Tcl is the time during the UAS was not within the VLOS due to landscape shadowing. The latter is obtained from the visualized operational environment since it is possible to detect interruptions of the visual line between the UAS and ground control station during the simulation. In addition, it can be checked whether the required amount of data can be stored on board during the losses or if an addition storage is necessary, see Section 2.2.2. In case if the UAS provides a buffer and a higher communication bandwidth it will allow to compensate the drop out. On the other side, it results in a high weight and high fuel consumption.

UOI: User Operating Issues

The User Operating Issues (UOI) parameter is introduced as an example of additional possible mission performance evaluation parameter. It considers information about launch/landing options based on the system weight, how easy it is to use the system, if it needs any special handling or storage facilities and how environmental sensitive the systems is. It can be represented in form of a scalar value within the range from 0 to 1, for example, for an agriculture application where issues as robustness, hand-launched and belly-landed, sensitivity to environment conditions and of course easy operation plays a role. For that, an additional metric has to be done, for example as Table, where each parameters become its weight in the range from 0 to 1. The UOI parameter is not considered in detail in the application studies presented in this work.

Weighting coefficients

Assignment of weighting coefficients is a complicated part of the MPI definition. Despite the fact that there are many methods for weight assignment, it is still a subjective process. Based on engineering insight and experience it has to be adjusted to every mission case by the design engineer individually. For example, for mapping task such as crop performance, surveying of a construction site, environment monitoring, aerial photography and etc. important parameters are coverage area, quality of gathered data, cost, and noise. Pipelines monitoring, traffic control, border patrol, wildlife monitoring, search and rescue missions, fishery protection, forestry monitoring can be attributed to search and rescue type of UAS missions. For these tasks in addition to coverage area and data quality, evaluation parameters like objects of interest detection probability, flight time to the search area, searching time and communication capabilities have to be taken into account during the mission evaluation process.

Weighting coefficient determine how a certain attribute influences the mission success. The higher the weighting coefficient the more important the certain parameter is. One of the widely used approaches for weighting assignment is called Analytic Hierarchy Process (AHP) and is represented by a weight decision matrix (Saaty 1990). Each criterion is weighted relative to all others with an importance index.

Based on these values a matrix of weights is obtained. Another method called Multi-criterion Analysis of Preferences by means of Pairwise Actions and Criterion comparisons (MAPPAC) (Matarazzo 1986) reduces the large number of ranking decisions by the decision maker. Each criteria is expressed as “poor”, “medium”, and “good”. Then the criteria are pairwise compared and ranked. The Rank-Order Centroid technique (Hutton Barron 1992) ranks the criteria from most important to least important and the weights are calculated based on a certain formula. Other ranking methods are presented in (Buede 2016).

In the presented work, the weighting coefficients are assigned just based on the initial requirements and an engineering experience as the goal of the application cases presented in Section 4 is to prove the UAS optimization process method.

2.5 Mission planning for the UAS mission simulation

Mission planning is an important part for the UAS mission simulation as it affects directly the sensor and communication performances. In the presented work mission planning consists of a calculation of a flight pattern for a desired mission area and for the specific mission sensor. It also takes into account the terrain shape. The following input parameters are used for flight path calculations:

- Desired overlap between flight laps;
- Desired GSD;
- Mission sensor;
- Pattern type.

After calculating the flight path for the mission it is simulated in the operation environment taking the terrain shape in the mission area into account. The following parameters are then obtained from the visualization environment and are used for further mission assessment:

- Sensor ground swath width at each mission time point;
- Area coverage and gaps;
- Detection probabilities of a certain object;
- Communication losses with the ground control station;

In addition, the required fuel and mission time parameters are calculated during the mission simulation.

The correct chose of the mission flight path influences mission performance parameters. In the next subsection, typical flight patterns and the calculation of the flight altitude as well as a general simulation model are presented.

2.5.1 Flight simulation model

A flight simulation model of an UAS is required in order to simulate a motion of the designed UAS, to calculate the trajectory and to assess mission parameters. In case when the flight simulation model is implemented into the visualized operational environment, one can evaluate the sensors and communication performances as well.

In the presented design approach, the flight simulation model is implemented in the MATLAB Simulink environment. In order to describe the dynamics of a fixed-wing UAS, the linearized equations of motion in polar coordinate form of a conventional aircraft are used:

$$\dot{V} = \frac{T - D}{m} - 9.81 \cdot \sin\gamma \tag{2.23}$$

$$\dot{\chi} = \frac{L \cdot \sin\mu}{m \cdot V \cdot \cos\gamma} \tag{2.24}$$

$$\dot{\gamma} = \frac{L \cdot \cos\mu}{V \cdot m} - \frac{9.81 \cdot cos\,\gamma}{V} \tag{2.25}$$

where $\dot{V}$ is kinematic acceleration, $\dot{\chi}$ is kinematic azimuth rate, $\dot{\gamma}$ is kinematic climb rate, γ is kinematic climb angle and μ is kinematic bank angle. D is aerodynamic drag force (2.27) and L is lift force (2.26). Both forces depend on the kinematic velocity V and air density ρ, which depends on the flight altitude h. Thrust T (2.28) depends on type of propulsion system, flight speed and flight altitude. The dependency on the thrust lever setting δ_T is realized in the simulation model as a thrust map calculated for each position of δ_T from 0 to 1 with the step of 0.01.

$$L = \frac{1}{2} \cdot \rho \cdot V^2 \cdot C_L \cdot S \tag{2.26}$$

$$D = \frac{1}{2} \cdot \rho \cdot V^2 \cdot C_D \cdot S \tag{2.27}$$

$$T = T_{ref} \cdot \left(\frac{V}{V_{ref}}\right)^{\eta_V} \cdot \left(\frac{\rho}{\rho_{ref}}\right)^{\eta_\rho} \tag{2.28}$$

Lift (C_L) and drag (C_D) coefficients depend on flight altitude h and aerodynamic angle of attack α for a given flight speed V. These coefficients can be derived from the trimmed aerodynamic polar as it is presented in (Feger et al. 2018). The coefficient η_V describes the dependency of the velocity for the thrust calculation and is $\eta_V = -1$ for a conventional piston engine with a propeller and $\eta_V = 0$ for a turbojet engine in the subsonic area. The coefficient η_ρ describes the influence of the altitude on the thrust and is $\eta_\rho = 0.7 - 0.8$ for altitudes below 11 km and $\eta_\rho = 1$ for an altitude between 11 and 20 km (Holzapfel 2017). T_{ref}, V_{ref}, ρ_{ref} are reference values defined by the engine manufacturer.

After the integration of equations (2.23) – (2.25) and neglecting the wind influence, the aircraft velocity is obtained in a north-east-down coordinate frame.

Attitude angles are simplified due to wind and sideslip neglecting:

$$\Psi = \chi \tag{2.29}$$

$$\theta = \alpha + \gamma \tag{2.30}$$

$$\Phi = \mu \tag{2.31}$$

Where Ψ is heading angle, θ is pitch attitude angle, Φ is bank angle.

In order to describe the position of the UAV in the environment, the world geodetic system WGS84 is used. By integrating the position differential equations, the UAV position at each time step is calculated:

$$\dot{\lambda} = \frac{V \cdot \sin\chi \cdot \cos\gamma}{(N_\mu + h) \cdot \cos\gamma} \tag{2.32}$$

$$\dot{\phi} = \frac{V \cdot \cos\chi \cdot \cos\gamma}{M_\mu + h} \tag{2.33}$$

$$\dot{h} = V \cdot sin\,\gamma \tag{2.34}$$

where λ is geodetic latitude and ϕ is geodetic longitude. According to WGS84, N_μ is the curvature radius of the earth ellipsoid main vertical axis and M_μ is the meridian curvature radius:

$$N_\mu = \frac{a}{\sqrt{1 - e^2 \cdot sin^2\mu}} \tag{2.35}$$

$$M_\mu = N_\mu \cdot \frac{1 - e^2}{1 - e^2 sin^2\mu} \tag{2.36}$$

Eccentricity e and flattening f are defined as:

$$e = 2f - f^2 \tag{2.37}$$

$$f = \frac{a - b}{a} \tag{2.38}$$

where $a = 6378137\,m$ is the length of the reference ellipsoids semi major axis and $b = 6356752.3142\,m$ is the length of the semi minor axis.

In the flight simulation model, the following assumptions have been made for aircraft performance calculations:

- Wind is not take into account;
- Consideration of a flat and not-rotated earth;
- Rotational dynamics are neglected;
- Small angle of attack α and zero sideslip β;
- Control through angle of attack α, roll angle μ and throttle setting δ_T.

2.5.2 Flight path planning

Flight path planning considers the speed and image quality requirements, terrain shape in the mission area and type of a flight pattern. The terrain shape especially with high gradients put limitations on:

- Sensor performance: the altitude has to be adjusted in such a way, that everywhere the desired image ground quality is achieved. For that, the flight altitude is optimized within the altitude range based on acceptable and unacceptable GSD values.
- Communication performance: LOS communication can be interrupted by terrain and losses might occur. For that either the flight altitude has to be increased or an additional equipment for buffer storage is then required onboard.
- UAV performance: additional climb performance and therefore thrust performance might be required.

This issues are taken into account in the presented approach for the flight path calculation. The details of flight path definition and optimization are presented in the next Subsections.

2.5.2.1 Flight patterns

Area coverage is one of the key performance parameters for civil missions. In order to cover the whole area of interest during the mission, the flight path has to be planned according to the sensor parameters. Based on it, the overlap between path lines, flight altitude and required speed have to be defined. Furthermore, mission requirements such as time, required quality of collected data and transmission requirements affect the chosen flight pattern and waypoints definition.

According to Kingston (Kingston et al. 2016) basic UAV tasks for civil mission requirements are the following:

- Point inspect task: based on the need to observe an object of interest at a known position and at a certain viewing angle;
- Line search task: based on the need to observe objects that can be modeled as lines – e.g., roads or area perimeters;
- Area search task: based on the need to observe an entire region of interest.

Based on the mission initial requirements and task type it can be fulfilled with different flight paths: line, lane, spiral or sector.

An example of the lane pattern is presented in Figure 2.14. This pattern can be also called lawnmower, line, raster, parallel and creeping lines. Lane pattern can be applied for survey of any area, but is especially effective at large search areas as with long strait lines and few turns the UAV can fly at a higher speed.

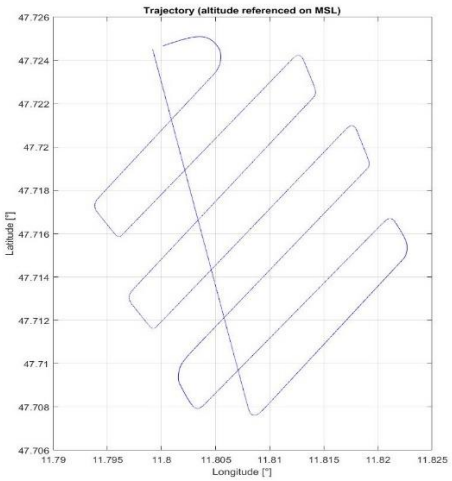

Figure 2.14: Example of a lane flight pattern

Figure 2.15 presents examples of spiral flight pattern. The usage of this flight path is based on the need to search for an object or a person from the last known location. The flight path starts at the last known location of the search object, which is the center of the area to be covered. Depending on the number of waypoints per roundtrip, the flight pattern can have for example a shape of triangle (left picture) or hexagon (right picture). The more waypoints the rounder the path will look.

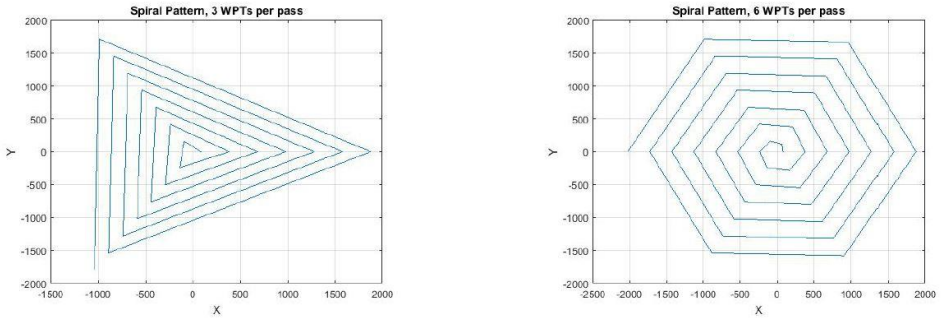

Figure 2.15: Examples of spiral flight patterns, graphs are unit less (de Serpa Marques e Braga Barbosa, Bernardo 2019)

The usage of sector pattern is based on the need to observe an object of interest from many different view angles or to observe a moving object that crosses the central point several times. For this pattern, the given area is defined by a circle, where the central point is an object that have to be observed and over flied several times. An example of a sector flight pattern is presented in Figure 2.16, where each pass consists of 3 waypoints. The number of passes is determined by the search area size.

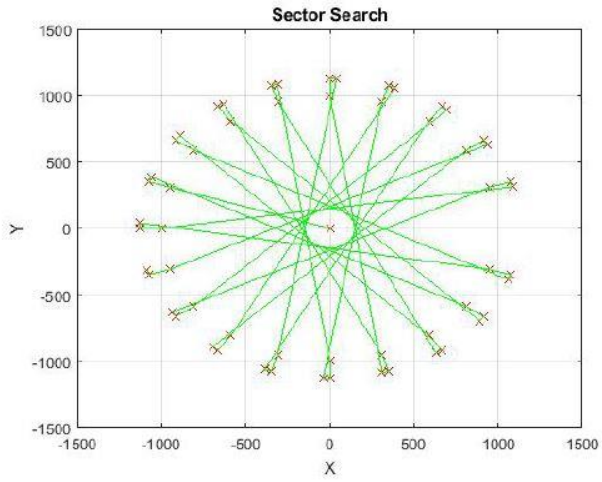

Figure 2.16: Example of sector flight pattern, graph is unit less (de Serpa Marques e Braga Barbosa, Bernardo 2019)

The patterns can be combined for flight path planning according to the mission complexity. The mission area can be divided into several subareas, where for each a different pattern has to be calculated. In the current approach during the mission planning one of the following patterns should be chosen: raster (lane), spiral or sector.

Flight patterns are defined in form of a set of GPS waypoints. Sensor camera characteristics and desired image quality influence the selection of overlap, flight altitude and airspeed. In order to calculate the waypoints, the following aspects have to be defined:

- Size and shape of the area of interest;
- Terrain elevation map of the area;
- Required ground sample distance for a desired image quality;
- Overlap between flight lines;
- Flight altitude;
- Airspeed during the mission.

However, there is no general agreement about which pattern is more appropriate for a certain mission. Therefore, it is necessary to simulate a mission with different flight patterns and parameters in order to find the one with best mission fulfilment.

In the presented work in order to calculate waypoints of a desired flight pattern, the mission area has to be defined as polygon in Google Earth and saved as a *.kml* file. This file is used in a MATLAB function *createMissionLARUS.m* in order to create a pattern with a set of waypoints. Each waypoint contains information about latitude, longitude, altitude in MSL and flight speed. In addition, there is a parameter called “sensor on”, which allows to avoid collecting data on the way from a starting point to the first waypoint of the survey area and on the way from the last point of the area to the end point

of the mission. Figure 2.17 presents an example of the mission area (in yellow) and the calculated flight pattern in Google Earth (in green).

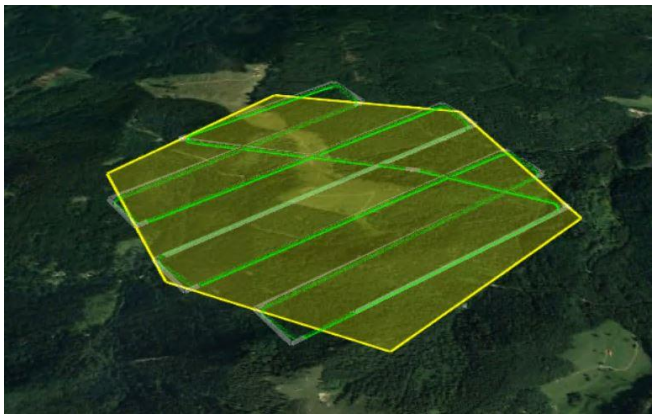

Figure 2.17: Example of a mission area and flight pattern definition

2.5.2.2 Flight altitude definition

For missions in areas where the terrain elevation has high gradients, the flight pattern has to be optimized in order to ensure that the obtained GSD is still acceptable, the coverage area has no gaps and that there is no collision between the trajectory and the landscape during the whole mission. Thus, for the flight path optimization the following aspects have to be considered:

- A flight path consists of a set of waypoints. The larger the distance between these points is, the less specific terrain landscape between these points is taken into account.
- The required (GSD_{req}) and inacceptable (GSD_{inacc}) ground sample distances define the minimum and maximum flight altitudes and in order to collect images with the desired quality the UAV has to fly within this region. These altitudes are calculated according to Eq. (2.39)-(2.40):

$$alt_{req} = \frac{H_{res} \cdot GSD_{req}}{2 \cdot tan \cdot \left(\frac{HFOV_{max}}{2}\right)} \tag{2.39}$$

$$alt_{max} = \frac{H_{res} \cdot GSD_{inacc}}{2 \cdot tan \cdot \left(\frac{HFOV_{max}}{2}\right)} \tag{2.40}$$

Where H_{res} is the number of pixels of the camera in horizontal plane and $HFOV_{max}$ is the maximum horizontal field of view of the camera. Required GSD (GSD_{req}) and inacceptable GSD (GSD_{inacc}) are defined by the user based on the object size that have to be observed. The lower GSD limit means that the resolution achieved on the ground is enough for 100% detection of the object of interest according to Johnson criteria. Further reduction of the GSD and therefore flight altitude, leads to smaller ground swath width and longer mission endurance.

The waypoints altitude can be defined in two possible ways in relation to mean sea level (MSL), see Figure 2.18:

a) As an addition of the target altitude based on required GSD (alt_{req}) and the highest ground elevation.

b) As an addition of the target altitude based on required GSD (alt_{req}) and the ground elevation of each waypoint.

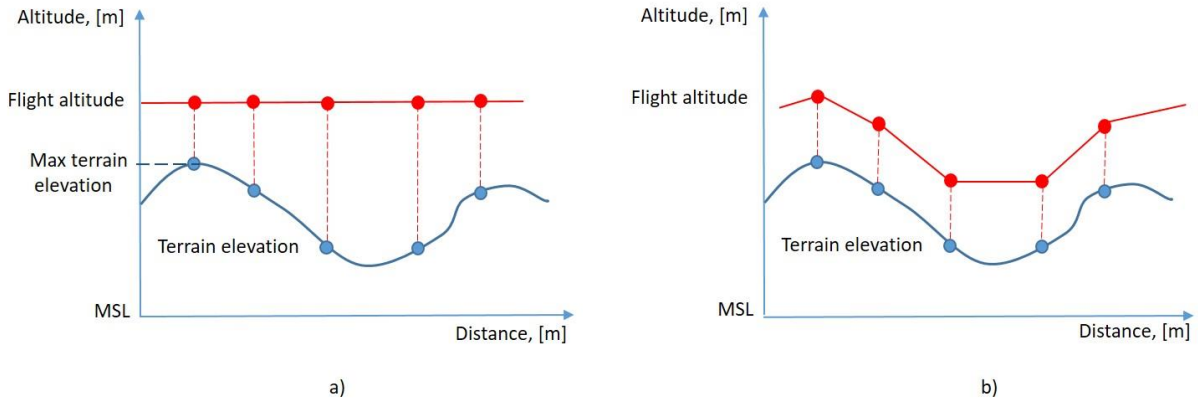

Figure 2.18: Waypoints altitude definition a) flight path altitude is constant and is based on the maximum elevation of the terrain b) terrain following flight path

In the first case, the flight altitude stays stable during the whole mission, which is an advantage for the aircraft performance as it will maintain the altitude. Nevertheless, it is necessary to ensure whether the whole area is covered without gaps as the ground swath varies during the mission performance.

In the second case, the flight altitude is changing which provides better coverage, however at the same time it is necessary to check whether the UAV provides sufficient climb performance as it has to follow to the shape of the terrain by climbing or descending.

2.5.2.3 Flight path optimization

For missions with a high landscape difference a flight pattern optimization algorithm for spiral and sector patterns (de Serpa Marques e Braga Barbosa, Bernardo 2019) is implemented into the presented UAS mission simulation environment.

During the flightpath generation the waypoint coordinates with ground elevation data and the flight altitude range are defined. The last one is calculated based on required and inacceptable ground sample distances, GSD_{req} and GSD_{inacc}, see Eq. (2.39)-(2.40). After that the optimization algorithm starts.

In the first step of the optimization the trajectory is shaped as it is represented in Figure 2.19. Waypoints are marked by numbers from 1 to 4. The goal of this optimization step is to relocate the waypoints into the desired GSD range which is marked with red and green lines. The flight altitude is set relative to MSL as a sum of the target altitude based on GSD_{req} and the highest ground elevation (on the discussed figure it is the waypoint 1) for all waypoints, see blue line on Figure 2.18 a). For the

waypoints which are located higher than the desired GSD region the altitude is set to maximum allowed based on GSD_{inacc} , (red line). If the altitude of a waypoint is lower than the trust region, then the altitude is set to target altitude (green line). The blue arrows represent the change in altitude for the points 2 and 3 by setting the altitude to maximum allowed GSD.

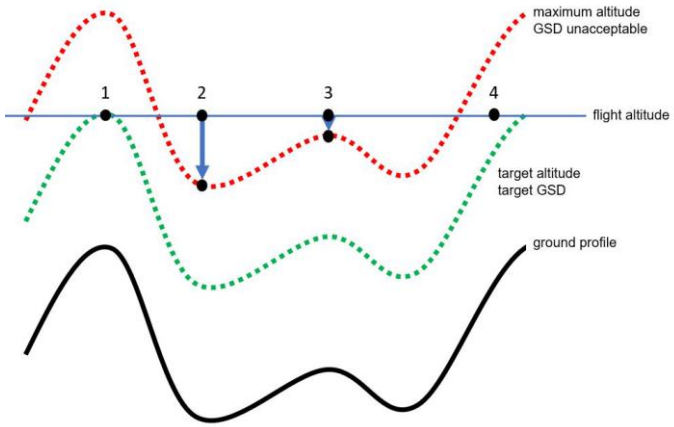

Figure 2.19: First step of the flight path optimization (de Serpa Marques e Braga Barbosa, Bernardo 2019)

However, the trajectory is not optimized yet since climb performance constraints of the UAS are not taken into account. The desired GSD region defined at the beginning gives the flexibility to create a trajectory where climb and descend distances between the waypoints can be minimized.

In the second step of the optimization, the required climb performance of the UAS is reduced by smoothing out the trajectory. For that, the altitude changes between the waypoints are minimized. It is checked whether it is possible to maintain the altitude between the two neighbor waypoints while staying inside the desired region. If this is possible then the altitude of the next waypoint is set to the same value as the previous one. If this is not possible, then for climbing the altitude of the next waypoint is set to the target altitude and for descending to the maximum altitude. Figure 2.20 presents the second step of the optimization. Waypoint 3 gets the altitude of waypoint 2 and waypoint 4 is set to the target altitude.

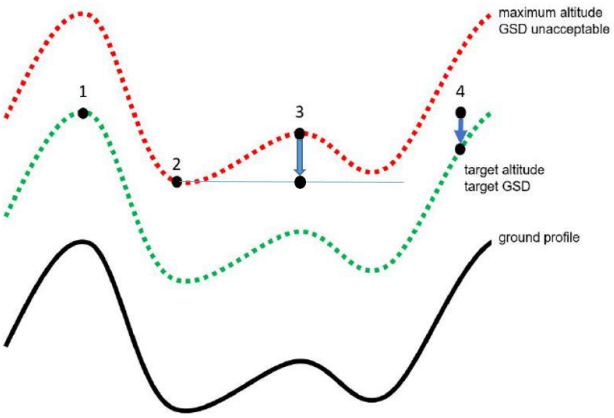

Figure 2.20: Second step of trajectory optimization (de Serpa Marques e Braga Barbosa, Bernardo 2019; modified)

In the third step of the optimization, the trajectory is further smoothed out by comparing altitudes of three neighbor waypoints. If in order to reach the waypoint $i + 2$ from the i waypoint a climb or a descend is necessary then the altitude of the point $i + 1$ is optimized according to one of the following approaches:

- Altitude of the waypoint $i + 1$ is set to the average altitude of waypoints i and $i + 2$ while maintaining GSD requirements. This case is presented in Figure 2.21 where the altitude of point 3 is set to the average altitude of points 2 and 4 in order to provide constant climbing between these three points.
- Otherwise, the altitude of waypoint $i + 1$ will be placed at maximum altitude for climbing or at target altitude for descending.

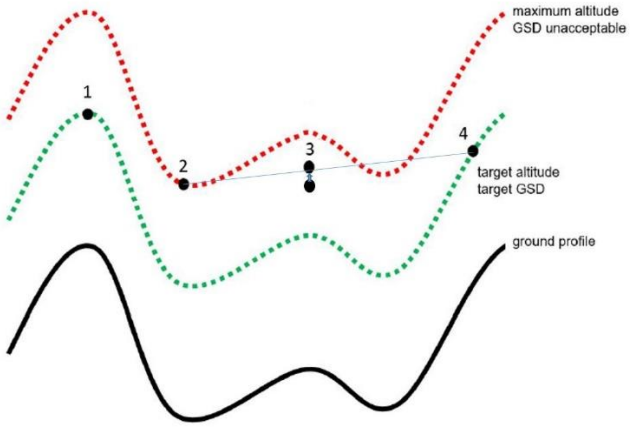

Figure 2.21: Third step of trajectory optimization (de Serpa Marques e Braga Barbosa, Bernardo 2019; modified)

One can see that due to the landscape shape the trajectory between waypoints 3 and 4 is higher than the maximum altitude. In order to avoid such situations, the number of waypoints for the generated flight path has to be increased.

The size of the desired GSD region is driven by the camera HFOV and horizontal resolution, see Eq. (2.39)-(2.40). The higher the resolution of the camera the larger the trust region and the bigger the ground coverage area. Thus the potential for the trajectory optimization is also higher. In contrast, the larger the HFOV of the camera the smaller the trust region. However, a smaller HFOV angle makes the ground swath width also smaller, which lead to more passes and a longer mission time. The influence of the altitude trajectory optimization on the mission performance is discussed in the UAS application case studies in Section 4 (Figure 4.37, Figure 4.38).

3 Mission simulation based design environment for UASs

In order to bring together mission requirements, aircraft design, payload, communication and other elements of an unmanned aerial system into a multidisciplinary design process the UAS design environment presented in this work is developed at the Institute of Aircraft Design. The UAS design loop includes the mission simulation and evaluation, which are programmed in MATLAB 2017a using the object oriented method. The visualized operational environment, which is the part of the UAS design loop, is programmed in Visual Studio 2013 using the OpenSceneGraph toolkit.

The UAS design environment is developed by Jens Feger (Feger et al. 2018). For the mission assessment a visualization environment is implemented into the design loop as well as additional functionalities for flight path planning and mission performance assessment. The interaction of the designed UAS with the environment as well as the sensor and communication performances are simulated and assessed in the visualized operational environment (Fokina et al. 2019). Owing to the elevation model and realistic representation of the terrain, the visualization environment provides information concerning sensor coverage area, probabilities of object detection, number of detected objects, slant range between the UAV and search objects, communication range, obstacles detection in the line-of-sight and time of communication losses. These information is used in the mission evaluation process and in the UAS design loop.

The visualized operational environment is based on the software osgVisual developed at the Institute of Flight System Dynamics at TU Munich (Dannhauer 2009; Hochstrasser 2012), which was updated with a set of new functions in order to be able to simulate the interactions between the UAV and other systems of an UAS. This allow to assess sensor and communication performances in correlation with the mission terrain area.

3.1 Overall description

3.1.1 Structure

The structure of the presented mission simulation based UAS design environment is presented in Figure 3.1. It consists of the following main parts:

- Initial mission requirements and mission definition
- UAS design
- UAS mission simulation and evaluation
- Visualized Operation Environment
- Optimization of the UAS design

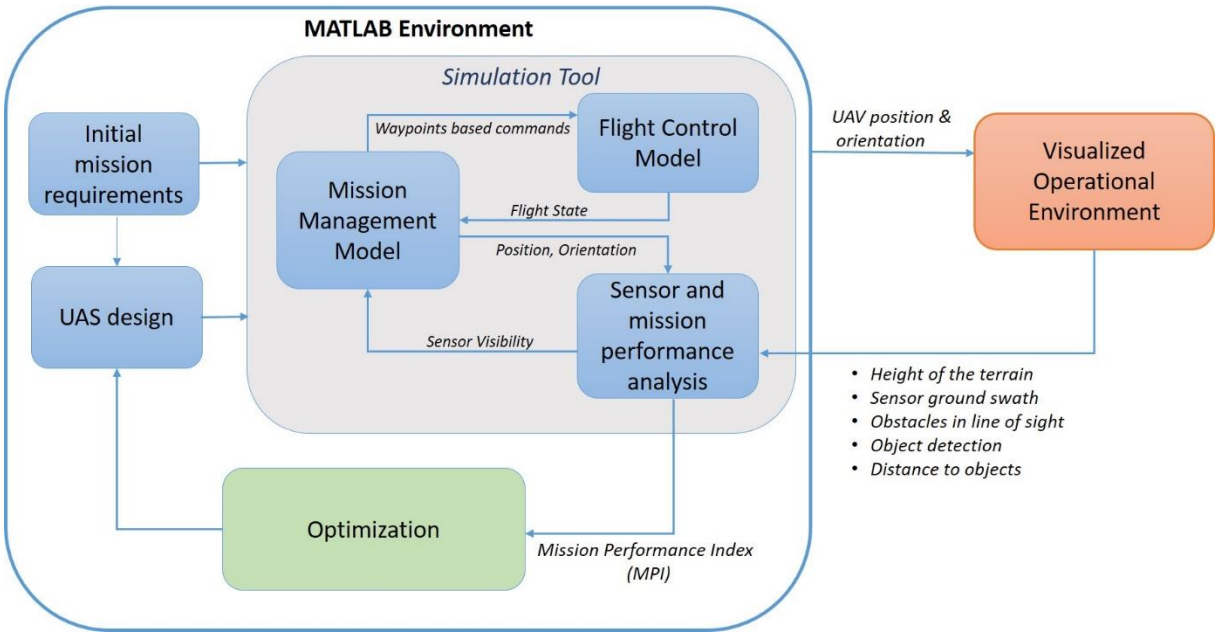

Figure 3.1: Structure of UAS mission simulation and evaluation environment (Fokina et al. 2018c)

All elements of the presented design environment except the visualization part are programmed in MATLAB and MATLAB Simulink environments (version R2017a) using the object oriented approach. As the design environment is modular it can be extended with new functionalities or some parts can be exchanged by another. The visualization part is written in C++ based on OpenSceneGraph Toolkit. In order to transfer the data between those parts the User Datagram Protocol (UDP) is used. With it different computer applications can send data to other hosts on an Internet Protocol (IP) network or within the same computer to other applications. Thus, the single parts of the UAS mission design environment can be split on different computer and different programs can exchange their data.

The UAS design process starts with the definition of objective function, constraints and design variables. In the presented work the following design parameters are taken: wing area, aspect ratio, design speed and camera index. The last one is a scalar variable representing an index of a mission sensor taken out from the list of possible sensors for the mission. In the presented in Section 4 application studies the mission sensor is represented by an optical camera. The following camera parameters are taken into account in the design process: resolution, VFOV and HVOF, frame rate and weight. The objective function of the UAS optimization is to maximize the MPI, which defines the mission performance success. Minimum stall speed is taken as constraint. These parameters are defined in *OptimizeConfigurationLARUS.m* and *objectiveFunctionLARUS.m* files.

The next step is to define initial mission requirements, mission area, UAS elements and a list of sensors for the mission. Initial settings are set in MATLAB within the configuration m-file called *initConfiguration.m*. The mission area is defined in Google Earth tool in order to calculate in MATLAB the desired flight path based on waypoints. Initial settings for flight path planning are defined in *createMission.m* file.

After the definition of the input data the process of UAS mission based design starts. An initial set (population) of UAS designs is generated from randomized values of the design variables. For each UAS

design (individual) a conceptual UAV design is carried out. The details of aircraft sizing method are presented in (Feger et al. 2018). Each of these UAS designs is then simulated in the mission simulation model in MATLAB Simulink and the visualized operational environment. The latter provides data for the further mission assessment of each individual in the sensor and mission performance analysis block. The following data are obtained during the mission simulation at each time step:

- Height of the terrain;
- Sensor ground swath;
- Obstacles in communication LOS;
- Object detection in the sensor FOV;
- Presence time of object in the sensor FOV;
- Distance between moving objects (e.g. UAV and object of interest).

Based on this data for each UAS design a MPI is calculated. The reference values for MPI elements are the average values of the 1st generation. These values are used for the next generations as well. All individuals are ranked by their mission performance indices and fulfilment of constraint functions. After the simulation and assessment of initial UAS designs (of the first generation) the next generation is created by using the methods of randomized recombination, mutation and preserving the best individuals of the parent generation.

In order to achieve an optimal UAS design, these processes are repeated until convergence so that an UAS tailored to the specified mission is designed. For that the following parameters have to be set in the *optimizeConfiguration.m* file:

- Ranges of design variables;
- Constraints definition;
- Population size and number of generations.

The process is convergent if after the evaluation of the population of the last generation the value of MPI does not changes. If that is not the case then numbers of generations and population has to be increased.

3.1.2 Mission simulation environment in MATLAB

The mission simulation and evaluation environment developed in MATLAB Simulink is a modular environment (Feger 2015; Feger et al. 2018) divided into functional blocks, which enable to simulate different missions and different subsystems of an UAS. It is implemented as a control flow model and consists of three major components: Mission Management Model, Flight Control Model and block for sensor and mission performance analysis. The architecture of the mission simulation environment in MATLAB is depicted in Figure 3.2.

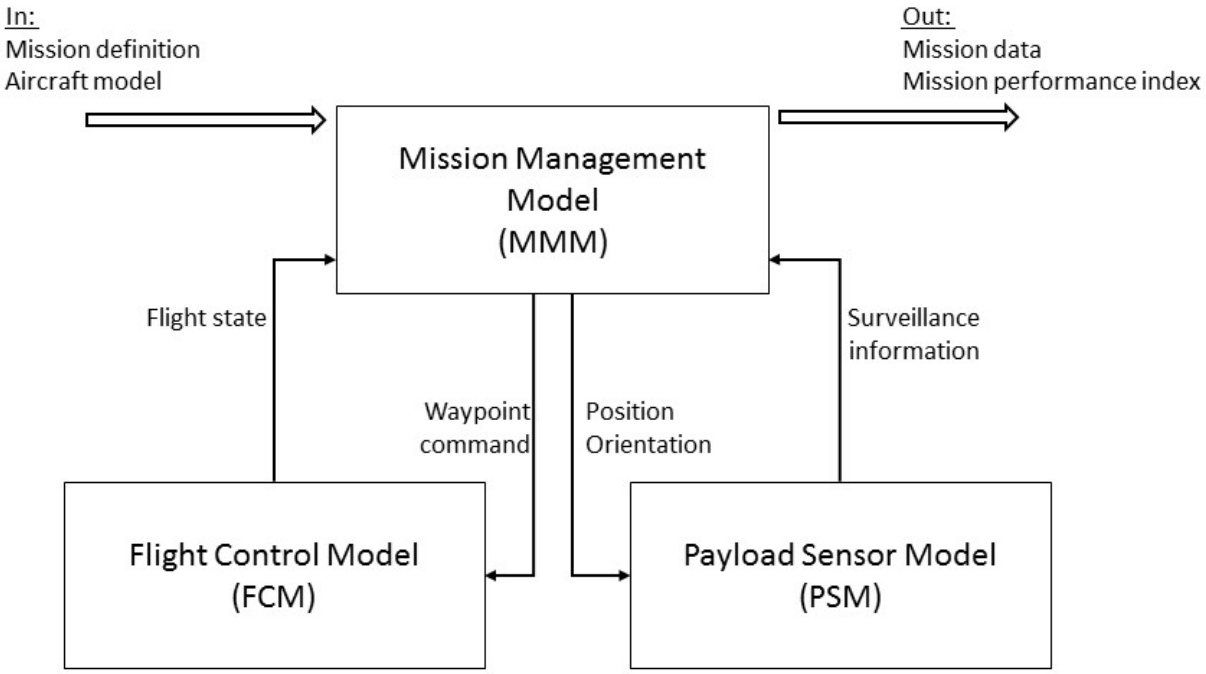

Figure 3.2: Architecture of mission simulation block (Feger et al. 2018)

The **Mission Management Model** is the central control element of the simulation model. It generates waypoint navigation commands, distributes flight state information and stores simulations results to the aircraft data model for further evaluation. In this block the selection of data to be provided for processing after the execution of the simulation model is also performed. Mission definition and aircraft model defined at the beginning are used as input data.

Mission definition data contain information about:

- Calculated flight path waypoints: reference altitude, latitude, longitude, altitude, elevation, initial heading angle, initial course angle, waypoint offset and design speed.
- Mission objective: target location, altitude reference, target dimension, reference values for detection/recognition/identification, GSD required, GSD inacceptable and image overlap.
- General: controller gains, time step, sample time and simulation pace.

The aircraft model contain the following data:

- Wing geometry data, area, span, aspect ratio and mass.
- Fuselage/horizontal tail/vertical tail: geometry and mass.
- Trimmed aerodynamic polar data: mass, reference area, polar alpha, polar altitude, polar Cl and polar CD.
- Propulsion system: mass, thrust map (thrust, altitutde, speed, throttle setting), power, max RPM, size and fuel tank (mass empty, fuel mass, size, mass).

- Other system elements: size, mass and other specific parameters such as sensor HFOV, VFOV and resolution.
- Overall mass.

The simulation results are represented by mission data and mission performance index. Mission data contain data for a discrete time calculated waypoint based flight path and mission results data. At each trajectory point the following data are calculated:

- Position in WGS84 coordinates as latitude, longitude and altitude;
- The Euler's position angles Ψ, θ, Φ;
- Speed in form of absolute value V, course angle χ and climb angle ϒ;
- Propulsion data: thrust setting, mass, fuel flow and used fuel;
- Total distance and mission flight time.

Mission result data contain:

- Mission performance index MPI and its elements: area coverage rate, mision time, required energy, detection probability and time of communication losses;
- Detection/ recognition/ identification probabilities of objects of interest at each time step, slant ranges and view angles from the UAV to the objects of interest;
- Actual GSD, swath width at each time step;
- Height of the terrain and height above the terrain at each time step.

The **Flight Control Model** estimates the vehicle current flight state at each time step. It calculates aerodynamic and propulsion forces and integrates the linearized equations of motion, see Eq. (2.23) - (2.25) and Figure 3.3.

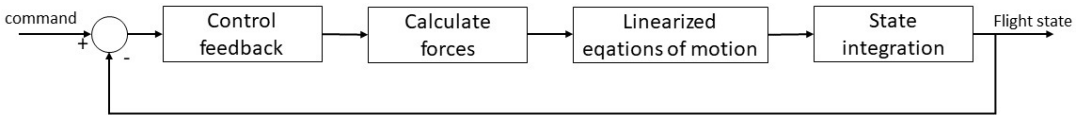

Figure 3.3: Working scheme of flight control model (Feger et al. 2018)

The flight control model receives coordinates of the next waypoint and the desired speed as input commands. The details of the flight control model are presented in Feger et al. 2018. The results of the flight simulation model are presented by vectors of data for each sample time point with the following information:

- Position in latitude, longitude and altitude in WGS84 coordinates;
- Kinematic velocity with speed, course angle and climb angle in North-East-Down coordinates;

- Attitude angles with heading, pitch and roll attitude;
- Current control variable settings (angle of attack, bank angle, thrust lever setting);
- For combustion engine: mass, used fuel mass and fuel flow;
- For electric propulsion system: used energy.

In the **Payload Sensor Model** the data exchange between the Simulink model and visualization environment is established, the sensor performance is evaluated and the mission performance index is calculated. For that the UAV flight state data are sent to the visualized operational environment, where the exact location of the UAS elements in the operational environment is simulated. In case when the sensor field of view is controlled by an operator (by a joystick in MATLAB Simulink) its coordinates are also sent to the visualization environment. The output data from the visualized environment are:

- Sensor ground swath width;
- Obstacles in LOS between the UAV and the ground control station;
- Distances and view angles to the objects of interest/ targets;
- Time slots when objects of interest are in the sensor FOV;
- Height of the terrain and height above the terrain,

Based on these data the MPI is calculated.

3.2 Visualization environment

The goal of the visualization environment is to simulate the operational environment and to evaluate sensor and communication performances taking into account the landscape of the mission area. The visualized operational environment is implemented into the mission based UAS design loop and provides it with data for the mission performance assessment: sensor swath width, area coverage, detection probabilities of objects and obstacles in LOS.

3.2.1 Targeted functionalities and state of the art

In order to simulate and evaluate sensors and communication performance in the operational environment, a special graphical tool is required, which fulfils the following requirements:

- High-resolution texture data and elevation based terrain data: to simulate the operational environment; to calculate intersections between simulated sensor field of view and terrain; to calculate height above terrain and height above mean sea level; to detect whether the calculated trajectory is colliding with the landscape or scenery objects.

- Geometry representation and geospatial simulation of the UAS in the visualized operational environment: to simulate the mission flight of a UAS in the mission area and motion of other elements of the system.
- Possibility to load and position new aircrafts models with different sensors onboard designed by the UAS design tool and other 3D objects in order to simulate UAS mission. For that a geometry representation of UAS elements is required.
- Simulation of sensor field of view and its intersections with the terrain in order to obtain at each time step of the mission simulation: sensor swath width on the ground, area coverage and gaps in it, information when an object of interest is in the field of view and for how long.
- Calculation of intersections between the geometry representation of the UAS elements and terrain. It allows to calculate sensor ground swath width, area coverage, losses of LOS and flightpath collision with terrain.
- MATLAB compatibility: as UAV design, mission simulation and evaluation tools are developed in MATLAB. The visualized operational environment have to be compatible with MATLAB, as input and output data are processed in MATLAB.
- Open source tool: in order to connect the visualization environment with the existing tools used at the Institute of Aircraft Design, TUM, and to extend the visualization tool with additional functionalities depending on mission scenario and requirements.

Table 3.1 presents an overview of other visualization tools, stated to the start time of this project. The most popular flight simulators Flight Gear, X-Plane and Microsoft Flight Simulator have a realistic environment representation and offer accurate flight dynamic models. However, it is not possible to modify X-Plane and Microsoft Flight Simulator for the UAS design needs as they are not open source codes. In Microsoft Flight Simulator it is also not possible to load new designed aircraft models. Flight Gear is an open source project and modifications are possible. It is also possible to load customized aircrafts. However, in none of these flight simulators it is possible to add additional graphic into the scenery for sensor field of view representation in order to simulate the ground trail and to obtain intersection points of it with the terrain.

Quite often research groups use rendering engines such as the high performance and open source 3D toolkit OpenSceneGraph for visual simulation, virtual reality and scientific visualization (Bertuccelli et al. 2009, Perez et al. 2013). For example, in the Australian Centre for Field Robotics, University of Sydney, the visualization environment for sensor performance analysis is developed. It allows to simulate the field of view of the sensor and to assess area coverage (Göktogan et al. 2005). However, to our knowledge it is not an open source project and it is also not possible to process data from the visualized operational environment for external usage such as mission performance evaluation block in the UAS design loop.

There are also available commercial software for sensor and communication performance evaluation in the visualized operational environment. For example UgCS software developed by SPH Engineering (SPH Engineering 2020). It uses an elevation based terrain landscape for mission planning and UAS performance simulation with the possibility to:

- automatically calculate key variables such as the course heading and track spacing necessary to provide the prescribed coverage area for a search target based on the initial flight altitude;
- create an user defined search area with selected sensor and flight altitude;
- calculate and visualize different flight paths that covers the specified area with no gaps and specified camera footprint;
- etc.

However, this very powerful visualization software is developed for mission planning purposes and it is not considered in it to load new designed aircrafts and sensors. Such commercial software are not open sources as well.

Despite the fact that there are several tools available with possibility to simulate UAS and its elements in the visualized operational environment, including simulation of the sensor field of view, the only one fulfiled all listed above requirements is the tool osgVisual (Dannhauer 2009; Hochstrasser 2012). It is based on OpenSceneGraph and using its functionalities it is possible to implement rendering functions for sensor field of view visualization and to simulate its motion together with the motion of the UAV. It also provides functionalities for calculation of intersection points between the graphical representation of UAS elements and terrain. Basic functionalities of osgVisual provides with the geospatial UAS simulation, where new aircraft models and sensors can be loaded.

Table 3.1: Overview of visualization tools with regard to targeted functionalities

Requirements	FlightGear	X-Plane	Microsoft Flight Simulator	osgVisual/NG	Other tools based on OSG	UgCS by SPH Engineering
High resolution texture data and elevation model based landscape	✓	✓	✓	✓	✓	✓
Geospatial simulation of UAS	✓	✓	✓	✓	✓	✓
Possibility to load and position new aircrafts	✓	✓ using additional Plug-Ins	–	•	• code extensions are required	–
Simulation of sensor field of view and other objects	–	–	–	✓	✓	✓
Calculation of intersections with terrain	–	–	–	✓	✓	–
Compatibility with MATLAB	✓	✓	✓	✓	✓	✓
Functional extension / Open source	✓	–	–	✓	–	–

3.2.2 Architecture of the visualization environment

The visualization part of the UAS mission based design process simulates the operational environment where the UAS performs a mission. As the basis for the development of the presented visualization part the high-definition environment for spatial display of aircrafts osgVisual (Dannhauer 2009) and its enhanced version osgVisualNG (Hochstrasser 2012) were taken. They have been developed at the Institute of Flight System Dynamics at the Technical University of Munich, Germany. Both are based on the OpenSceneGraph (OpenSceneGraph 2020) rendering engine and on a special real-time simulation environment written in C++.

Figure 3.4 presents the structure of the visualization environment. Models of airplanes and sensors, terrain and other objects are imported via an XML configuration file from MATLAB into the main body of the visualization environment. This is done in order to bypass changes in the code for every new UAS design. The aircraft model is calculated in MATLAB and transferred in STL format. Sensor model contains data of its location on the UAV, gimbal angle, FOV and resolution needed for its graphical representation in the scenery. Terrain data are obtained with the help of OSGEarth or Virtual Planet Builder tools (details in Hochstrasser 2012) and are loaded in .osgb format into the scenery. In the XML configuration file are defined the parameters of the user viewing positions on the UAV such as distance to the object and view angle.

There is an interface allowing the data exchange with MATLAB Simulink via freely definable channels using IP data protocol (UDP). Position coordinates and attitude obtained from the simulation model in MATLAB Simulink are applied directly to the aircraft model with the sensor onboard in the visualization environment at each time step. Information such as the height of the terrain, sensor ground swath width and etc. obtained in the visualization environment are sent back at each simulation time step to the Simulink model in MATLAB.

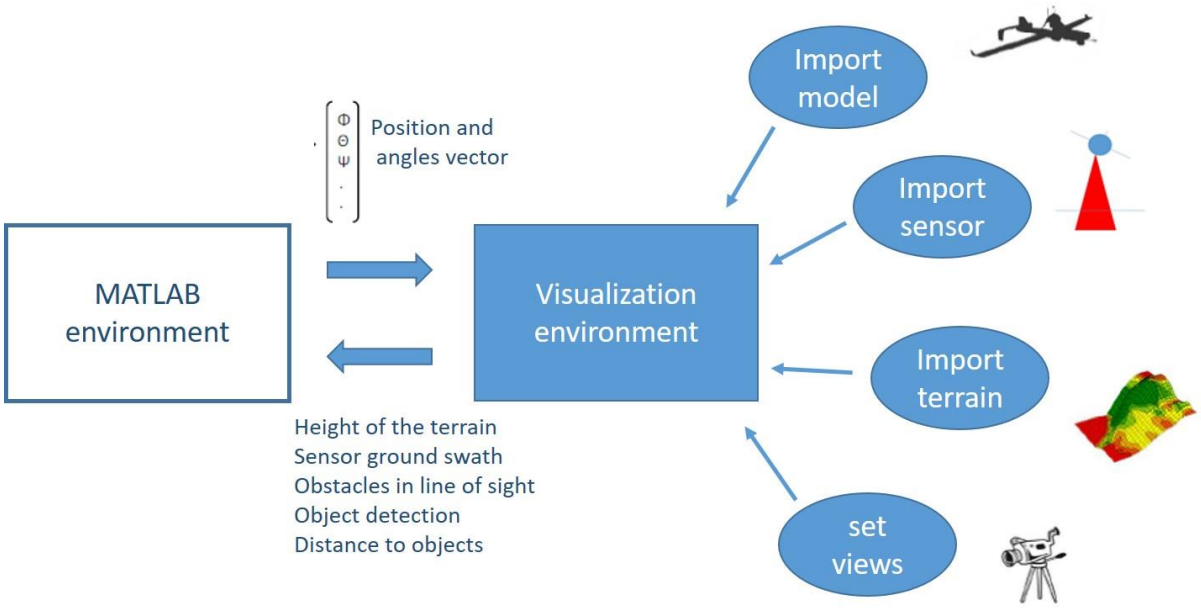

Figure 3.4: Structure of the visualization environment

OpenSceneGraph is a well-designed rendering application using a low-level OpenGL application. It concepts modularity and object-orientation. Based on this it allows to manage graphics primitives, materials and different visual data sets in user applications, saving much development time and allowing new functionalities to be combined as modules and plugins. OpenSceneGraph is based on the theory of scene graph, which records rendering commands and data in a buffer, for executing at some other time (OpenSceneGraph 2020). A data structure represented typically as a hierarchical graph is called scene graph. It defines the spatial and logical relationship of a graphical scene for efficient management and rendering of graphics data. Scene graph contains a top-level root node, a number of group nodes each of which can have any number of child nodes, and a set of leaf nodes.

Figure 3.5 illustrates the scene graph built in the visualized operational environment, which corresponds to the structure of the XML configuration file. The last one is created by the function *createVisualConfigOSG.m* for each new UAS design. The tree depicts main elements and nodes each of which has further sub-nodes responsible for transformations of the geometry. The scene graph is assembled in the function *VisualCore :: initialize()* and its sub-functions.

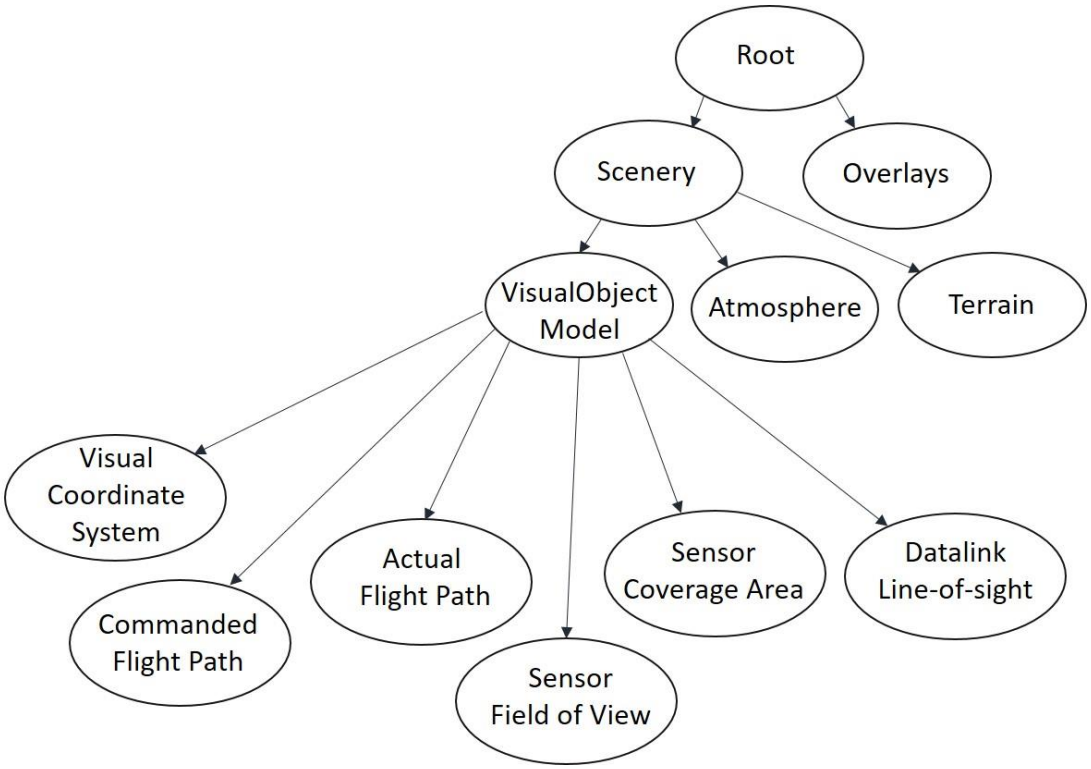

Figure 3.5: Scene graph of the visualized environment

The configuration of the visualized operational environment is done in an XML file. An example of a full configuration file is presented in A.1. The file consists of six sections: modules, viewing windows, overlays, atmosphere, terrain and models. A short example of the module specification is presented in Figure 3.6. The commercial software from Sundog-Soft (Sundog Software LLC) called “sky silverlining” represents a module, which allows to visualize atmosphere, clouds and weather. The module “dataio” allows bidirectional communication with external applications such as a parallel simulation in MATLAB Simulink via UDP. Using the module “model” an object can be positioned into

the scenery. There is a set of attributes in this module, in order to specify the positioned object, such as geometry file, position, orientation, updater and etc. More details about these settings can be found in (Hochstrasser 2012). The list of input and output signals between the visual environment and MATLAB is described and configured in a second XML file created by the function *createUDPConfigOSG.m* for each new UAS design. The detailed UDP configuration file is presented in A.2.

```
<!-- MODULE SECTION -->

<module name="sky_silverlining" enabled="true"></module>

<module name="dataio">
      <udp socket="vcl"
           filename="Protocol_osgVisual_inout.xml" />
</module>
```

Figure 3.6: Example of module specification in the configuration file (Hochstrasser 2012)

The basic elements of the scenery representation in the visualization environment are presented in Figure 3.7. The functionality presented in osgVisualNG includes:

- Aerial vehicle position and orientation control;
- Possibility to load and position additional 3D objects into the scenery;
- Several viewing positions und possibility to switch between them;
- Module for creating overlays;
- Atmosphere, cloud and weather module;
- Terrain module.

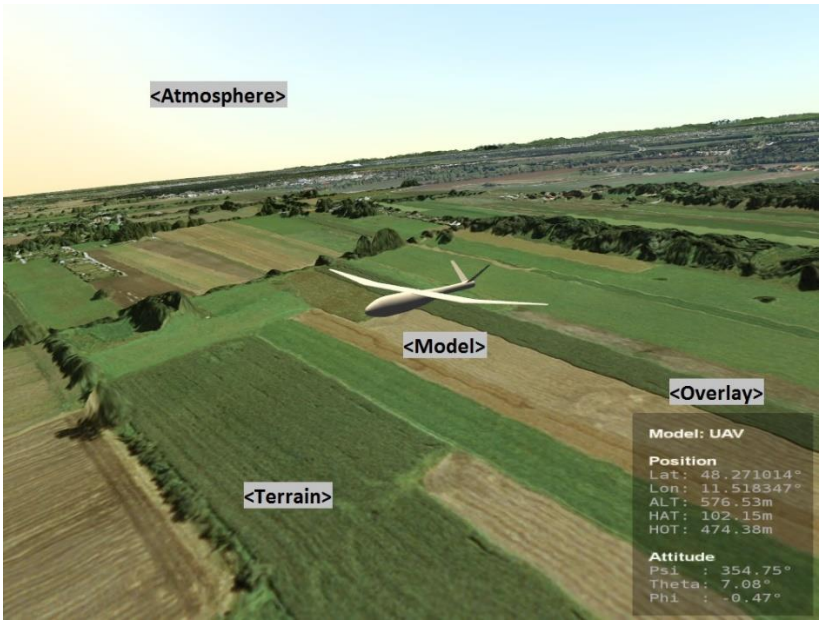

Figure 3.7: Basic elements of the scenery in the visualized operational environment

Other elements of the basic configuration are presented in Figure 3.8 (Hochstrasser 2012). With keys F1 up to F5 it is possible to switch between different user viewing positions. A different window configuration is presented in Figure 3.9. Here, it is possible to observe the model during the simulation from different viewpoints (observer camera positions) at the same time and to present additional simulation data in overlay windows.

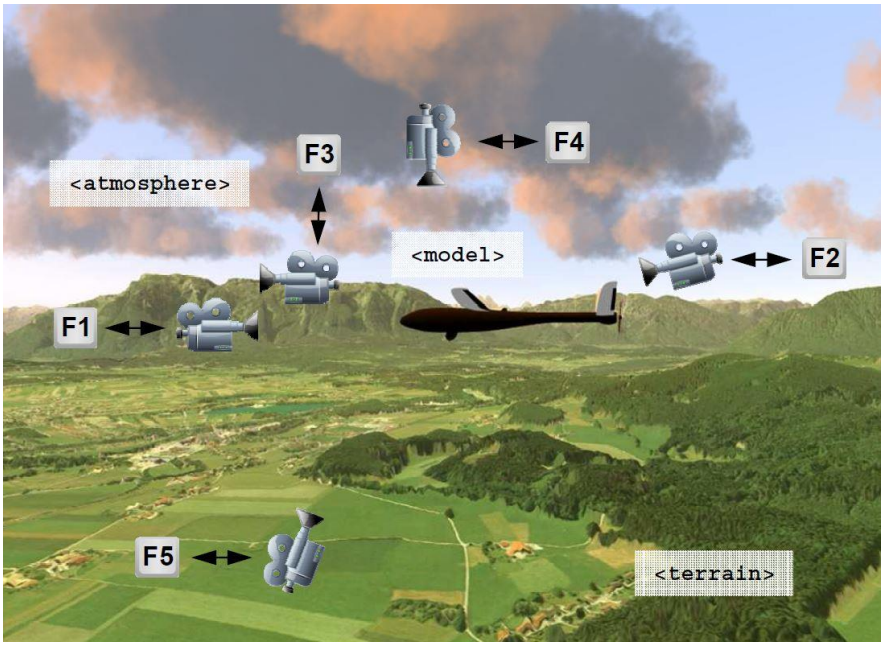

Figure 3.8: Main elements of the osgVisual NG configuration (Hochstrasser 2012)

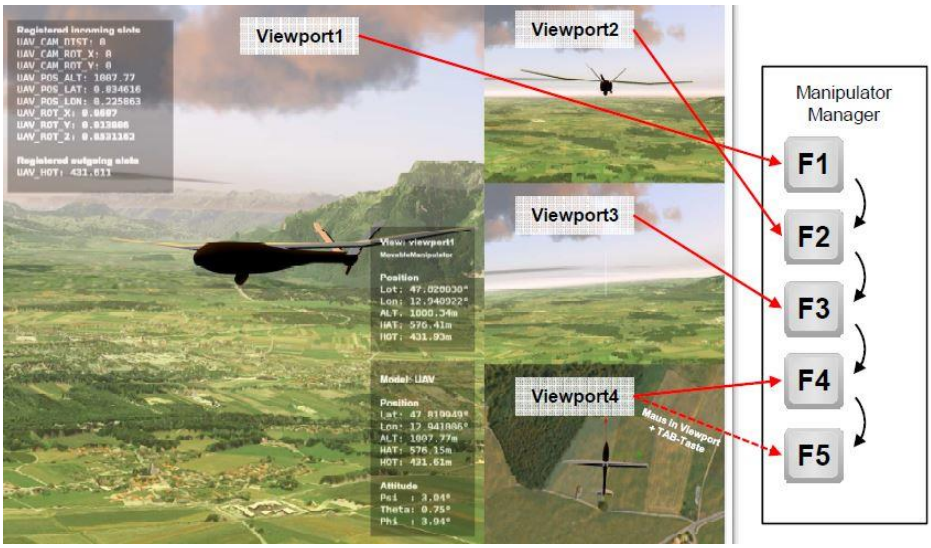

Figure 3.9: Window configuration in the visual environment (Hochstrasser 2012)

3.2.3 Sensor performance analysis

Key sensor performance parameters are sensor field of view, sensor ground swath width and pixel density on the ground. Simulation in the visualized operation environment allows to obtain the ground swath width taking into account the terrain elevation in the mission area and the angle of installation of the sensor on board or gimbal motion.

These issues are addressed in the visualization environment by the geometry representation of the sensor's FOV by a pyramidal shape (see Figure 3.10) and its intersection with other scenery objects. The size of the pyramid is determined by horizontal (HFOV) and vertical (VFOV) field of view angles of the sensor. The intersection area of the pyramid with the terrain represents the footprint of the sensor on the ground.

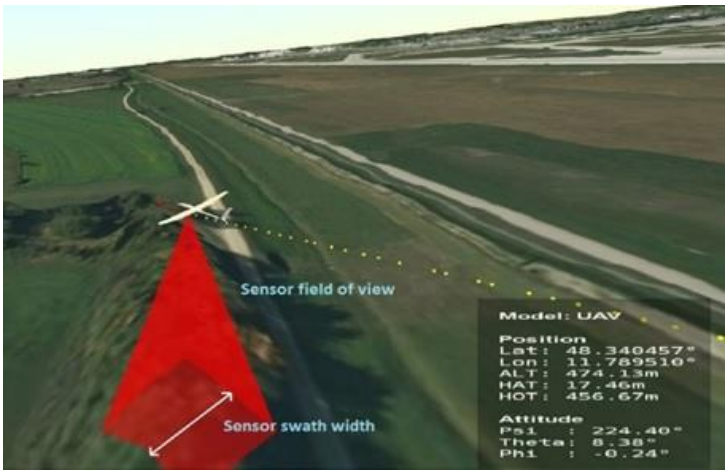

Figure 3.10: Representation of the sensor´s field of view (Fokina et al. 2019)

To calculate the sensor´s footprint on the ground, it is necessary to know intersection points between the sensor FOV and terrain. In the visualization environment OpenSceneGraph functionalities allow to calculate intersection points between objects in the scenery by the ray tracing approach. This approach is realized in OSG by an internal function util::intersect(), which allows to obtain coordinates of an intersection point along a defined line with a certain object. Thus, this function provides with the intersection points along the pyramid ribs and the terrain, which are obtained at each time step during the mission simulation. Using these coordinates of the intersection points, a geometry representation of the sensor ground footprint is rendered and precisely located in the scenery. Therefore, it is not necessary to calculate the sensor´s footprint location with separate algorithms. Thus, the actual footprint area is obtained in real time during the mission flight simulation, which issues higher accuracy for area coverage and actual GSD calculations.

The sensor ground swath width is determined as the distance between the two middle points on the sides of the pyramid intersection area parallel to the flight direction, see Figure 3.11. This value is used in Eq. (2.6) for the calculation of the actual GSD during the mission at each simulation step. Especially in regions with high gradients of the terrain the sensor swath width derived by the presented approach would make significant difference compared to the sensor swath width on a flat terrain (Fokina et al. 2019).

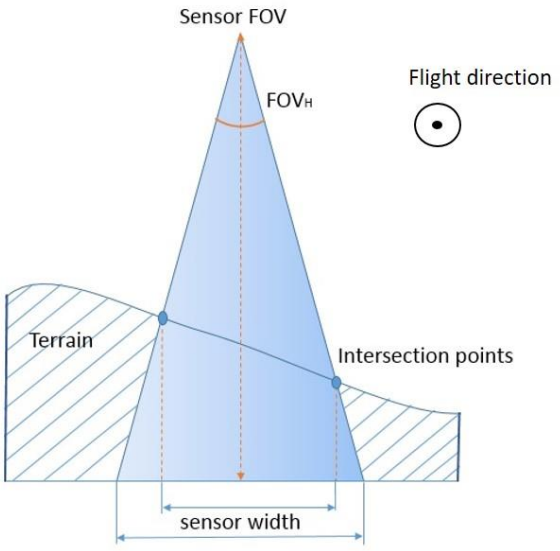

Figure 3.11: Sensor ground width calculation (Fokina et al. 2019)

The pyramid follows the orientation of the sensor and its orientation is defined by rotation matrices in respect to the motion of the UAV. In the visualization environment it is possible to simulate 2 sensor operation modes: without and with gimbal, see Figure 3.12. Thus, the field of view of the sensor can change its orientation together with the UAV angular movements, stay stable pointing towards the ground or is fixed on a certain point in the geospatial space. The sensor operation mode with gimbal onboard minimizes ground swath width, stabilizes image quality, but at the same time brings additional weight to the UAV.

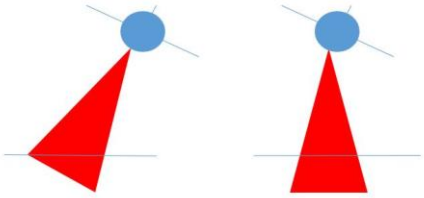

Figure 3.12: Sensor FOV orientation without gimbal (left) and with gimbal (right)

Figure 3.13 presents simulations with two different sensor operation modes. It can be observed that in the configuration without gimbal (left picture) the coverage area at the turns increases and therefore also the probability to detect objects compared to the configuration with gimbal (right picture) (Fokina et al. 2018c). Without gimbal the GSD is increased at the turns in the remote area and shows high variations. This operation mode shows higher coverage area, but at the same time not stable image quality. Furthermore, it carefully has to be checked whether gaps in the coverage area arise.

Figure 3.13: Sensor on board without gimbal (left) and with gimbal (right) (Fokina et al. 2018c)

Another feature of the visualized operational environment for the sensor performance analysis is the ability to simulate the FOV of the camera installed on the UAV. For that the osgVisual functionality for observing the UAV model during the simulation from different viewpoints is used, see Figure 3.8 and Figure 3.9. The window view of the visual camera called “Mounted” is taken and its parameters are set in accordance with the parameters of the sensor, where the window height and width correspond to sensor horizontal and vertical resolution. The distance from the sensor to the ground is calculated during the mission simulation taking into account the terrain elevation and is set in the window view settings. An example of the code lines is presented in A.3. An example of the view is presented in Figure 3.14, where the object of detection is presented by a shape of a cow and is marked as “Object 1”. This functionality is helpful in order to evaluate the probability of an object detection by an operator. Thus, the visualized operational environment can be also used for operator trainings.

Figure 3.14: Simulation of the FOV of the camera

3.2.4 Communication analysis

In the presented work for the communication assessment the following aspects are taken into consideration: communication range, obstacles in the line of sight and time of communication losses. The elevation model and realistic terrain representation in the visualized operational environment allow to assess the communication performance. For that the OSG functionalities for calculation of intersection points between objects in the scenery is used. The communication range is represented as geometry line with the dynamic starting point onboard the UAV, moving together with it, and the end point at the location of the ground control station. Using the callback functionalities the coordinates of the starting point are updated at each time step. Thus the LOS between the UAV and the control station is simulated during the mission flight (yellow line in Figure 3.16). At each simulation time step it is verified whether the intersections between the terrain and the LOS line occurs using the same OSG function *util::intersect(),* as for intersection calculations between the pyramid and terrain. In the visualization environment this information is displayed on one of the overlay windows, see Figure 3.15, as Boolean value, where “0“ means no intersection and “1” an intersection takes place. Using a time counter time of the communication losses is obtained. The same technique is applicable for the beyond-line-of-sight communication simulations with the geometry representation of data link between the UAV and a satellite or another airborne relay.

This technique of LOS simulation in the visualized operational environment allows to detect areas where the LOS is unavailable due to high terrain gradients. Despite the fact that the flight altitude is high enough and the flight path does not collide with the terrain, there can be still losses in the communication line of sight between the UAV and the ground control station as the VLOS intersects with the terrain.

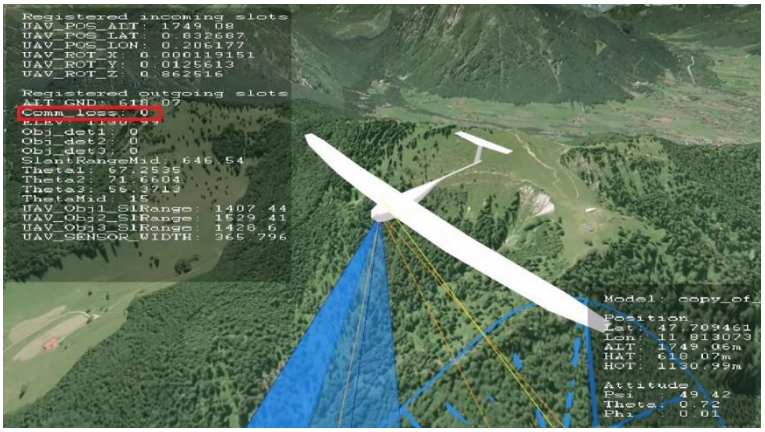

Figure 3.15: Communication losses data on one of the window overlays during the mission simulation in the visualized operational environment

3.2.5 Additional rendering functionalities for the mission performance assessment

For the visual data representation and for the visual UAS mission performance assessment the visualization environment has been enhanced with the following functions, see Figure 3.16 and Figure 3.17:

- Actual (blue line) and commanded (white line) flight paths in Figure 3.16

  The commanded flight path represents the result of the mission planning and consists of the calculated flight waypoints. The actual flight path represents the UAV motion during the mission simulation and consists of points calculated by a flight controller for each time step in the simulation model.

- Area coverage on the terrain (blue marking on ground in Figure 3.17)

  The blue area on the ground in Figure 3.17 represents the sensor ground trail or the sensor area coverage. Using the coordinates of the intersection points between the pyramid back ribs and the terrain curve lines along the flight direction are depicted on the ground. With each time step new points are added to this lines. Together with additional lines between them the geometry representation of the sensor area coverage is depicted. The area coverage is accurately located on the terrain and precisely calculated for the mission performance analysis taking into account the terrain gradient.

- Slant range between the UAV and objects of interest (orange line in Figure 3.17)

  The slant range is represented by a line geometry where the starting point is dynamic and connected with the UAV motion and the end point is located at the object of interest, which can also be dynamic. This geometry representation of the slant range allows to obtain information when the object of interest is in the sensor field of view. For that it is verified for intersections between the line and the pyramid representing sensor field of view at each time step of the mission simulation. When the intersection occurs it means that the object is in the

field of view of the sensor. Using the time counter the time is calculated and together with the distance to the object and the sensor properties is used for detection probability calculation, see Figure 2.13.

Thus, owing to rendering functionalities besides the visual assessment it is possible to obtain information about obstacle detection, time of communications losses and detection of objects in the camera field of view which are used for MPI calculation.

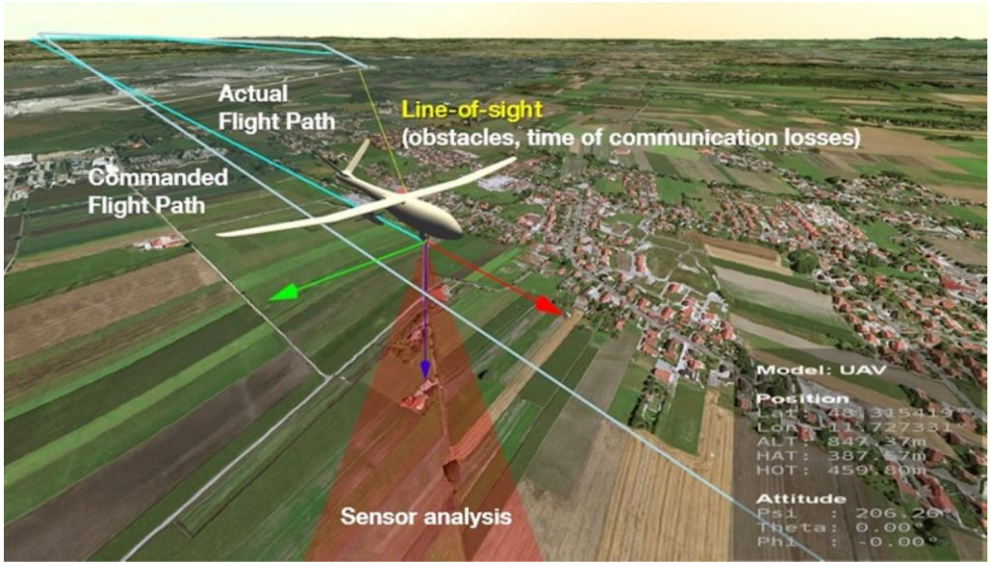

Figure 3.16: New rendering functionalities (Fokina et al. 2019)

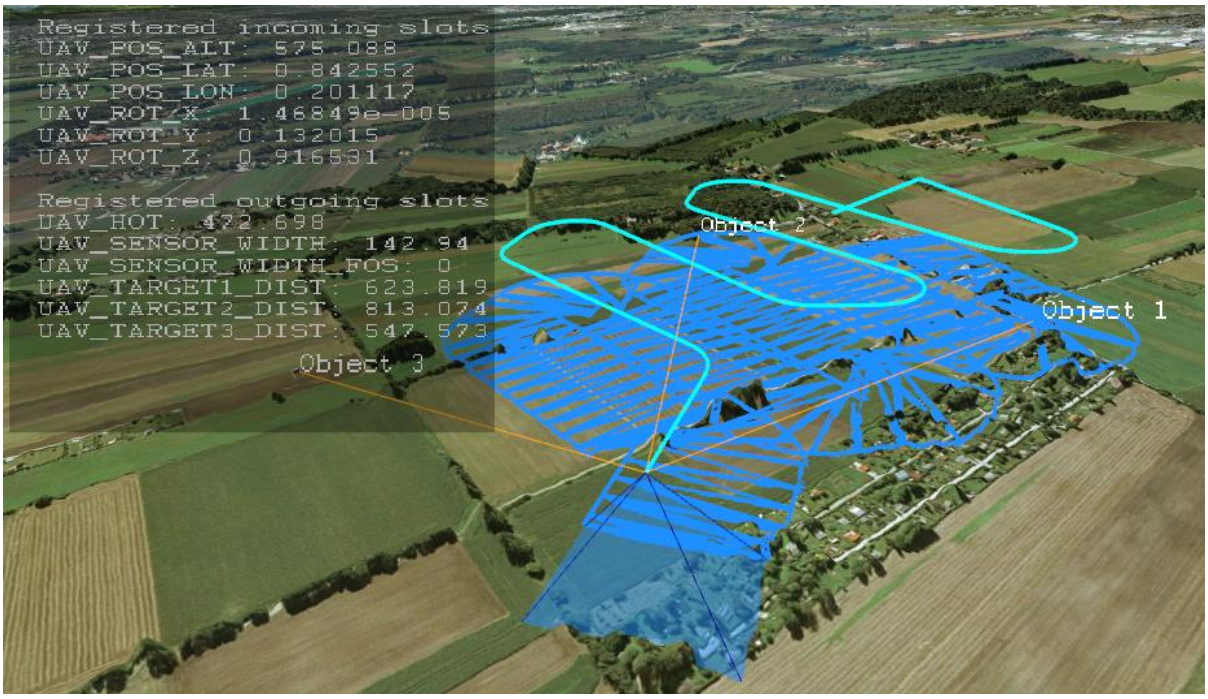

Figure 3.17: UAS general mission representation in the visualized operational environment (Fokina et al. 2018, AIAA)

The visualization of the UAS mission task can be simulated in real time or with a defined simulation pace, which allows to simulate missions faster and to reduce the overall UAS optimization time. For example, the simulation pace of 20 means that the mission simulation time in the visualized environment is 20 times shorter, compared to real mission time. Due to the fact, that the visualization environment uses a graphical representation of the UAS elements and its interaction with the terrain, the slower the simulation pace the more time steps there are and the more accurate are the values of the sensor ground swath width, detection probability and coverage area. Therefore, by setting the simulation pace value a tradeoff between accuracy and simulation time takes place.

4 Application studies

In this Section, two application studies are presented in order to show the feasibility of the developed approach for the mission simulation and evaluation based UAS design. The first application study concerns UAS usage in agriculture and the second a search and rescue mission.

For both application studies the designed UAS consists of a platform, an onboard camera, a flight control system, a generic data link and a data recorder element. The camera and the UAV are variable elements of the system, while the other subsystems stay the same for each UAS configuration during the optimization process (Fokina et al. 2018a). Table 4.1 presents weights for the subsystems taken for the UAS optimization.

Table 4.1: Weights of UAS basic payload elements (Fokina et al. 2018a)

Component	**Weight [kg]**
Flight Control System	0.62
Generic Datalink	0.58
Data Recorder	0.3
Mission Management Computer	0.4

The design parameters for UAS optimization and their allowed ranges are presented in Table 4.2. The resolution, field of view, size and weight of the chosen cameras influence the design of the UAS. An overview of the camera list is presented in Table 4.3.

Table 4.2: Design variables for UAS optimization (Fokina et al. 2018a)

Design variables	**Range**
Wing Area	0.2 … 3 [m^2]
Aspect Ratio	5 … 15 [-]
Design Speed	10 … 30 [m/s]
Camera Index	1 … 5 [-]

The objective function of the optimization process is to maximize the MPI, compare Eq. (2.17). Minimum stall speed of $V_{stall} = 17\ m/s$ is introduced as a constraint and it proves that the results show acceptable handling characteristics of the UAV (Feger et al. 2018).

Table 4.3: Selected camera types for UAS optimization

Camera Index	Resolution	Max horizontal FOV	Weight
Cam 1	1920 x 1080	59°	1.2 kg
Cam 2	1280 x 720	31.5°	4 kg
Cam 3	1280 x 720	55.7°	3.5 kg
Cam 4	1920 x 1080	31.2°	16.8 kg
Cam 5	720 x 480	57°	1.02 kg

During the UAS optimization process, several generations with a certain number of individuals are generated. Each individual represents a UAS configuration. The key evaluation criteria for MPI are obtained during the mission simulation for each individual. The mean values of the key evaluation criteria of the first generation are used as reference values and kept through the optimization.

In the next sections application case studies of the presented evaluation method and tool chain are presented. Different weighting schemes and their influence on the final UAS configuration are investigated. Depending on the mission type and desired performances with respect to area coverage rate, mission time, detection probability or required energy are taken as prevailing criteria. In addition, possible communication losses between the UAV and control station are taken into account as well as the mission flight route planning.

4.1 Aerial survey for precision vegetation analysis

According to (Gundlach 2016), agriculture may become one of the most demanding applications of UASs as with population growth it has to be more productive. By using a UAS, it is possible to improve land management practices, increase yields and reduce costs.

For agriculture UAS applications, the system has to be simple to use and inexpensive. Runway-independent fixed wing or VTOL systems have advantages as they can be operated close to the field or directly from it. An advantage for agriculture application can be hand-launched and belly-landed UAS where no special launch equipment is required. For the presented case study, the example from (Fokina et al. 2018c) is taken. Additional studies concerning overlap size, communication performance and weighting assignment are conducted.

4.1.1 Mission description and design trade-offs

A field farm with the size of 4 km² in the north of Munich has to be observed for vegetation analysis, see Figure 4.1. In order to detect the smallest pieces of plants, the required GSD is 5 cm and the

inacceptable GSD is 15 cm. The flight altitude is calculated for each UAS configuration based on the camera properties installed on board. In order to get a stable image quality, the altitude has to be constant during the flight. In reality for civil UAS applications, there can be altitude limitations, which should be considered as a constraint as well. However, the goal of the presented application study is to verify the presented methodology for the UAS design and therefore any restrictions are neglected.

Figure 4.1: Area of investigation for the agriculture application study

The forward overlap responsible for data processing is taken 60%, compare Section 2.2.1.2. The side overlap is required to ensure that there are no gaps in the coverage and is recommended to be a minimum of 30% (Qassim A. Abdullah). As the application study is about the UAS design, it is also assumed that there are no wind, rain or fog. Otherwise, corrections for the flight path planning and additional calculations are necessary.

The aerial imagery should be delivered in natural colors in file format with 8 bits per band or 24 bits for all three bands.

Communication between the platform and the ground control station is within direct LOS.

In case of precise agriculture applications, the mission key evaluation criteria are quality of collected data, area coverage rate and energy consumption. In order to improve the area coverage rate, the UAS has to fly at higher altitudes, with higher speed and with a higher resolution onboard camera. However, camera resolution and FOV set a maximum flying altitude for the UAV for a desired GSD. In order to obtain images with a desired quality, the required GSD has to be maintained and the flight speed should not exceed the maximum speed limited by the camera frame rate. In addition, the communication system bandwidth can restrict the data transfer rate from the payload to the ground control station. Thus, improving one key evaluation criteria can lead to the deterioration in the quality of another parameter. These tradeoff studies are conducted in the presented agriculture case study.

4.1.2 UAS mission modelling

For the agriculture application study the following weighting scheme is chosen:

$$\alpha\ (ACR) = 0.4\ ,\ \beta\ (E) = 0.4,\ \gamma\ (Pdet) = 0.05,\ \delta\ (T) = 0.05,\ \varepsilon\ (CA) = 0.1.$$

During the UAS optimization, 10 generations with 15 individuals each are designed and optimized. In total 150 UASs are designed, simulated and evaluated in order to find the one, which fulfils the mission requirements the best. Each UAS and its mission performance is assessed with a MPI. The goal of the objective function of the optimization is to maximize the MPI. Figure 4.2 and Figure 4.3 present progresses of the MPI and design variables during the optimization. In the first generation, 15 UASs are simulated and evaluated. For each individual, values of area coverage rate, energy consumption, mission time, detection probabilities and communication losses are obtained. Mean values of these parameters are taken as reference values in order to calculate MPIs, see Eq. (2.17), and are kept during the optimization for other generations.

The best individual is taken to the next generation and new individuals are created using methods of reproduction, crossover, and mutation. The highest MPI value of 1.56 has the UAS in the 1st generation with the camera 1 onboard and the following parameters: wing area 2.42 m², aspect ratio 10 and designed speed of 21 m/s. The final optimized UAS, obtained from the last generation, is presented in Figure 4.4 and has camera 1 onboard, a wing area of 1.45 m², an aspect ratio of 13.35 and a design speed of 21 m/s. The MPI value of the final UAS design is 1.72 and the stall speed constraint is 9 m/s. Figure 4.5 presents the mass fraction of the designed UAS.

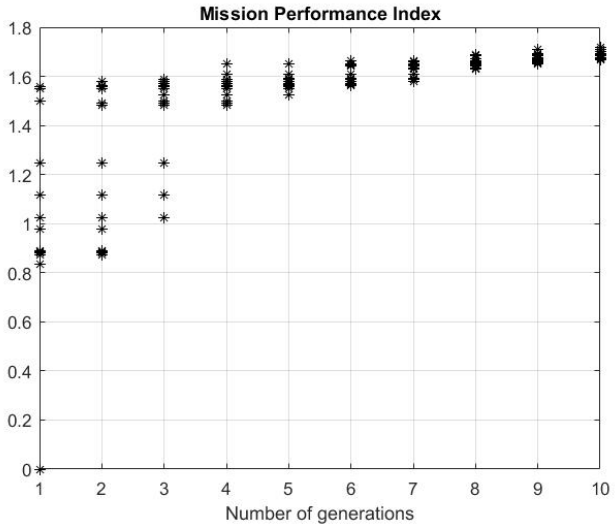

Figure 4.2: MPI progress during the UAS optimization for the agriculture application study

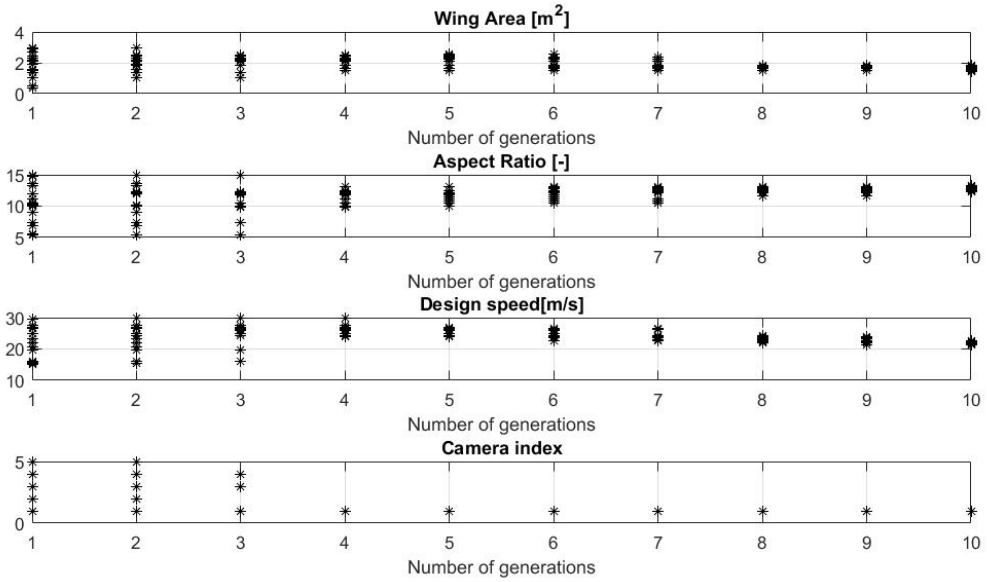

Figure 4.3: Progress of design variables during the UAS optimization for the agriculture application study

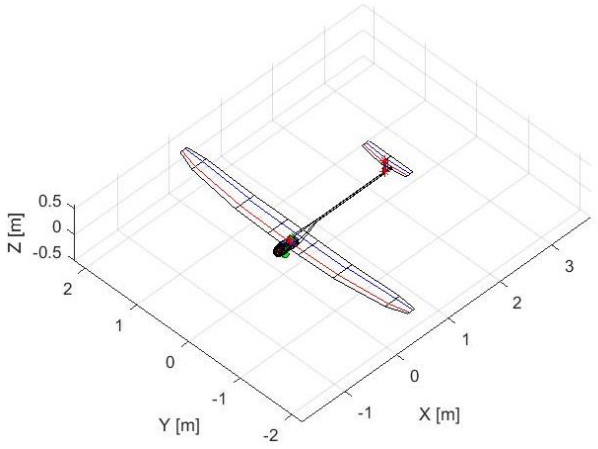

Figure 4.4: Designed UAV for the agriculture application study

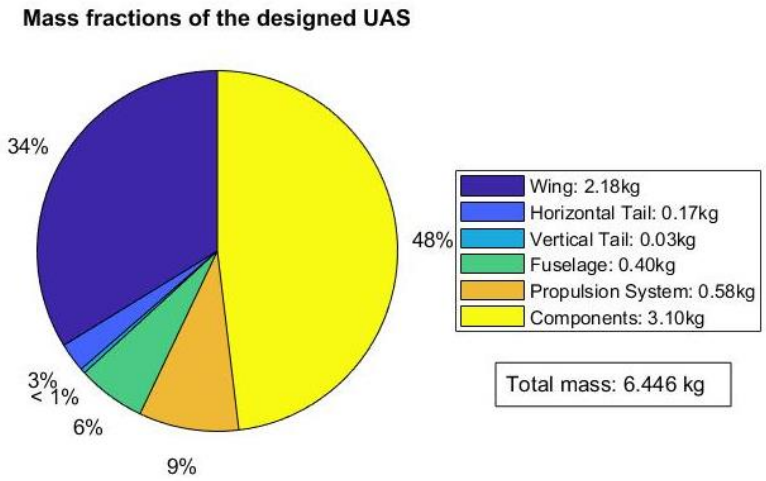

Figure 4.5: Mass fractions of the designed UAS for the agriculture application study

The mission is fulfilled in 52 minutes with the airspeed of 21 m/s at the altitude of 564 m over MSL or 85 m over ground. The flight altitude is calculated according to the required GSD of 5 cm, see Eq. (2.5)-(2.6), and is constant during the flight.

Results of the mission simulation are presented in Figure 4.6. The lane flight pattern is chosen for this simulation and is presented on the right side of the figure. In total there are 90 waypoints necessary to perform the mission. On the left side results of altitude and speed, angles and control inputs variations are presented. One can see over shootings of angles and control inputs values on the turnings. It is caused by the fact that the control model of the flight dynamics simulation is not optimized to each designed UAS during the simulation since the dynamic of the UAV behavior during the flight is not the issue of this research project.

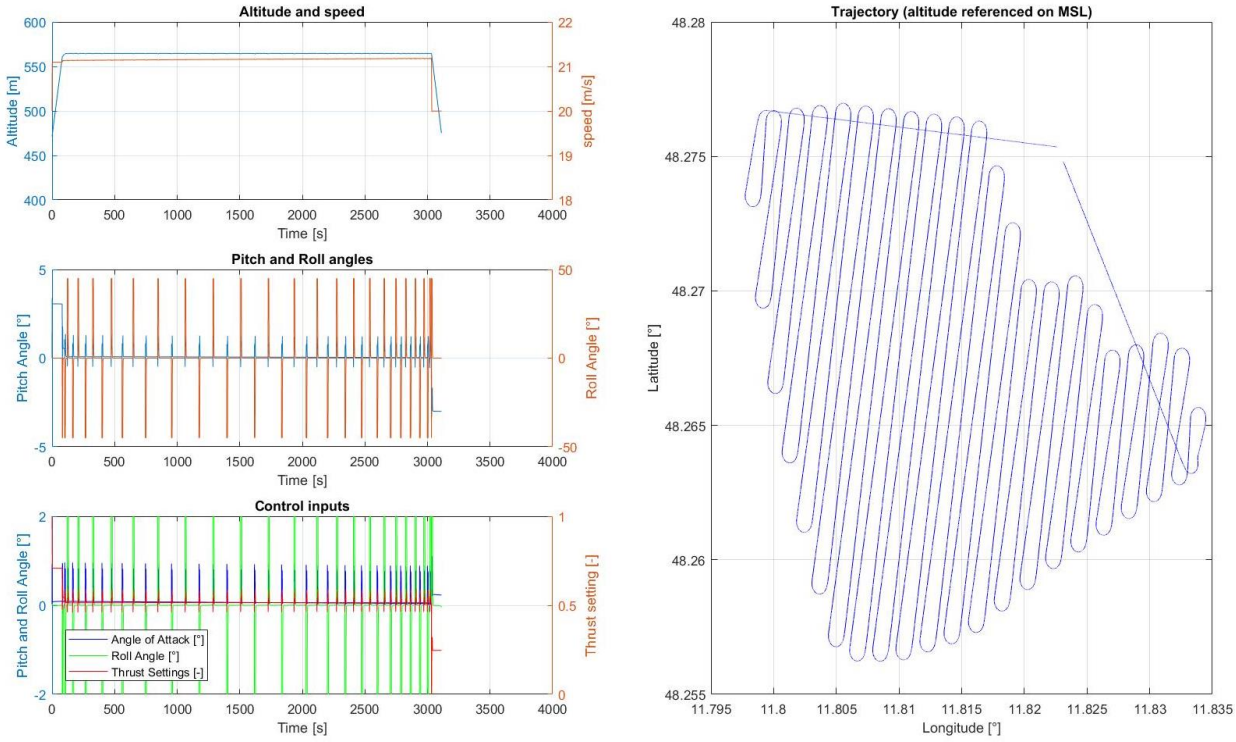

Figure 4.6: Result of UAS mission simulation for agricultural application study

Figure 4.7 presents the agriculture mission simulation in the visualized operational environment where blue color depicts the area coverage and cyan color the flight trajectory. One can see that the area is covered without gaps due to the overlap set to 30% and the flat landscape.

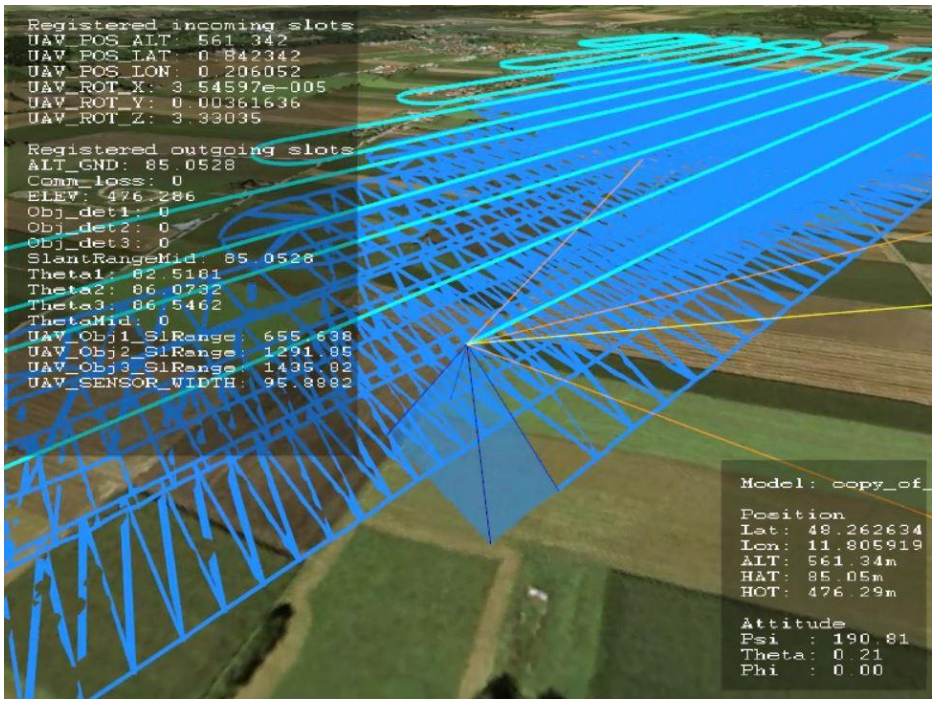

Figure 4.7: Agriculture mission simulation in the visualized operational environment

Communication analysis

Based on the initial requirements for collected images, the forward overlap should be 60%. That means that the distance between two successive images along one flight line, which is also called airbase, is 21.6 m, see Eq. (2.7), for the installed onboard camera with the resolution of 1920 x 1080 pixels. Thus for the designed speed of 21 m/s the frame rate of shooting images is 0.97 Hz, see Eq. (2.8) . This required frame rate should not be higher than the maximum frame rate of the camera, which defines the maximum airspeed for the UAV. Usually the maximum frame rate of a camera is 10 – 20 Hz. That means that for the presented example the speed can be higher than 21 m/s and it will not influence the image quality.

According to the initial mission requirements, an image has the size of 8 bits per color band, which is 1 byte per pixel. That means that according to Eq. (2.13) one image has a size per band of 2.1 Mb. The total number of images is obtained as a product of the mission time while the sensor is collecting images, which is 3022 seconds, by the calculated frame rate leads to a total amount of 2932 images. Therefore, the total storage requirement for the collected images is 18.5 GB and is obtained according to Eq. (2.15), where the number of bands for a RGB image is 3. The longer the mission the more onboard storage capacity is required.

In case when the collected data have to be transmitted to the ground control station, the data transfer rate has to be assessed, see Eq. (2.14). For the presented application case it is 4.1 Mb/s. This value should not be higher than the maximum transfer rate of the communication system.

Thus, increasing the airspeed leads to higher frame rate values. Higher frame rate or higher camera resolution require a higher transfer rate or a bigger storage capacity. Image requirements such as RGB color or monochrome and amount of pixels per byte influence the transfer rate and the total images size as well: higher image requirements drive higher values of the transfer rate and storage requirements.

Feasibility of the simulation

To demonstrate the functionality of the mission simulation and evaluation environment, the presented application study is performed several times with identical start parameters, such as weightings and mission area. In order to decrease the simulation time, the mission area of these five optimization runs is taken smaller compared to the presented above main agricultural application study. There are calculated 10 generations of 15 individuals each for each optimization run. The final design parameters of the optimized UAS such as wing area, aspect ratio, design and stall speed, as well as camera are presented in Table 4.4 for these five optimization runs. In addition, the percentage deviations from the mean value of these five simulations are indicated in brackets. All optimizations have chosen camera 1 as the best option. The average deviation of the optimized wing area of the different simulations is around ±11%. Significantly smaller are the deviations in aspect ratio, design and stall speed with only ±5%, ±3% and ±2.2%, respectively. The magnitude of the deviations of the five simulations to each other is even smaller than the deviation of the 15 individuals in the last generation of a single simulation, as it is shown in Figure 4.8, where the values of the 15 individuals in the last generation of simulation 1 are presented. The MPI values for these 15 individuals, see Figure 4.9, differ from minimum value of 1.8816 to a maximum value of 1.8873, which corresponding to a deviation of 0.3 %, despite the fact that the wing area and the aspect ratio are varying by 20% and 16% respectively.

Table 4.4: Comparison of 5 optimization runs for the same mission

Simulation	Wing area, [m²]	Aspect ratio, [-]	Design speed, [m/s]	Stall speed, [m/s]	Camera Index
1	1,173 (+3,1%)	10,65 (+5,2%)	15,88 (+3,6%)	9,10 (- 1,2%)	1
2	1,142 (+0,4%)	10,48 (+3,6%)	15,00 (-2,2%)	9,06 (- 1,6%)	1
3	1,026 (- 9,9%)	9,63 (- 4,8%)	15,79 (+3,0%)	9,47 (+2,8%)	1
4	1,070 (- 6,0%)	10,24 (+1,2%)	15,00 (- 2,2%)	9,25 (+0,4%)	1
5	1,280 (+12,5%)	9,58 (- 5,3%)	15,00 (- 2,2%)	9,19 (- 0,2%)	1
Average	***1,138***	***10,12***	***15,33***	***9,21***	***1***
30/20 1	0,950 (-16,6%)	9,05 (- 10,6%)	15,26 (- 0,5%)	9,64 (+4,7%)	1
30/20 2	0,926 (-18,7%)	8,89 (- 12,1%)	15,41 (+0,5%)	9,74 (+5,8%)	1
30/20 3	0,923 (-18,9%)	8,96 (- 11,4%)	15,19 (- 0,9%)	9,69 (+5,2%)	1

Furthermore, the same procedure is carried out with 30 individuals and 20 generations to generate and simulate significantly more combinations of the four design variables, which means 600 UAS configurations. These are named in Table 4.4 and Table 4.5 as “30/20 1-3”. The values in brackets describe the percentage deviation of the results of these simulation in reference to the mean value of the five missions described above. One can see that the wing area and the aspect ratio differ from the results with only 15 individuals. However, the deviations of the design variables within each group are much smaller, which shows that the results are better converged. Compared to the results of the first 5 optimization runs, the wing area became 18% smaller that means also a cheaper UAV. From the aircraft design point of view the more generations the more accurate UAV model is designed.

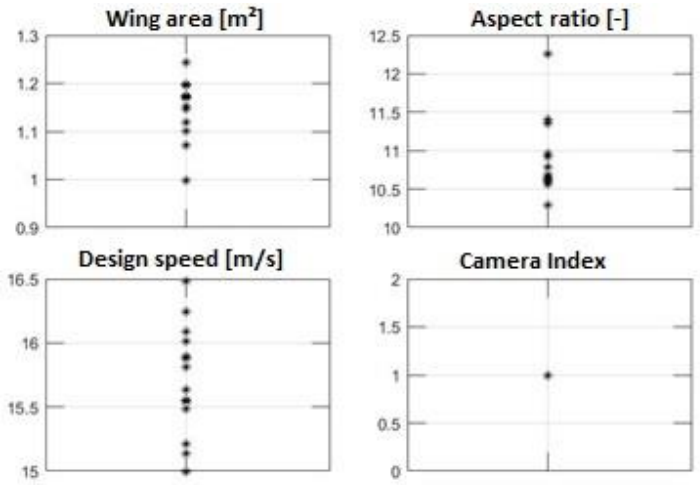

Figure 4.8: The values of design variables of the 15 individuals in the last generation of simulation 1

Figure 4.9: MPI of the last generation of simulation 1

Table 4.5: Values of evaluation parameters used for MPI calculation

Simulation	Mission time [s]	ACR [m²/s]	Detection probability [%]	Energy consumption	Comm. performance
1	1229 (- 3.1%)	1433 (+3.8%)	0.4474 (- 0.6%)	0.0352 (+1.3%)	0.9998
2	1292 (+1.9%)	1351 (- 2.2%)	0.4432 (- 1.5%)	0.0342 (- 1.6%)	0.9998
3	1236 (- 2.5%)	1419 (+2.8%)	0.4432 (- 1.5%)	0.0351 (+1.0%)	0.9998
4	1292 (+1.9%)	1350 (- 2.2%)	0.4739 (+5.3%)	0.0343 (- 1.3%)	0.9998
5	1291 (+1.8%)	1351 (- 2.2%)	0.4418 (- 1.8%)	0.0349 (+0.5%)	0.9998
Average	***1268***	***1381***	***0.4499***	***0.0347***	***0,9998***
30/20 1	1274 (+0.5%)	1374 (- 0.5%)	0.4404 (- 2.1%)	0.0349 (+0.6%)	0.9998
30/20 2	1263 (- 0.4%)	1386 (+0.4%)	0.4301 (- 4.4%)	0.0351 (+1.0%)	0.9997
30/20 3	1279 (+0.9%)	1367 (- 1.0%)	0.4753 (+5.7%)	0.0350 (+0.8%)	0.9998

Table 4.5 shows the calculated values for mission time, ACR, detection probability, energy consumption and communication performance, which are used for MPI calculation. For the detection probability evaluation, 3 objects are placed on the mission area. Based on the presence time in the sensor field of view, flight altitude, GSD and sensor resolution the probability of object detection is assessed. The percentage of deviations of the evaluation parameters compared to the average values are indicated in brackets in the table. The deviations of the parameters of the MPI are only < ±1.1% for these five simulations. The small deviations of the evaluation parameters indicate that despite quite few individuals and generations compared to the amount of design variables the results are accurate enough for the mission performance assessment in the presented approach.

Figure 4.10 and Figure 4.11 present the results of the optimization process for the simulation “30/20 1”. The rest results are presented in Table 4.4 and Table 4.5. The parameters mostly influencing the MPI, such as camera and design speed, are almost identical. Also the results of the MPI variables like mission time, ACR, detection probability, energy consumption and communication performance are in good agreement.

The results show that the deviation of the wing area and aspect ratio between the simulations with higher number of generations are much smaller compared to the case with 10 generations and 15 individuals. Thus, the more generations and individuals in the optimization the smaller are the deviations for the design variables and mission key performance parameters. This result also shows that the improvements in the aircraft design process are required. These is one of the future next steps for the presented approach.

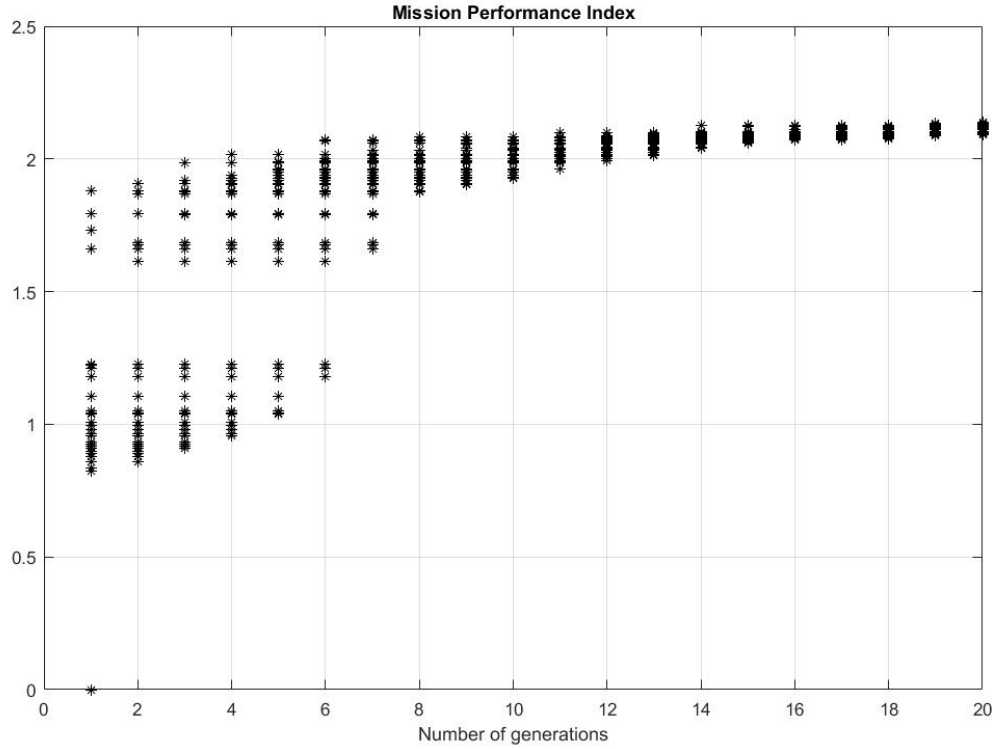

Figure 4.10: MPI variation for the optimization with 30 individuals and 20 generations

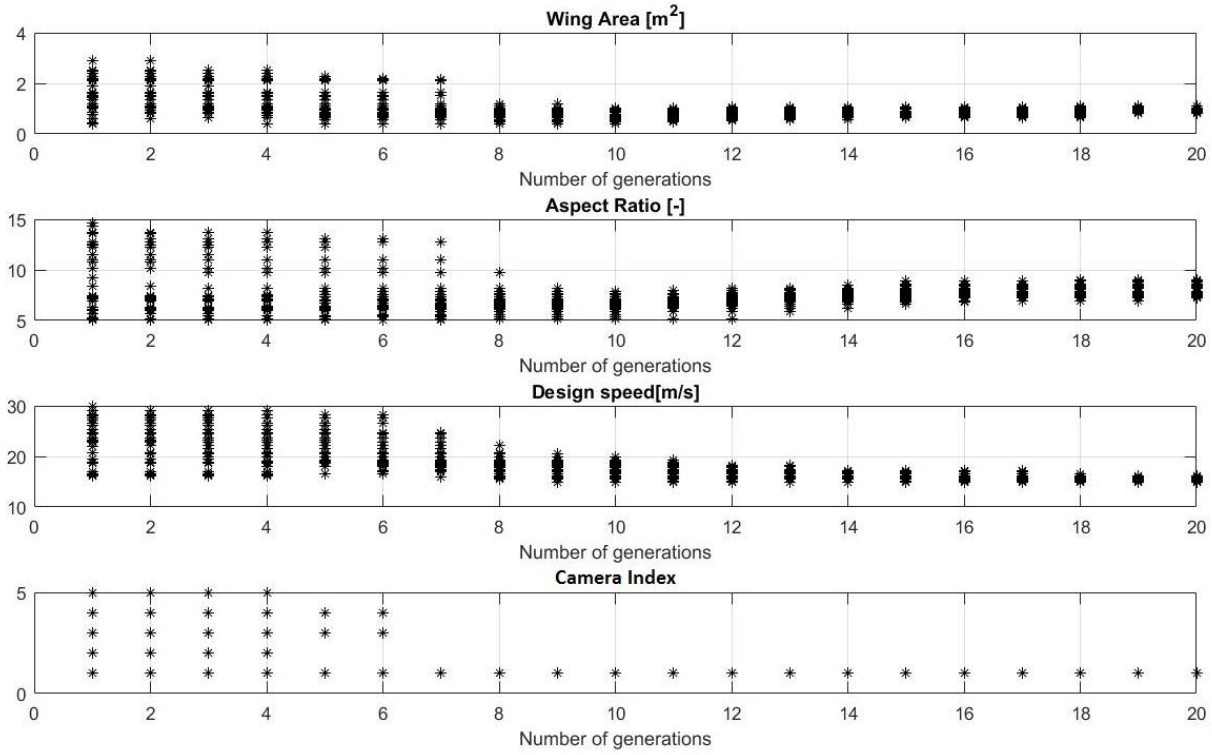

Figure 4.11: Variation of design variables for the optimization with 30 individuals and 20 generations

4.2 Search and Rescue in mountain area

The usage of the terrain based visualization environment for the mission performance evaluation gives significant results in the regions with high terrain gradients, for example in mountain areas. There, the terrain puts limits on search pattern, communication range and sensor performance. In the presented search and rescue (SAR) UAS application study which is an extended version of the study presented by (de Serpa Marques e Braga Barbosa, Bernardo 2019), additional attributes of assessment and UAS optimization are taken into account. In order to design possible UAS configurations the wing geometry and different camera types are taken as design parameters. The study is conducted for lane and spiral search patterns with elevation based optimization, see Section 2.5.2.2.

For search and rescue type of missions, it is important to find the missing person by exploring the search area:

- within the shortest possible period of time;
- with the desired image or video quality, so that an operator at the ground control station is able to detect the missing person.

Short mission time can be obtained through high altitude combined with larger sensor ground swath width. However, better image quality can be obtained with lower altitudes. In addition, a smaller camera field of view produces a smaller footprint on the ground and better resolution.

Therefore, the tradeoff study has to be conducted between required image quality, airspeed, flight path construction, communication attributes and UAS elements.

4.2.1 Mission description and design trade-offs

For the presented case, the area between Tegernsee and Schliersee, Germany, is chosen. It is assumed that a person is missing in this area and the last known position is at coordinates 47°42'56.42''N, 11°48'21.13''E, which corresponds to 47.715672, 11.805869. For the flight path calculation, the mission area is defined as a polygon in Google Earth, see Figure 4.12. The search area is 2.68 km^2 with a perimeter of 6.15 km. The terrain elevation in this area varies from 934 m up to 1326 m above MSL. Such a high elevation difference implies difficulties for mission planning as it requires sufficient thrust performance of an UAV in order to overcome the possible height differences of consecutive waypoints.

The flight time should be as short as possible and the whole search area should be covered without any gaps, thus the side overlap is taken as 10%. Higher overlap means better image quality but longer mission time. As for the presented application study mission time is a critical parameter, the overlap is taken smaller compared to the agriculture application.

It is assumed that the camera is installed together with a gimbal and the FOV of the camera is directed vertically towards the ground during the whole mission simulation, see Figure 3.13. The UAV should be within the LOS from the ground station during the flight. The position of the ground station is marked with a red point in Figure 4.12 on the right picture and is defined at the following coordinates: 47.716300, 11.809803. It is assumed that the weather conditions are good and there is no wind during the mission.

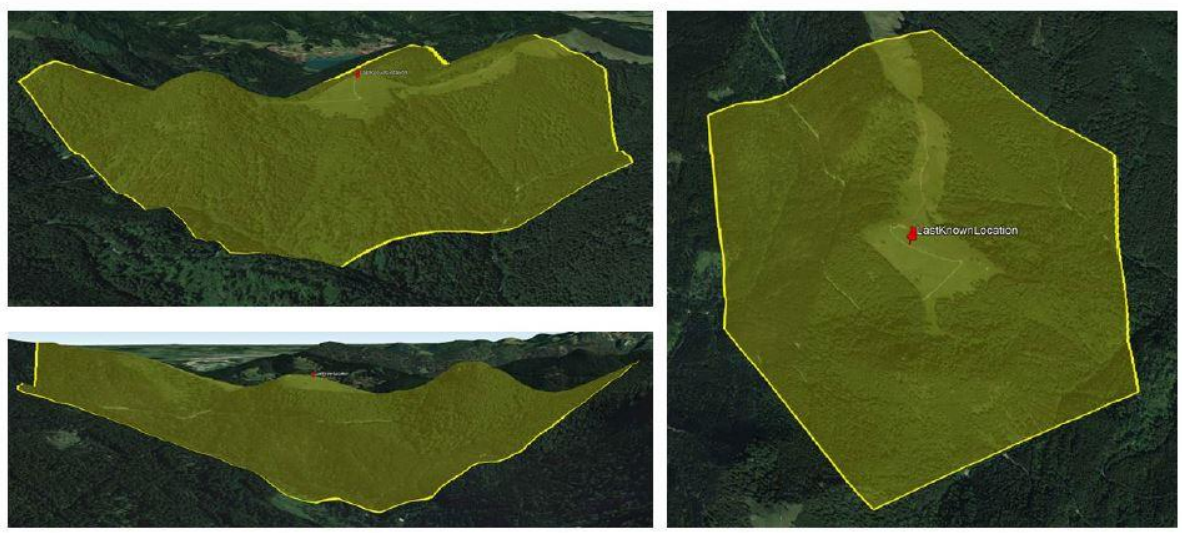

Figure 4.12: Mission area definition for SAR mission in Google Earth (de Serpa Marques e Braga Barbosa, Bernardo 2019)

The dimension of the searched person for the Johnson Criteria is taken 1.5 x 1.5 x 1.5 m^3. Based on Figure 2.6 and Eq. (2.11) the number of cycles is taken 5, which is a good compromise between a still acceptable GSD and relatively good probabilities of detection and recognition. The required GSD is 0.15 m/pix and the inacceptable GSD is 0.25 m/pix.

The probabilities of detection, recognition and identification are calculated during the optimization according to Eq. (2.21) for 3 possible locations of the missing person with the following coordinates:

1. 47.717837, 11.801029
2. 47.7211380, 11.804426
3. 47.719981, 11.815940

The average value of detection probabilities for these three points is used in MPI calculation, see Eq. (2.17).

The following design trade-offs are investigated:

- UAV, sensor and mission matching;
- Optimum flight path: comparison between lane and spiral search patterns.

At the first sight, the spiral pattern is more suitable since the UAS starts at the last known position and gradually increases the search range with the probability to find the person faster. However, depending on the sensor performance and terrain shape the lane search pattern can be faster as it is shorter and the flight path has less turns and the UAV can fly faster.

4.2.2 UAS mission modeling

For missions where human lives are in danger, the mission time and detection probability become the prevailing criteria. It is also important that the whole area is covered during the mission especially in the regions with high elevation difference. Thus for the SAR application study the following weighting scheme is chosen:

$$\alpha\ (ACR) = 0.1\ ,\ \beta\ (E) = 0.05,\ \gamma\ (Pdet) = 0.4,\ \delta\ (T) = 0.4,\ \varepsilon\ (CA) = 0.05.$$

User Operating Issues are not taken into account in this example as usually these missions are performed by experienced operators and issues such as type of landing or storage requirements do not play a role.

4.2.2.1 Optimization with lane search pattern

In this subsection the results of the UAS mission based optimization with the search lane pattern are presented. During the optimization, 10 generations with 15 UAS configurations each are designed, simulated and evaluated. Figure 4.13 and Figure 4.14 present the progress of the MPI and design variables during the optimization. The optimization algorithm maximizes the MPI. In case if the designed UAV cannot fulfil the mission from the performance point of view the MPI gets a zero value.

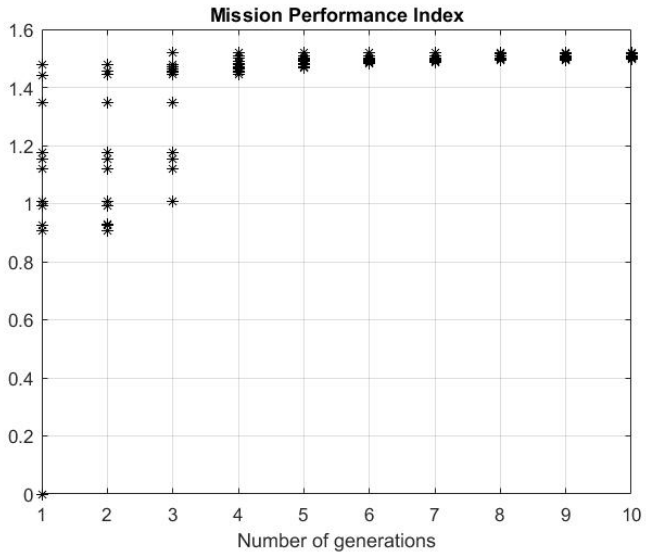

Figure 4.13: Progress of MPI during the optimization with lane search pattern

In the first generation UAS configurations with all possible cameras on board are designed, simulated and evaluated by the MPI. The characteristics of the cameras are presented in Table 4.3. The best individuals are taken to the next generation. Already in the 4th generation one can see that camera 4 yields the highest MPI. In the next generations, the MPI is further increasing and the range of the design variables is narrowed down. The progress of the design variables for the first 6 designs of the 4th generation is presented in Table 4.6. Figure 4.15 shows UAV designs for this individuals. One can see that although the type of the camera doesn't change anymore, the wing area and aspect ratio still needed to be optimized.

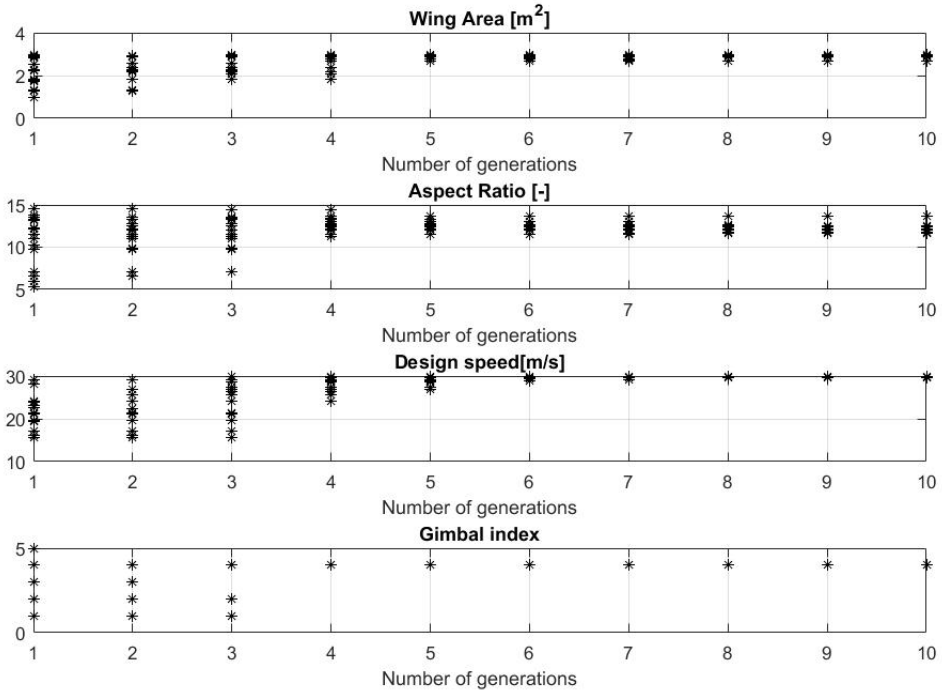

Figure 4.14: Progress of design variables during the optimization with lane search pattern

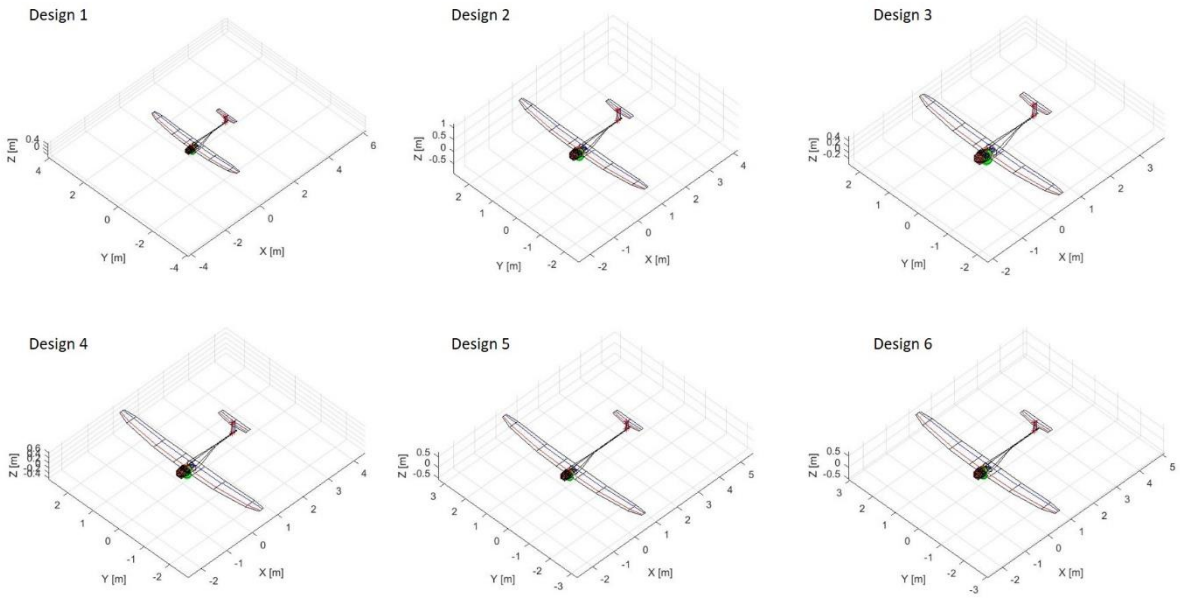

Figure 4.15: First 6 UAVs designs from the 4th generation

Table 4.6: Design variables and MPI values for the first 6 UAS designs from the 4th generation

Design	Wing Area [m²]	Aspect ratio [-]	MPI [-]
1	2.15	11.30	1.4461
2	2.05	13.45	1.4511
3	1.8	12.53	1.4575
4	2.35	12.75	1.4577
5	3	14.37	1.4652
6	3	12.43	1.4673

The optimized UAV with its onboard systems is presented in Figure 4.16. The wingspan is 6 m and the fuselage length is 3.7 m. The optimized UAS reaches a MPI= 1.52 and has the following characteristics: stall speed of 13 m/s, design speed of 30 m/s, a wing area of 3 m², aspect ratio 12 and camera 4 onboard.

Figure 4.17 presents the mission simulation of the designed UAS with camera 4 onboard in the operational environment. The search area is fully covered and the LOS between the ground control station and the UAV (yellow line) was not interrupted by the terrain. For the overall detection probability assessment three possible locations of the missing person are taken and marked in the mission area with points. At these points objects of interest are placed in the visualized environment. The orange colored lines depict the slant ranges between the UAV and these objects. When one of the lines intersects the graphical representation of the sensor FOV the object of interest is counted being in the FOV and its presence time is calculated. The presence times for all three objects are then used for detection probabilities calculation and MPI.

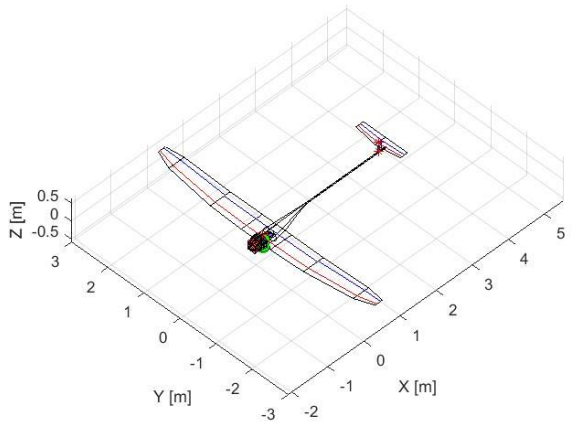

Figure 4.16: Optimized UAV for the case of lane pattern

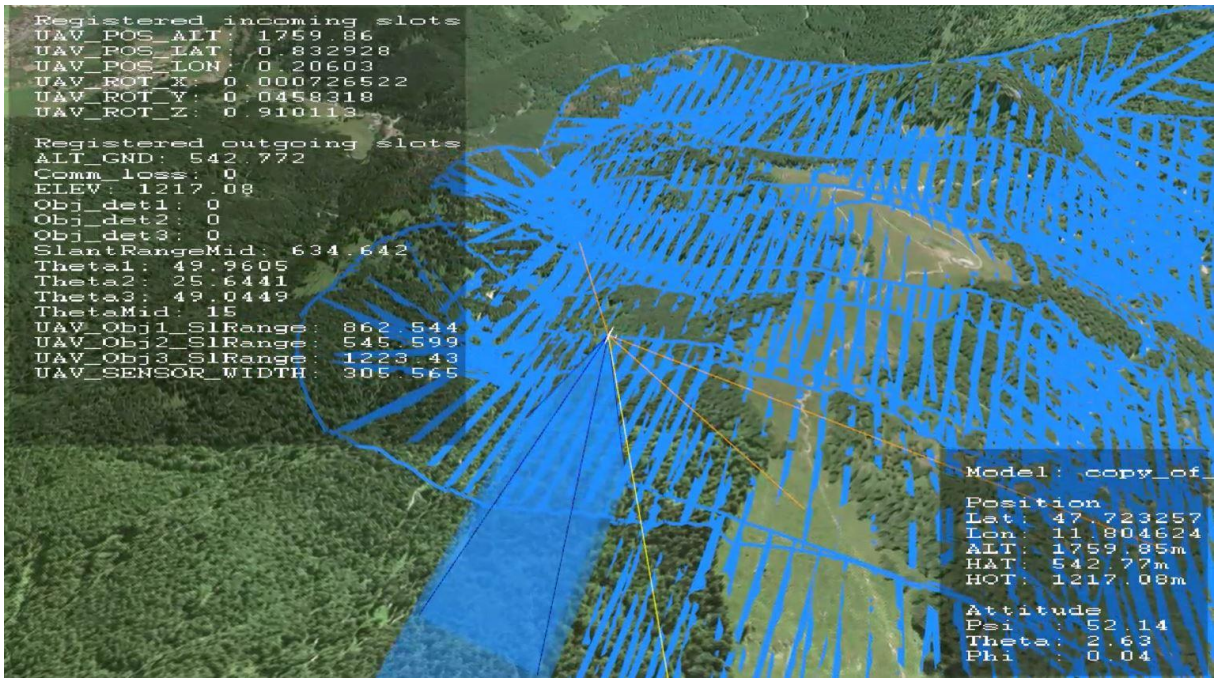

Figure 4.17: UAS mission simulation in the operational environment with camera 4 onboard and lane search pattern

The mission is fulfilled in 9 min with an airspeed of 30 m/s. In Figure 4.18 the trajectory (right), altitude (left top), speed (left top) and control inputs (left middle and bottom left) are presented. At turns, one can see an overshooting of control inputs and angles. The reason for that is that a 180° turn consist of 2 waypoints and a PID (proportional integral derivative) flight controller has to be adjusted for each generated UAS design which is not realized within the scope of the work. The values for the flight dynamic controllers are set at the beginning of the optimization process and are fixed for all UAS designed configurations since.

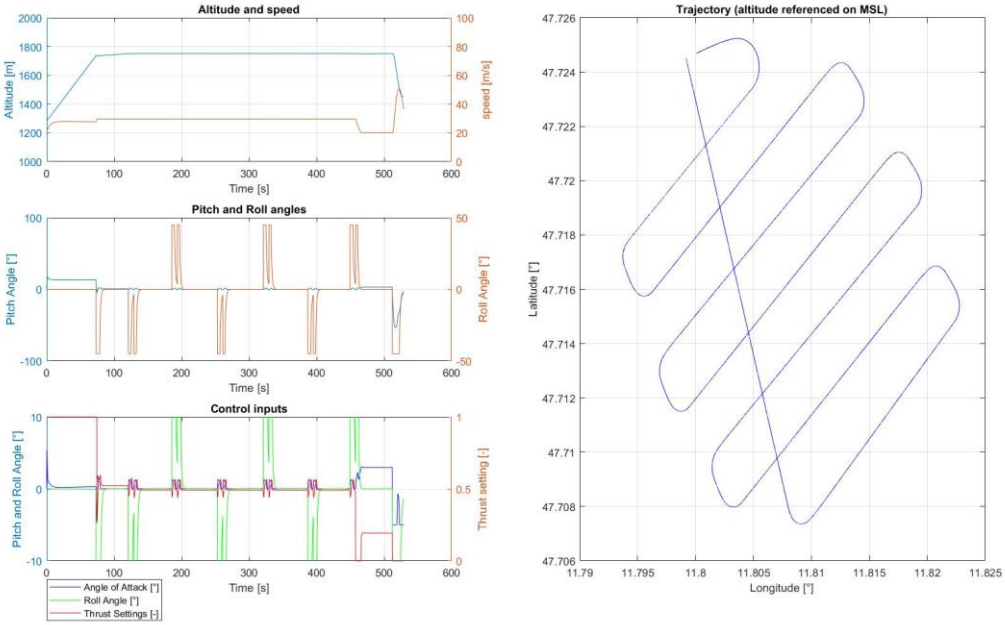

Figure 4.18: Results of the mission simulation for the lane search pattern

Figure 4.19 presents the elevation of the terrain (blue line) and the optimized flight altitude over MSL during the mission simulation (orange line). The altitude for each waypoint is calculated according to its elevation Eq. (2.5), camera FOV and resolution. The maximum altitude for the acceptable GSD is 424 m over ground and the altitude for the required GSD is 254 m over ground. Results of the mission simulation with not optimized flight path are presented in B.1. The not optimized flight path requires more thrust performance and is considered as non-flyable as it has constantly to climb or to descend on the way from a waypoint to a next one. With the optimization, the trajectory is smoothed so that the flight altitude stays almost stable and the GSD of collected data is also within the required range.

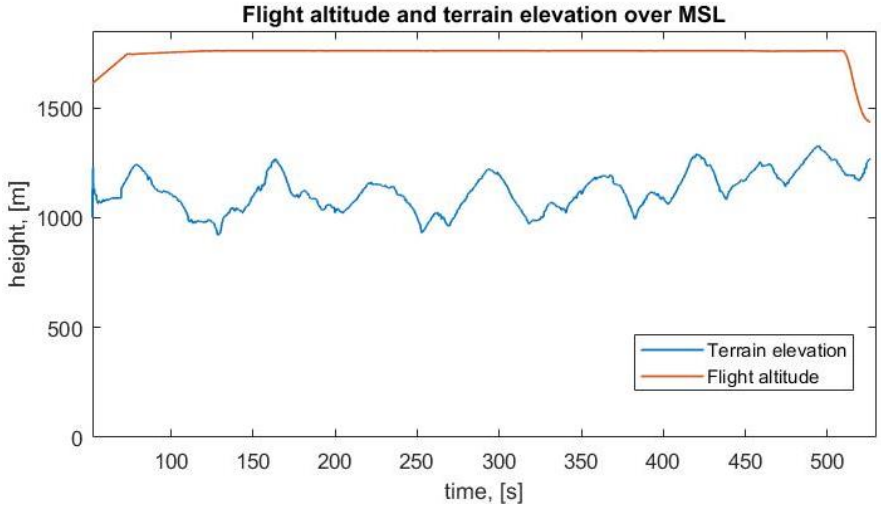

Figure 4.19: Flight altitude and height of the terrain over MSL

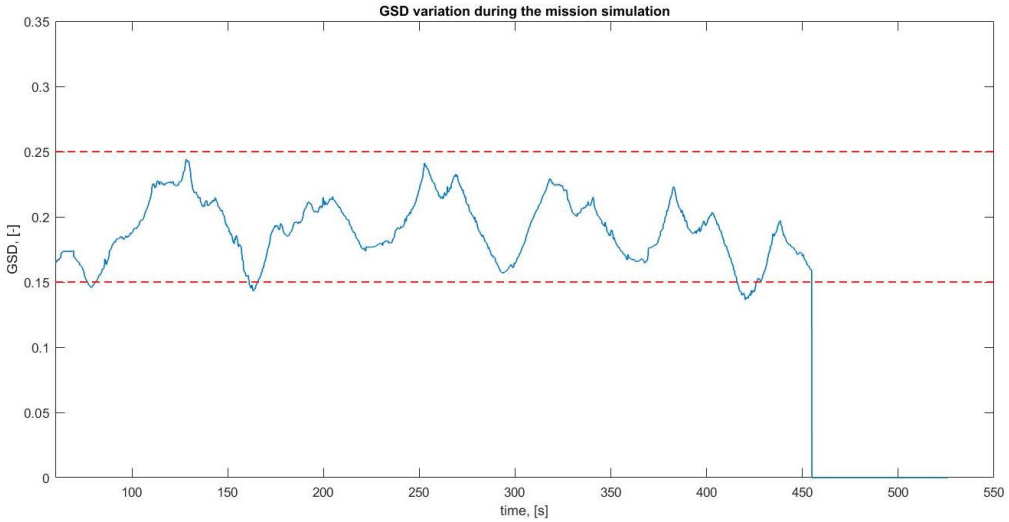

Figure 4.20: GSD during the mission simulation in the visualized operational environment

Figure 4.20 presents actual values of the GSD during the mission simulation in the operational environment (blue line) and the trust GSD region (red dotted lines), which is defined by the required GSD=0.15 m and the inacceptable GSD=0.25 m. Even though the GSD is varying during the simulation, it is located within the desired GSD range. Values for GSD are collected from the take off point and during the search and not on the way from the last waypoint of the search flight path to the landing point. This is why the values are zero at the end of the mission time on Figure 4.20.

Results of the detection probability of the missing person in 3 possible locations are presented in Figure 4.21. The first graph shows the slant ranges from the UAV to the location points on the ground at each time step. Detection probabilities presented in the second graph are based on the slant range distance and are calculated according to Johnson Criteria, see Eq. (2.10). These values are above 94% during the whole mission. However, the location points are in the FOV of the camera only for a limited amount of time. The maximum residence time is marked on the graph with vertical lines and is used in Eq. (2.21) for MPI calculation. During this time the detection probabilities calculated according to Eq. (2.21) are:

- For the first location point 83%;
- For the second location point 81%;
- For the third location point 95%.

One can see that at the beginning the slant ranges to the 1st and 2nd points are short, which means that the UAV flew close to these points on the way from the starting point to the waypoint, which defines the beginning of the search area and therefore the probabilities of detection are high. As the UAV climbs at that moment these slant ranges are short due to the low flight altitude. However, these values of the detection probabilities are not taken into account as these points are not in the camera FOV.

The third and fourth graphs present the probabilities of recognition and identification of the missing person in three possible locations based on Johnson criteria. One can see that the recognition probabilities for all location points is higher than 60%. However, the identification probabilities for locations 1 (red line) and 2 (green line) are lower than 30% and in order to have better values the UAS has to fly lower or with a camera with a higher resolution.

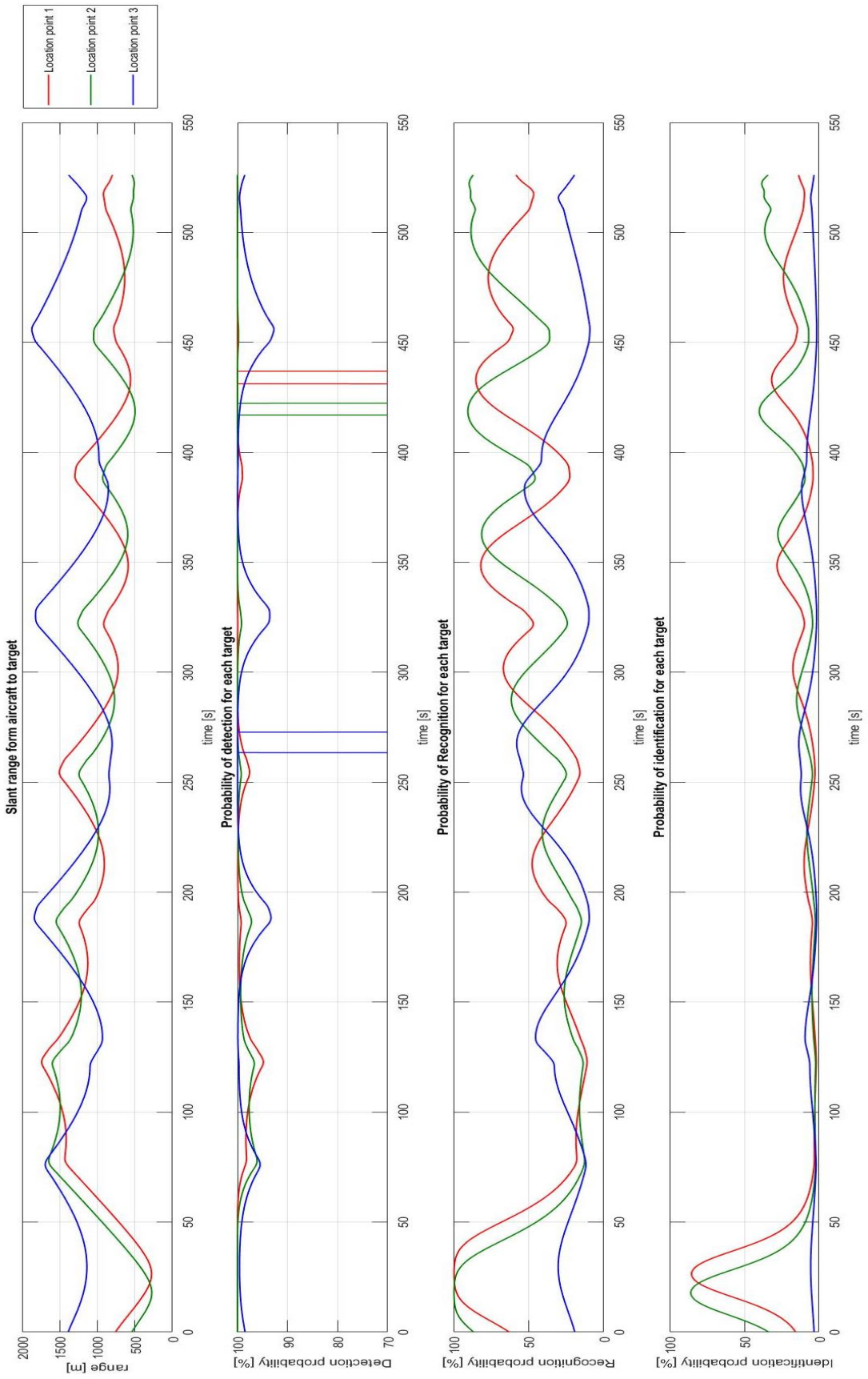

Figure 4.21: Probabilities of objects detection, recognition and identification during the mission simulation with lane search pattern in the visualized operational environment

An example of the simulated FOV of the camera so called “what does the camera see” is presented in Figure 4.22. The size of the screen window corresponds to the resolution of the camera onboard on the UAV, which resolution is 1920 x 1200 pixels. Such a simulation allows to see the size of the objects the way it will be visible in a real camera.

Figure 4.22: Simulation of camera FOV during the mission and the object for detection in it

In the optimization process presented above the designed UAS has camera 4 with a FOV of 31.2° and a resolution of 1920 x 1080 pixels. The total weight of the designed UAS is 28.3 kg, 16 kg of which is the weight of the camera, see Figure 4.23. Despite the high weight of the camera it was chosen in the optimization process as time and detection probability have the highest weighting coefficients, 0.4 each, and energy weight coefficient is set very low, 0.025.

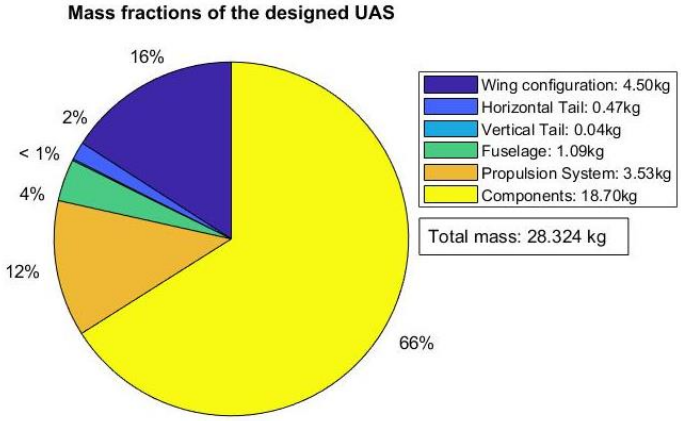

Figure 4.23: Mass fractions of the designed UAS for lane pattern

UAS optimization with E and ACR as key evaluation criteria and for lane search pattern

In this example a UAS is optimized for the same mission requirements but with a different weighting scheme. The following weightings for the MPI calculation, see Eq. (2.17), are considered:

$$\alpha\,(ACR) = 0.3\,, \qquad \beta\,(E) = 0.6, \qquad \gamma\,(Pdet) = 0.05, \qquad \delta\,(T) = 0.025, \qquad \varepsilon\,(CA) = 0.025.$$

In this case, the focus of the optimization lies on increasing the ACR and reducing the energy consumption. The final designed UAS is presented in Figure 4.24. It has a wing area of 2 m^2, aspect ratio of 13.2, wingspan of 5.3 m and a fuselage length of 2.4 m. The design speed for the mission is 15.4 m/s.

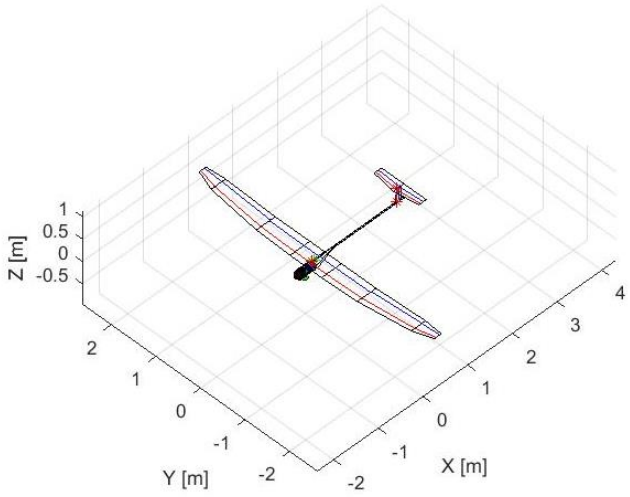

Figure 4.24: UAV designed for E and ACR priorities and lane pattern

A high priority to the energy weighting coefficient means less energy consumption and therefore drives reduction of the overall weight of the UAS. The mass fraction of the designed system is presented in Figure 4.25. For the presented case, during the optimization camera 1 with FOV = 59°, resolution 1920 x 1080 and with a weight of 1.2 kg is chosen. The overall weight of the system compared to the previous example is much lower due to the light camera. The overall weight of the UAV elements is 3.7 kg compared to 6 kg of the UAS designed with camera 4 onboard. The propulsion system weight is also much lighter, 0.60 kg compared to 3.53 kg, since a lighter UAS needs a smaller propulsion system. Furthermore, the reduced system weight leads to a smaller wing area and wing span since less lift is required.

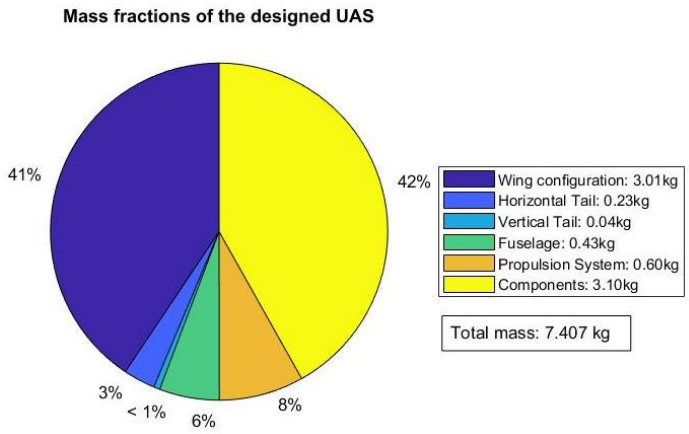

Figure 4.25: Mass fractions of the designed UAS with E and ACR priorities and for lane search pattern

The mission is fulfilled in 16 min compared to 9 min of the designed UAS with camera 4 onboard. This is a result of reduced weighting of the mission time and the increase of the weighting of the energy consumption. Figure 4.26 and Figure 4.27 present the flight altitude and the terrain elevation above MSL and the variation of the GSD obtained during the simulation. The mission is fulfilled at the average altitude of 1400 m above MSL. The flight altitude is reduced compared to the previous mission since camera 1 has a FOV of 59° compared to camera 4 with FOV of 32.1°. In order to maintain the desired GSD value with the decreased FOV, the flight altitude has to be reduced, see Eq. (2.5)-(2.6). For most times the GSD values are within the desired range and there are moments when the GSD values are slightly above the acceptable threshold.

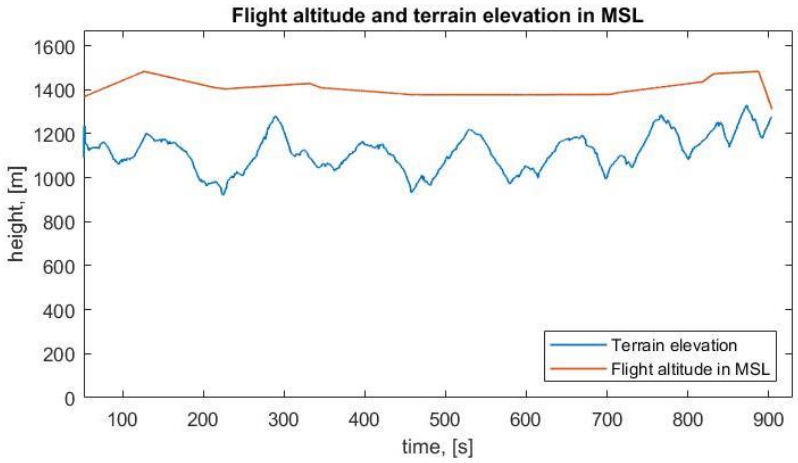

Figure 4.26: Flight altitude and terrain elevation for the UAS designed for E and ACR priorities

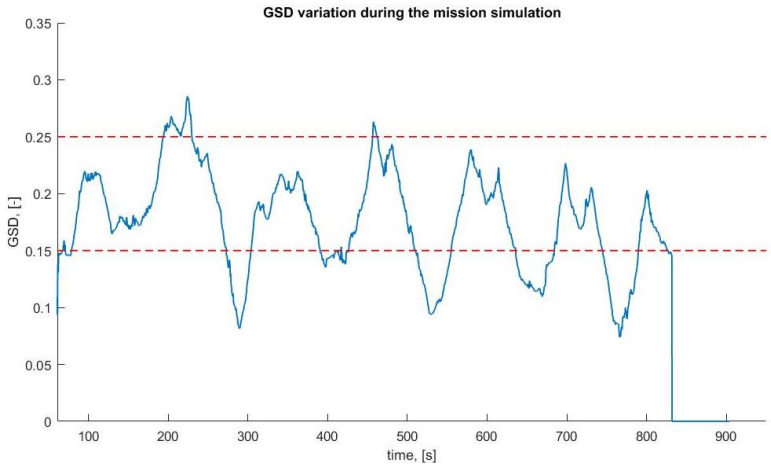

Figure 4.27: GSD variation during the simulation for the UAS designed for E and ACR priorities

However, the mission simulation with the designed UAS in the visualized operational environment shows that the coverage area has gaps, see Figure 4.28. As camera 1 has the larger FOV the UAV has to fly lower in order to maintain the desired GSD range. In relation to the low flight altitude any terrain elevation change leads to a larger GSD variation compared to a higher flight altitude. Due to the limited UAV thrust performance, it cannot follow perfectly the landscape shape and there are areas where the GSD is outside the desired range. On the areas with the small GSD the resolution on the ground is higher and the ground swath width is smaller, which might cause gaps in the area coverage. Although camera 4 is heavier, it allows flying with a more constant GSD level and therefore with a full area coverage of the high elevation difference landscape.

In order to improve the results of the presented simulation, the following can be done:

- increase overlap which will increase mission time;
- increase altitude which will increase ACR, however will reduce detection probability;
- improve waypoint locations which require to check GSD, UAV performance and communication LOS.

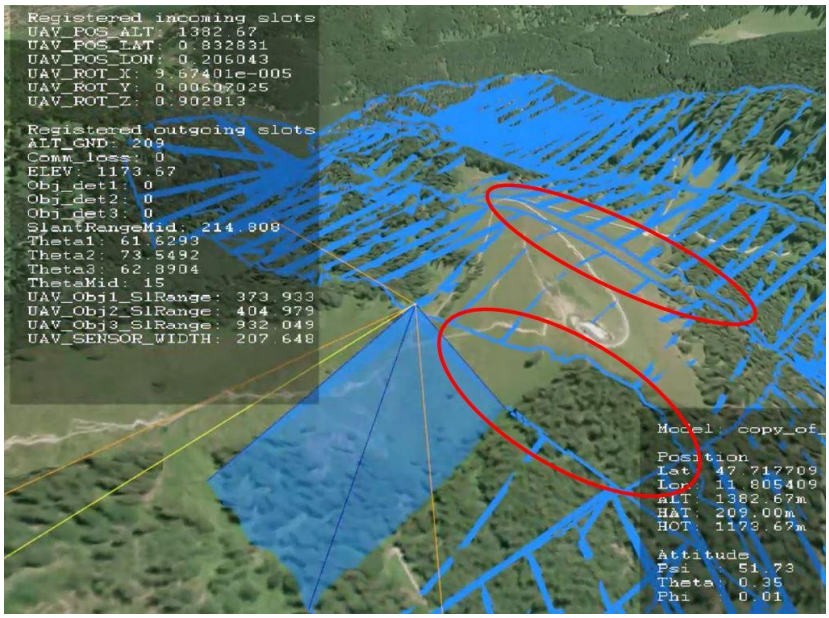

Figure 4.28: Gaps in the area coverage for the mission simulation in the operational environment with camera 1

Results of the detection probabilities are presented in Figure 4.29, Figure 4.30 and in Table 4.7. According to the Johnson criteria the probability to detect the missing person during the mission simulation is higher than 99% at each location point, see second graph. However, taking into consideration the time of the location points being in the field of view (vertical lines on the second graph), the probability to detect the person at location 1 is reduced to 94% and at location 2 is 0%. It is caused by the fact that point 2 turned out to be in one of the gaps in the coverage area and is not in the FOV of the camera, see Figure 4.29. Thus, the mission simulation in operational environment yields information about gaps and detection probabilities at the chosen location points.

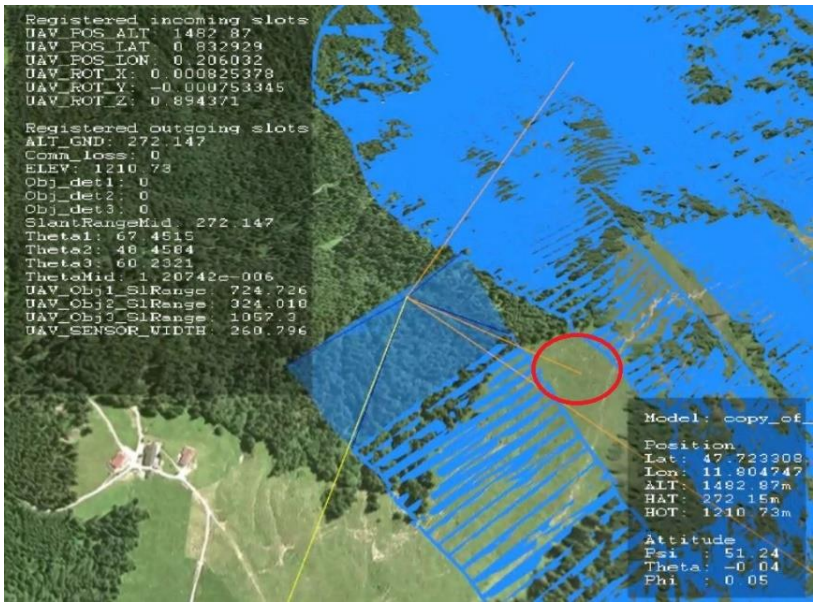

Figure 4.29: Location point 2 is in the gap during the mission simulation

Table 4.7: Probability detection at 3 location points for the UAS designed with E and ACR priorities and lane pattern

Location point	P_{det}	Time in the FOV	Final P_{det}
Location point 1	> 99 %	8 s	94 %
Location point 2	> 99 %	0 s	0 %
Location point 3	> 99 %	26 s	99 %

The presented examples show the influence of the onboard camera and the mission requirements on the UAS design and mission success. The size and weight of the camera as well as weights of other system elements drive the overall weight of the UAV and requirements for the propulsion system. However, in this example the UAS with heavier camera onboard fulfils the mission within the shortest period of time, full area coverage and with high probabilities of detection. By changing the mission requirements where the energy is the key evaluation criteria for the mission success the UAS optimization process resulted into a system with the lighter camera with bigger FOV onboard. Thus the UAV became smaller and lighter and requires less fuel for the mission. To maintain the desired image quality it has to fly with a lower flight altitude, which leads to gaps in the area coverage in case if the mission area is in mountains. Thus, one can see the interdependencies between the mission requirements, UAS design and payload performance. Additional graphs for this case are presented in B.2.

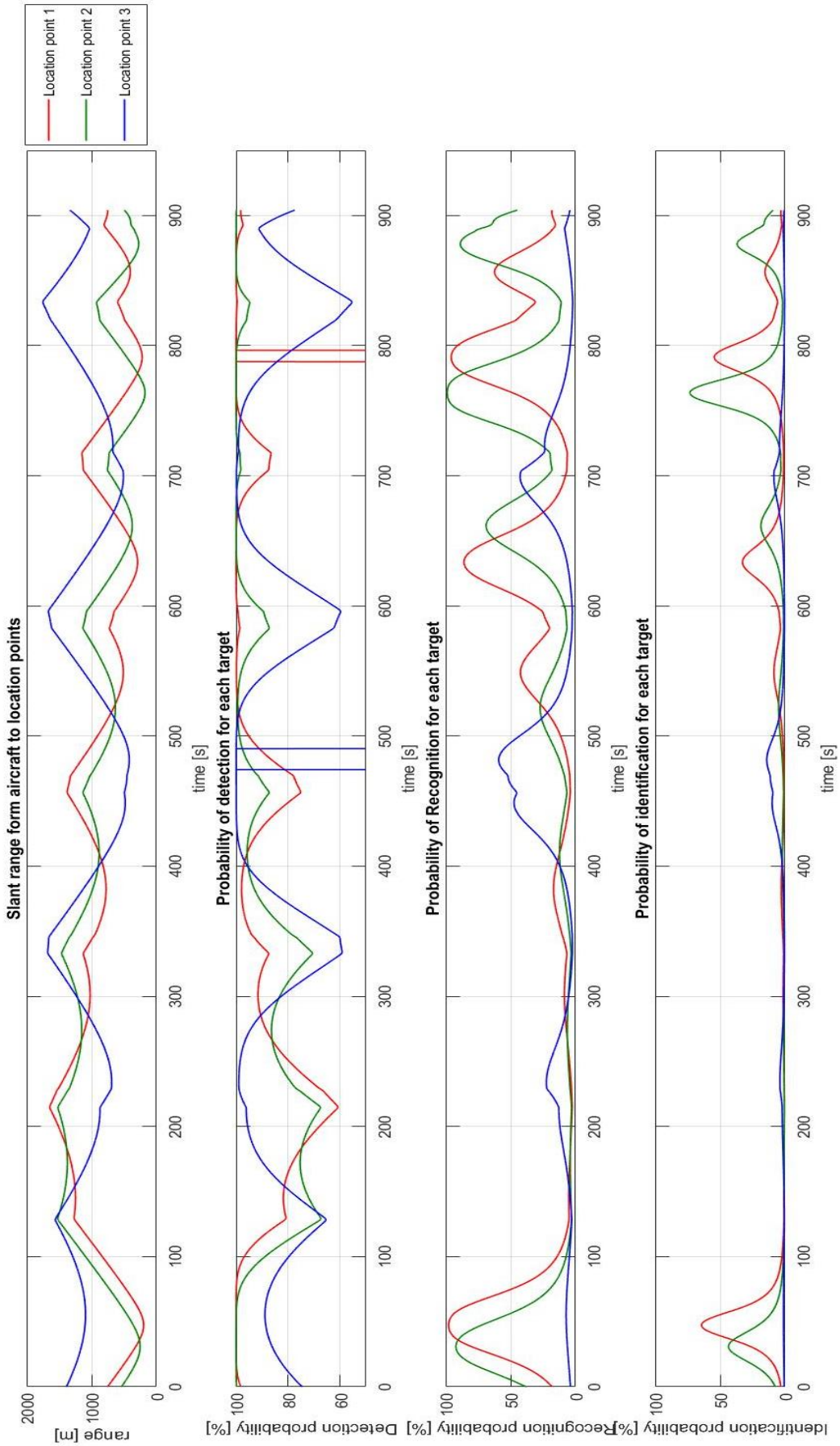

Figure 4.30: Probabilities of objects detection, recognition and identification for the UAS designed with E and ACR priorities and with the lane search pattern

4.2.2.2 Optimization with spiral search pattern

In this subsection the results of the UAS mission based optimization for the case with spiral search pattern are presented. The following weighting scheme for the key evaluation parameters is considered:

$$\alpha\,(ACR) = 0.1\,, \qquad \beta\,(E) = 0.05, \qquad \gamma\,(Pdet) = 0.4, \qquad \delta\,(T) = 0.4, \qquad \varepsilon\,(CA) = 0.05.$$

Same as for the previous example, the optimization is performed for 10 generations with 15 individuals so that in total 150 UAS different configurations are designed and evaluated. Figure 4.31 and Figure 4.32 present the progress of the MPI and design variables during the optimization. The highest MPI is achieved by three UASs, two of them with cameras 4 (MPI = 1.48 and MPI = 1.4) and one with camera 1 (MPI = 1.36). The best individuals are taken to the next generation and additional new UAS are generated. In the 5th generation UAS with camera 4 yield the highest MPIs and already from the 6th generation UAS only with camera 4 onboard are generated. The further optimization is necessary in order to narrow down the ranges of the other design variables.

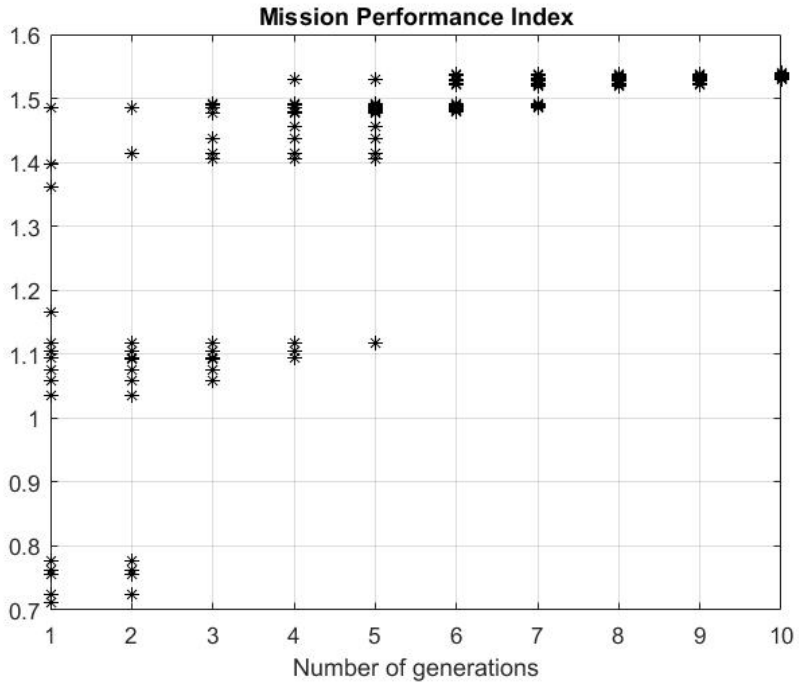

Figure 4.31: Progress of MPI during the optimization with spiral search pattern

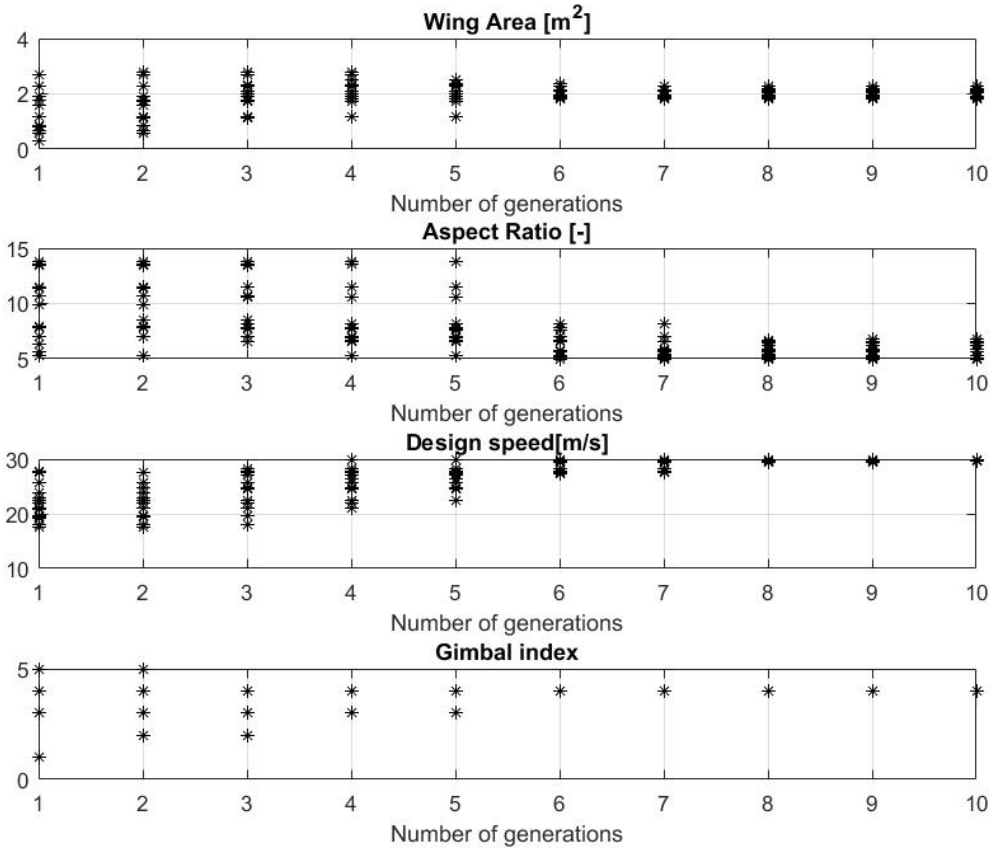

Figure 4.32: Progress of design variables during the optimization with spiral search pattern

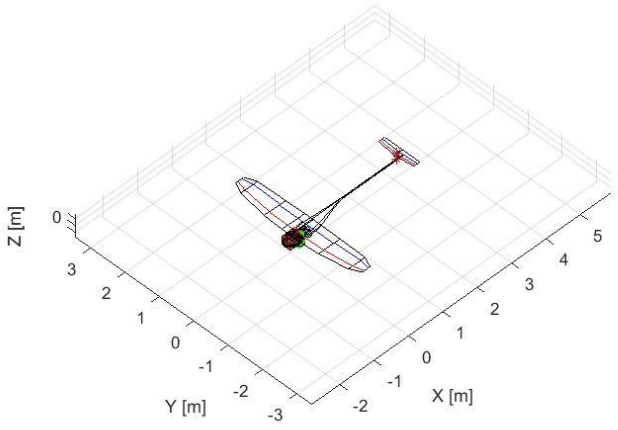

Figure 4.33: Optimized UAV for the case of spiral pattern

The optimized UAS yields a MPI= 1.54 and has the following characteristics: stall speed of 15.8 m/s, design speed of 30 m/s, a wing area of 2.09 m², 6.45 aspect ratio and camera 4 onboard. The optimized UAV with its onboard systems is presented in Figure 4.33. The wingspan is 3.68 m and the fuselage length is 3.42 m. The mass fractions of the designed system are presented in Figure 4.34. In the presented optimization study the designed UAS has camera 4 onboard, which has a weight of 16 kg.

This camera with the highest weight was chosen by the GAME algorithm due to the fact that time and detection probability have the highest weighting coefficients, 0.4 each, and energy weight coefficient is set very low, 0.025. The overall weight of the system is 29.6 kg, where onboard components have a total weight of 18.7 kg and the UAV structure together with the propulsion system is 10.9 kg.

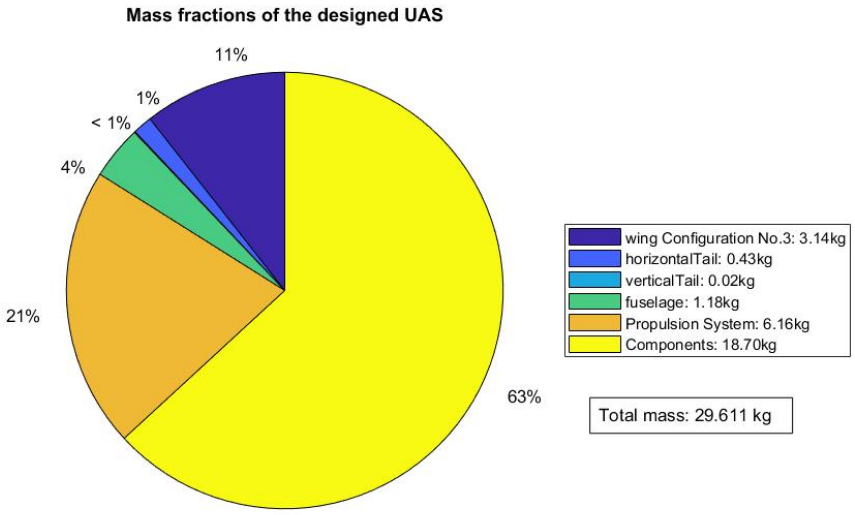

Figure 4.34: Mass fractions of the designed UAV for spiral search pattern

Figure 4.35 presents the mission simulation of the designed UAS with camera 4 on board in the operational environment. The search area is fully covered and the LOS between the ground control station and the UAV (yellow line) was not interrupted by the terrain. The orange colored lines depict slant ranges between the platform and the location points. This picture is done at the moment when location point 3 was in the camera field of view as evidenced by the visual location of the slant range line colored in orange and the signal data from left overlay window: Obj_det3 = 1 (Boolean “true”).

The mission is fulfilled in 14.5 min with an airspeed of 30 m/s. In Figure 4.36 the trajectory (right), altitude (left top), speed (left top) and control inputs (left middle and bottom left) are presented. The spiral flight path is calculated with 145 waypoints, leading to a round shape of passes. The flight system dynamic modelling is not the issue of the research in this work, therefore one can see imperfection of the trajectory planning expressed in additional circles (right picture in Figure 4.36, 3 small circles left) when moving from one full circle of the spiral path to another. This is caused by the fact that the values for PID controllers are set at the beginning of the optimization process and are not tuned during the optimization for each designed UAS, which lead to overshooting of the control inputs and roll angles during the flight simulation.

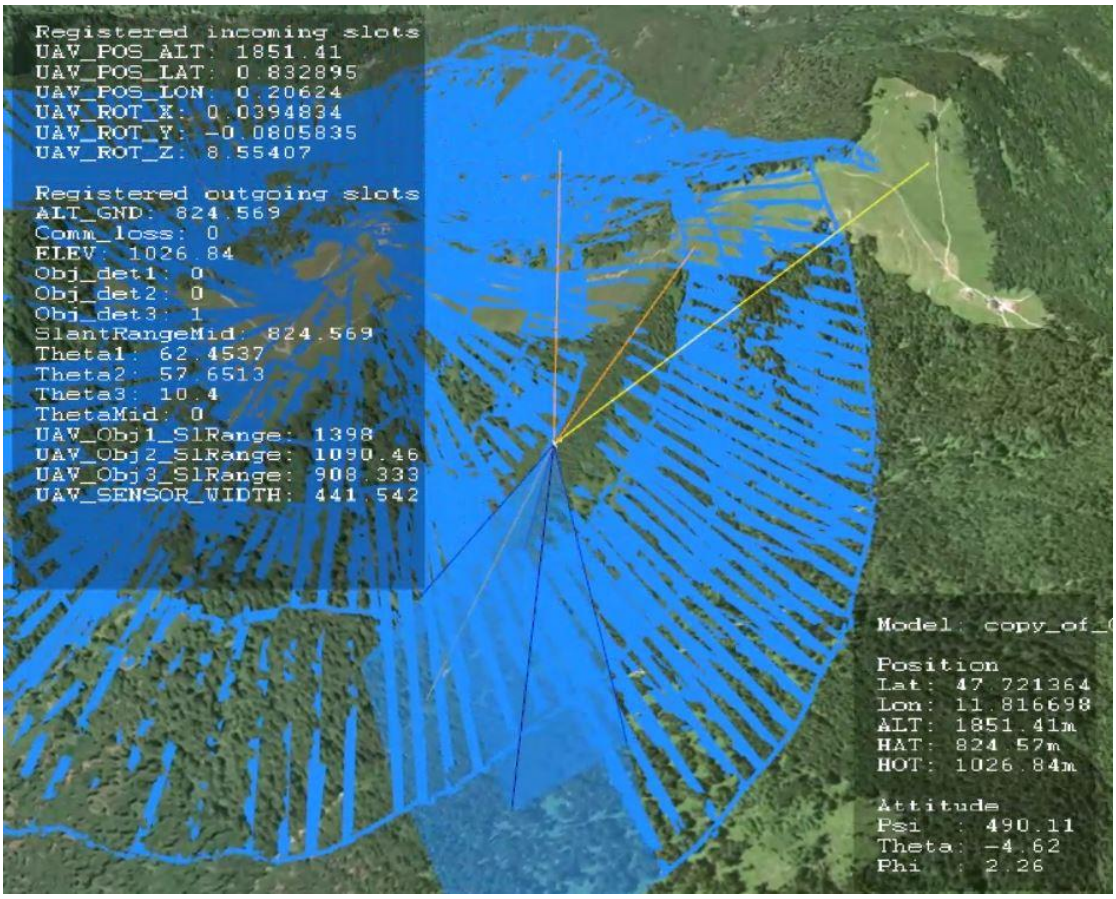

Figure 4.35: UAS mission simulation in the operational environment with camera 4 onboard and spiral search pattern

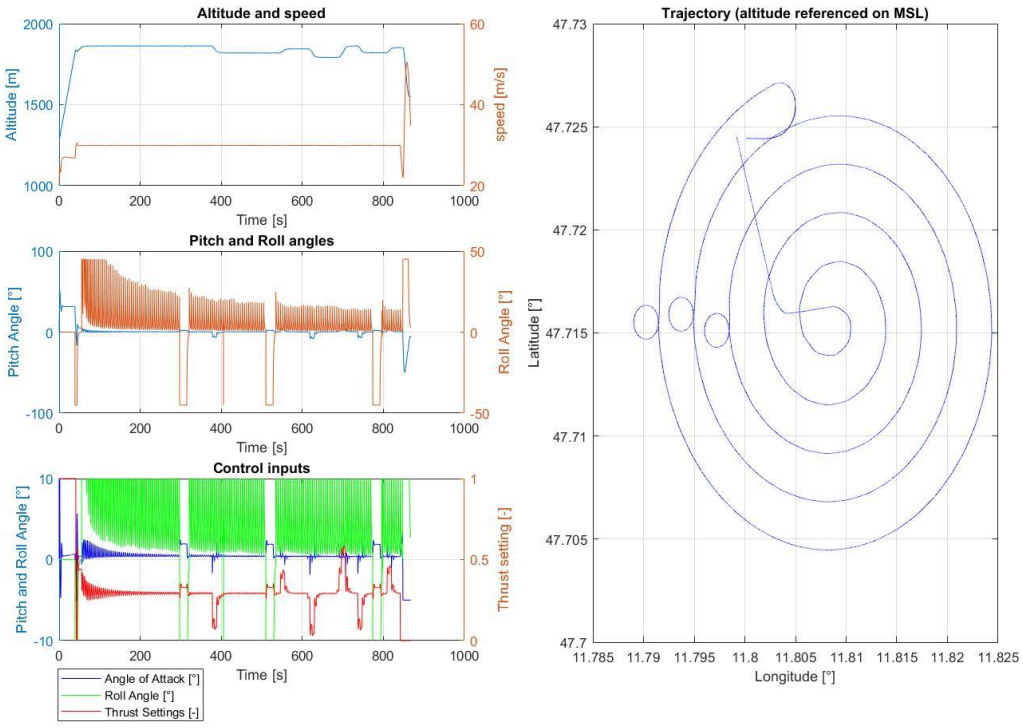

Figure 4.36: Results of the mission simulation for the spiral search pattern

The calculated flight path is presented in Figure 4.37. The altitude variation of the flight path is high and therefore requires significant thrust performance in order to fulfil all climbs and descends. Otherwise, when at the end of the simulation the thrust range is out of limits the mission is considered as non-flyable and MPI=0. Figure 4.38 presents the elevation of the terrain (blue line) and optimized (red line) flight altitude profiles above MSL. The altitude for each waypoint is calculated according to its elevation Eq. (2.5), the camera FOV and resolution. The optimized flight path is smoothed out and the collected GSD has an average value of required GSD=0.15, which is presented in Figure 4.39. The actual measured GSD values obtained during the mission simulation in the operational environment are colored with blue line and the trust GSD region is limited by red lines, where the required GSD=0.15 and the inacceptable GSD=0.25.

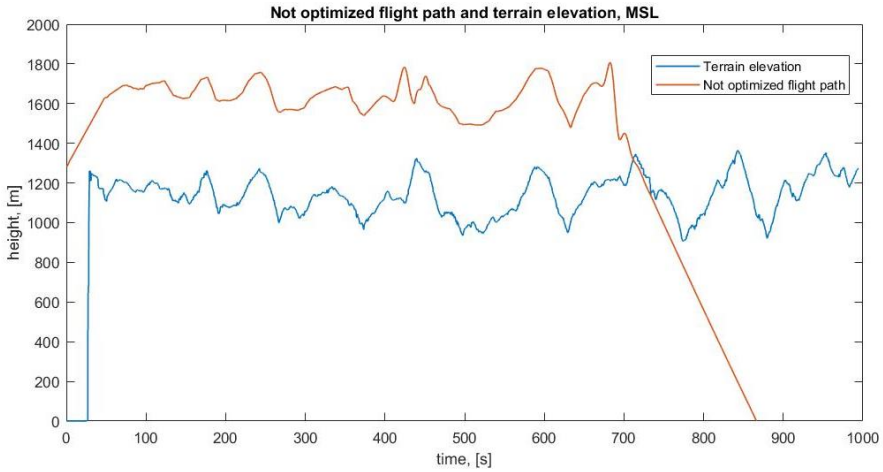

Figure 4.37: Not optimized flight path for SAR mission with spiral pattern

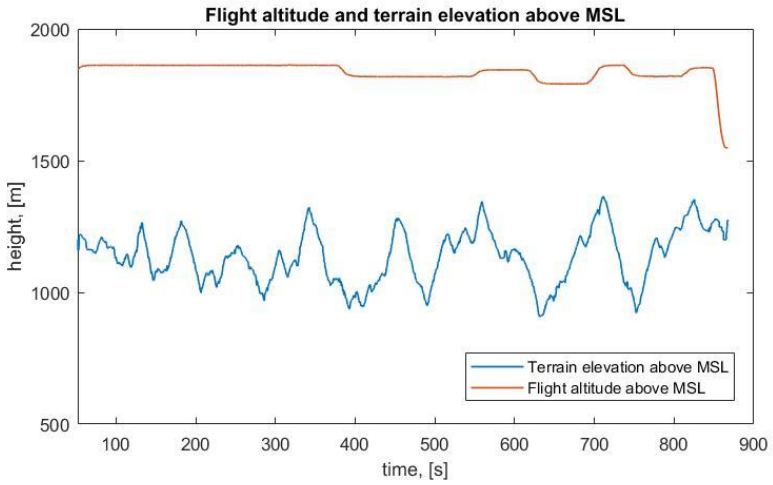

Figure 4.38: Flight altitude and height of the terrain in MSL for SAR mission and with spiral pattern

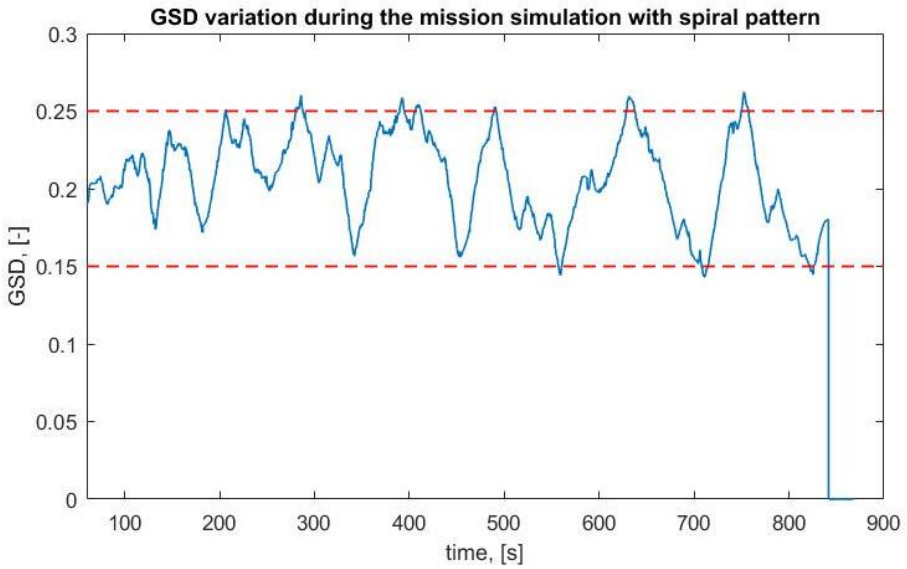

Figure 4.39: Measured GSD during the mission simulation with spiral search pattern in the visualized operational environment

The results of the detection probability of the missing person in 3 possible locations are presented in Figure 4.40. Slant ranges from the UAV to the location points on the ground at each time step are shown on the first graph. Based on it the detection probabilities according to the Johnson Criteria Eq. (2.10) are calculated and presented in the second graph. At each time step for all 3 locations the values are higher than 85%. The maximum residence times of the locations points in the FOV of the camera are marked on the graph with vertical lines and are used in Eq. (2.21) for MPI calculation. Thus, the following detection probabilities are obtained:

- For the first location 97%;
- For the second location 86%;
- For the third location 99%.

The third and fourth graphs present the probabilities of recognition and identification of the missing person. The recognition probabilities for locations 1 and 2 are higher than 60% during the residence time in the FOV and for the location 3 this value is only 50%. The probability to identify the missing person is 30% for location 2 and less for the other locations. In order to improve these values, the UAS has to fly lower or has to be equipped with a camera with a higher resolution.

Same as in the previous example with the UAS designed for the lane pattern, see Section 4.2.2.1, the detection probabilities at the beginning and at the end of the simulation are high. It is caused due to low altitudes when the UAV is climbing at the beginning and landing at the end of the mission.

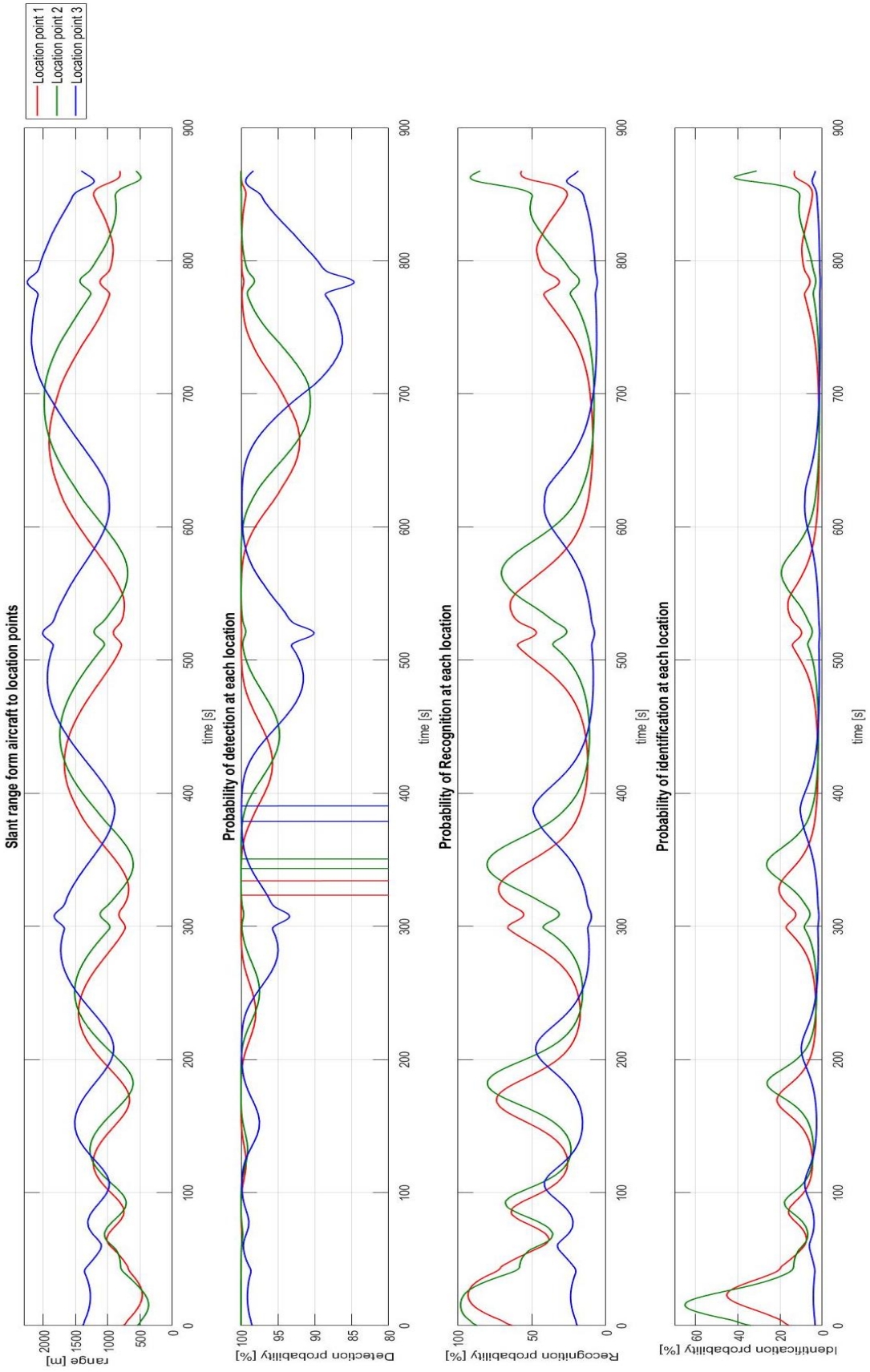

Figure 4.40: Probabilities of objects detection, recognition and identification according to Johnson Criteria during the mission simulation with spiral search pattern in the visualized operational environment

The dependency between the location points and flight circles is presented in Figure 4.41. Taking into account the longest time when each point is in the field of view of the camera (see Figure 4.40 vertical lines) one can see that location point 1 is in the field of view at the 3rd circle, which corresponds to the 320th second of the mission time. The detection time for this case is 9.5 s. However, according to the slant range distance (see Figure 4.40, first graph) to location point 1, it should be detected with a higher detection probability already at the 2nd circle, which corresponds to time 170 s. Here, the detection time is only 6.3 s, which reduces the detection probability, see Eq. (2.21). It should be noticed, that the flight altitude during the detection time for both circles is 1861 m above MSL with the same sensor ground swath width. Thus, the reason for the different detection times is that on circle 2 the location point is on the outer side of the flight path and on circle 3 it is on the inner side of the curved flight path, where the inner and outer areas of the camera's field of view have different angular velocities. In the outer area, the FOV of the camera sweeps over a certain area more quickly, resulting in a shorter detection time compared to the inner part with a smaller velocity.

The graphical representation of the UAS elements and its precise location in the visualized operational environment allows with high accuracy to assess detection probabilities of the sensor for a specified mission. The presented above effects can hardly be detected without a visualization environment.

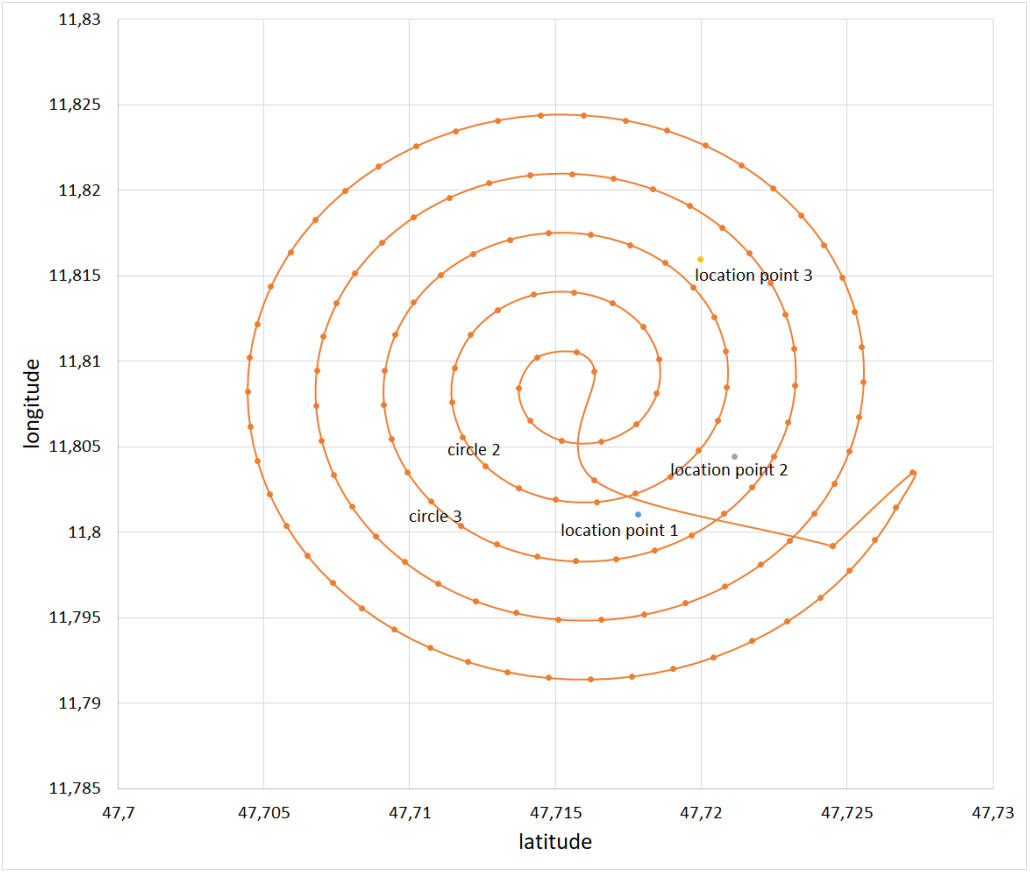

Figure 4.41: Flight path circles and detection probabilities for SAR mission

UAS optimization with E and ACR as key evaluation criteria and for spiral search pattern

In the following example a UAS is optimized for the same mission requirements as the presented above example but with a different weighting scheme:

$$\alpha\ (ACR) = 0.3\ \ \beta\ (E) = 0.6\ \ \gamma\ (Pdet) = 0.05\ \ \delta\ (T) = 0.025\ \ \varepsilon\ (CA) = 0.025$$

In this case energy and area coverage rate have the highest priority for the mission assessment and detection probabilities, mission time and communication losses have less impact. The results of the optimization are similar as for the UAS optimized with the same weighting scheme and for the lane pattern, see Section 4.2.2.1, where camera 1 was chosen for the optimum designed UAS.

Here, for the designed UAS camera 1 is chosen by the optimization process with the following parameters: FOV = 59°, resolution 1920 x 1080, weight 1.2 kg. The designed UAV is presented in Figure 4.42 and it has a wing area of 1.44 m², 13.3 aspect ratio, wingspan is 4.4 m and the fuselage length 1.55 m. The mass breakdown of the UAS is presented in Figure 4.43. Compared to the UAS designed for the detection probabilities and mission time priorities with camera 4 onboard, the overall weight of the structure of the designed UAV including the propulsion system is reduced from 10.9 kg to 3.5 kg.

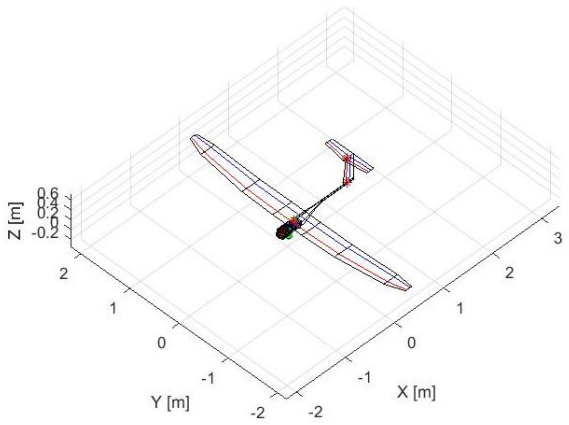

Figure 4.42: UAV designed for the case with E and ACR priorities, spiral pattern

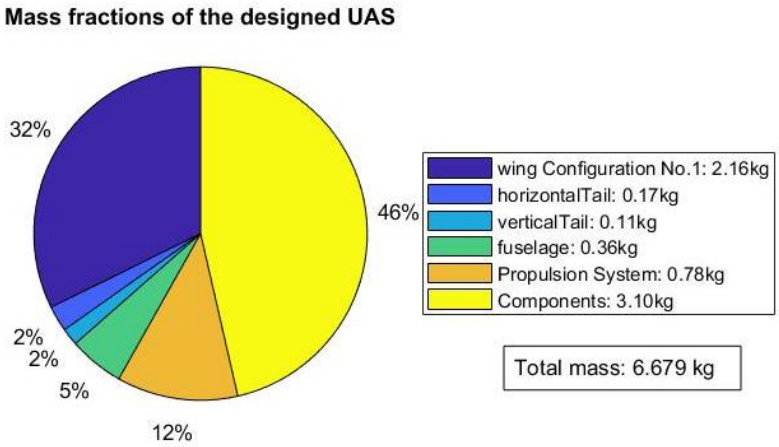

Figure 4.43: Mass fractions of the designed UAS for E and ACR priorities

The mission is accomplished in 25 minutes with a design speed of 15 m/s. Thus one can see that increasing of the weighting coefficient for energy reduces the design speed during the optimization compared to the previous example.

Figure 4.44 presents the GSD variations for the studied case. Most of the time the GSD stays in the desired range and at some points values are higher than the acceptable GSD = 0.25. That means that at these points quality of the collected data will not match the required. This is considered in the MPI over Johnson criteria as for it calculation the actual GSD value is taken. There are no gaps in the coverage area due to the good chosen overlap and the large amount of waypoints.

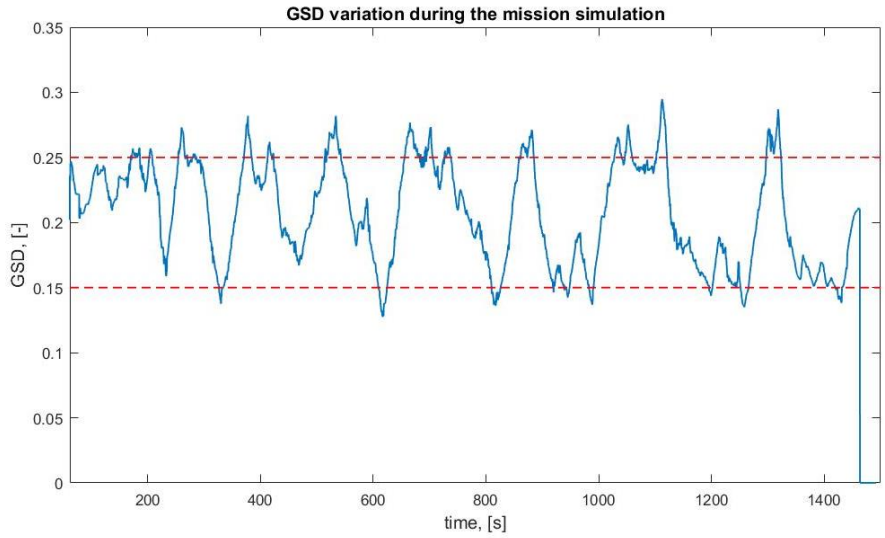

Figure 4.44: GSD variation for the UAS designed with E, ACR priorities and spiral pattern

The results of detection, recognition and identification of the missing person at 3 possible location points are presented in Figure 4.45. The detection probabilities for all 3 points according to Johnson criteria and residence time are 99%. Point 1 and 3 are detected at the same mission time as in the previous example, see 4.2.2.2. Since the airspeed is significantly lower one would expect to detect object 3 to a later mission time. But the bigger FOV of the mission camera onboard the designed UAS cause a bigger ground swath width, which allow to detect object 3 already at the second flight path circle. At point 2 the result is as expected, the designed UAV in this example needs more time to get to location point 2 due to a smaller sensor ground swath and therefore longer mission time.

The location point 1 is in the FOV of the camera for the longest time on the second circle of the spiral flight path which corresponds to mission time 260 s, see Figure 4.45. As it is described in the example above with UAS with camera 4 onboard, one would expect the longest detection time on circle 3 as well, especially since the waypoints in both simulations are identical. However, in this simulation with camera 1, the flight altitudes of the UAV on circle 2 and circle 3 above the location points are different. On circle 2, the UAVs' flight altitude is about 58 m higher than on circle 3 and therefore has a larger swath width along the flight direction, which compensates for the higher angular velocity and leads to a longer detection time. This is influenced by the flight path optimization. The same holds true for location point 3. Additional graphs describing the simulation result are presented in B.4.

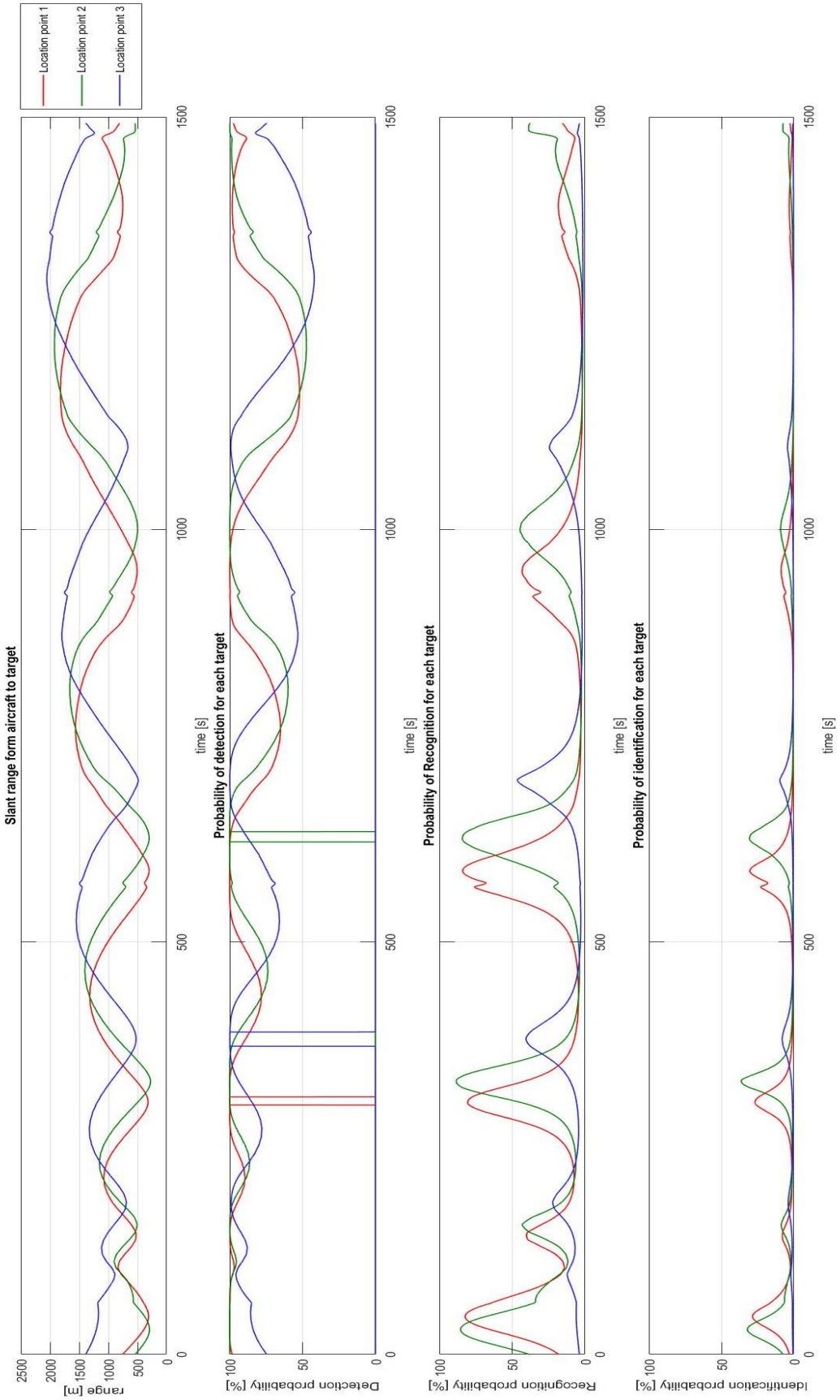

Figure 4.45: Probabilities of objects detection, recognition and identification during the mission simulation with spiral search pattern for the UAS design with E and ACR priorities

4.2.2.3 Comparison of designed UASs with different search patterns

In this section, a comparison between 2 designed UASs for spiral and lane patterns is described. In addition, each UAS is simulated with the different flight pattern: the UAS designed for the SAR mission with lane pattern, is now simulated with spiral pattern as well and the other way round.

Hereinafter, the following notation are adopted:

- UAS 1.1 is the UAS 1 designed and optimized for the mission with lane search pattern (a detailed description is given in section 4.2.2.1)
- UAS 1.2 is the UAS 1 designed and optimized for the mission with lane search pattern but the mission is simulated with spiral pattern
- UAS 2.1 is the UAS 2 designed and optimized for the mission with spiral search pattern (a detailed description is given in section 4.2.2.2)
- UAS 2.2 is the UAS 2 designed and optimized for the mission with spiral search pattern but the mission is simulated with lane pattern

Both UASs were designed with priorities in weightings coefficients for time and detection probabilities:

$$\alpha\ (ACR) = 0.1 \quad \beta\ (E) = 0.05 \quad \gamma\ (Pdet) = 0.4 \quad \delta\ (T) = 0.4 \quad \varepsilon\ (CA) = 0.05$$

Table 4.8 presents the results of the various mission simulations. UAS 1.1 is taken as a reference for the MPI calculation in order to provide a means of comparison.

Table 4.8: Comparison of mission simulation results

UAS vs search pattern	Pattern type	Mission time	Pdet at location 1 | 2 | 3 average	Energy	ACR	CA	MPI
UAS 1.1	lane	526 s	84% | 81% | 96% **87.0%**	0.1893	11018 m²/s	0.9994	1
UAS 1.2	spiral	885 s	99% | 88% | 99% **95.3%**	0.3213	11747 m²/s	0.9993	0.86
UAS 2.1	spiral	868 s	96% | 87% | 99% **94.0%**	0.3338	12090 m²/s	0.9997	0.86
UAS 2.2	lane	520 s	82% | 78% | 94% **84.7%**	0.2002	11132 m²/s	0.9998	0.99

Figure 4.46 and Figure 4.47 show the Johnson Criteria and residence time in the sensor's FOV for the simulations UAS 1.2 and UAS 2.2, respectively. The Johnson Criteria and the residence times of UAS 1.1 and UAS 2.1 are presented in section 4.2.2.1 and 4.2.2.2, respectively.

Comparison between lane and spiral flight path

The comparison between the simulations with lane flight path and spiral flight path shows that the missions with spiral flight path take considerably longer. To fly over the same area, the spiral flight path requires a longer distance than the flight path with lane pattern. Since all simulations show an almost identical flight speed, the UAS needs a longer time on the spiral flight path. The longer flight time leads to a higher energy consumption compared to the lane pattern.

Furthermore, the UAS flies on the optimized spiral flight path at a higher altitude (1859 m MSL) compared to the lane pattern, where the flight altitude is 1750 m MSL. The higher flight altitude leads to a larger ground swath width parallel to the flight direction, which results in a higher ACR. At the same time, the larger ground swath width parallel to the flight direction leads to a longer presence of the object in the FOV. The higher flight altitude also leads to a larger slant range to the object and thus to a smaller detection probability. However, this is close to 100 % according to Johnson Criteria for all simulations (compare Figure 4.46, Figure 4.47, Figure 4.21, Figure 4.40) and therefore the effect of the longer detection time outweighs the lower detection probability.

In summary, the larger ACR, the higher energy consumption, the longer mission time and the higher detection probability, together with the defined weightings, generally result in a significantly smaller MPI for the spiral flight path compared to the MPI for lane pattern simulation. Mainly the strongly reduced mission time for the lane pattern lead to this results, despite the lower detection probabilities.

Comparison between UAS 1 and UAS 2

When comparing the two different UAS used for the missions one can see that the UAS 1 has a longer mission time for both spiral and lane pattern. Table 4.9 shows the average mission design speed for the four simulations. The lower flight speeds lead to longer detection times and thus to a higher probability of detection of the objects during the missions flown with UAS 1, as Table 4.8 shows. The lower airspeed is also detectable in a smaller ACR. Furthermore, the total weight of UAS 1 is about 1 kg lighter than UAS 2 (see Sections 4.2.2.1 and 4.2.2.2). Together with the lower flight velocity, it leads to a lower energy consumption for UAV 1. In summary it can be stated that the higher detection probability and the lower energy consumption compensates for the longer mission time and the smaller ACR for the assumed weighting factors and therefore hardly any difference in MPI between UAV 1 and UAV 2 can be detected.

Table 4.9: Average flight design speed of the UASs during the mission

UAS 1.1	UAS 1.2	UAS 2.1	UAS 2.2
28.95 m/s	29.47 m/s	30.00 m/s	29.25 m/s

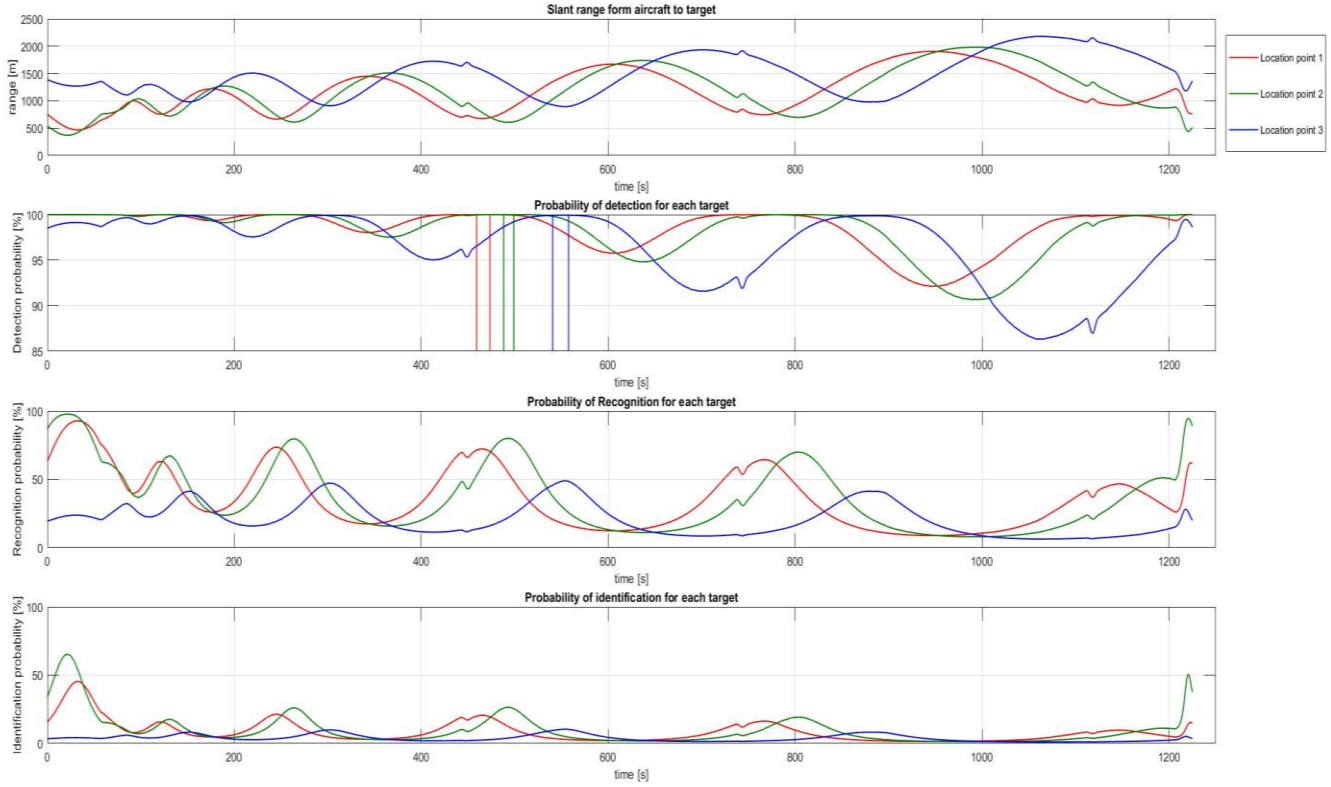

Figure 4.46: Results of detection probabilities for the mission simulation with UAS 1.2

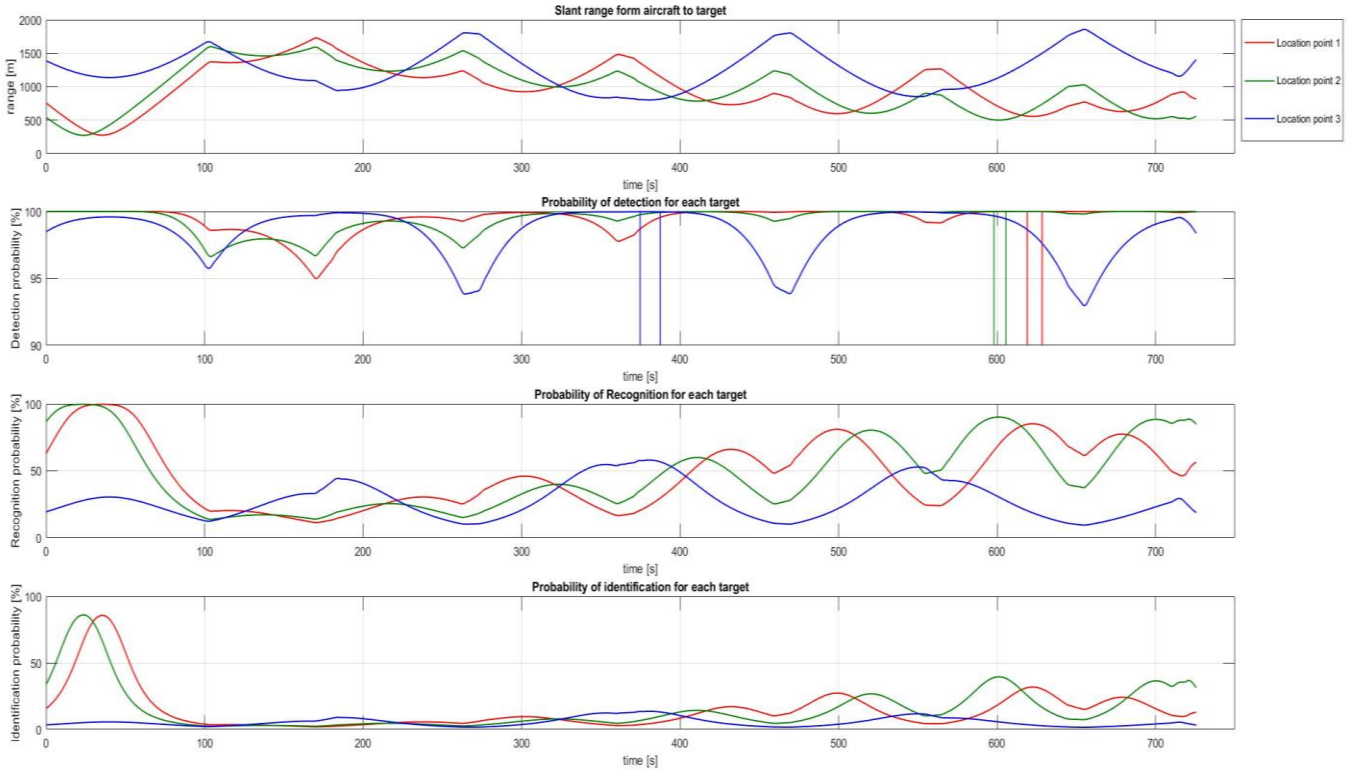

Figure 4.47: Results of detection probabilities for the mission simulation with UAS 2.1

4.3 Comparison of UASs designed for agriculture and SAR type of missions

In this section the UASs which have been optimized for the agriculture mission (see Section 4.1) and the search and rescue type of mission (Section 4.2) are compared. For this the simulations where each UAS performs the other type of mission, for which it was not optimized, are simulated.

UAS SAR is the UAS optimized and designed for the search and rescue type of mission, whereas UAS AG is designed for the agriculture mission.

Table 4.10 presents the results of the key performance parameters for both mission types and the calculated MPI referred to the optimized UAS for the specific mission, respectively.

Due to the different obtained design speeds, UAS SAR = 29.9 m/s compared to UAS AG = 21.2 m/s, the mission time and ACR differ for both UASs. UAS SAR performs the missions in a shorter time and with a larger ACR value. However, the high design speed leads to more fuel consumption. In addition, UAS SAR is equipped with the much heavier camera 4, compared to UAS AG with camera 1 on board, which increases the fuel consumption.

Table 4.10: Comparison table of UASs designed for agriculture and SAR type of missions

UAS	T	ACR	E	C	D	Pdet 1	Pdet 2	Pdet 3	MPI
Search and rescue mission									
UAS SAR	526	8469	0.1893	0.9994	0.8678	83%	81%	95%	1
UAS AG	689	5955	0.0375	0.6391	0.8575	85%	7%	99%	0.965
Agriculture mission									
UAS AG	3111	2020	0.1596	0.9998	0.6915	69%	69%	68%	1
UAS SAR	2470	2929	0.8465	0.9999	0.6251	68%	63%	56%	0.861

By comparing the detection probabilities of objects in three possible locations, one can observe that UAS AG shows mostly higher probabilities of detection. Since the required GSD within each mission type is the same, the different probabilities are a result of the different design speed only, since this directly influences the time within the camera range.

UAS AG reaches a relatively high MPI for the SAR type of mission. The high difference in energy consumption (factor of 5) push up the MPI despite its small weighting factor of 0.05, since the other key performance parameters vary much less and therefore are balanced out by the energy. However, due to camera 1 on board there are gaps in the covered area, which can be noticed during the visualization of the mission and is also detectable in the small detection probability of object 2. It was only detected within a small period of time, since the object lies at the border of the visible camera range. The same behavior with gaps was observed and described in detail in the mission simulation presented in section 4.2.2.1. Furthermore, the communication key performance parameter CA for the UAS AG in the SAR mission has smaller value. It is caused by the reduced flight altitude and strongly varying flight profile, which is a result of camera 1. There are line-of-sight interruptions because of shadowing effects of high terrain. Thus, according the high value of MPI of UAS AG and with respect to maximum flexibility one would rather use it for other missions.

The difference of MPIs for the agriculture type of mission is significant. UAS SAR performs much worse according to the desired mission performance criteria. Mainly the high energy consumption leads to the strongly reduced MPI value. For a real user, this will be the strongest argument to choose UAS AG despite the reduced ACR value.

5 Summary and Outlook

The goal of the presented thesis is to introduce an advanced mission simulation based methodological framework for the design of UAS, which combines mission requirements, aircraft design, payload, communication and other elements of an unmanned aerial system in a multidisciplinary design process. The result of such a process is a UAS tailored to the mission requirements fulfilling the mission best as possible.

5.1 Summary of the results

In classic aircraft design approaches sensor and communication performances are not part of primary requirements and are taken into account on the operational analysis stage, only. However, especially for UAS operations the interaction of the aircraft with the environment during the mission through the onboard sensors is of utmost importance for the success of a mission. Hereby, the camera sensor and communication performances become important. Therefore, in order to design an effective UAS solution beside the aircraft also the onboard systems have to be taken into account during the conceptual design.

For this, the multidisciplinary design environment is introduced. It consists of several environments presented in the sequence of utilization order in the design process:

- UAS design;
- UAS mission simulation and evaluation;
- Visualized operational environment;
- UAS optimization.

The mission based UAS design loop contains the optimization method called Genetic Algorithm for Multi-criteria Engineering in order to tailor a UAS to certain mission requirements. The design variables for the optimization are: wing area, aspect ratio, design speed and camera type. The following camera parameters are taken into account: resolution, VFOV and HVOF, frame rate and weight. Minimum stall speed is taken as constraint. The objective function of the UAS optimization process is to maximize the introduced in this work mission performance index, MPI, which defines mission performance success. The MPI is represented as a weighted sum of the following key mission performance parameters: area coverage rate, required energy, mission time, communication losses, detection probabilities and user operating issues.

The UAS design process starts with the analysis and definition of the mission requirements and weighting coefficients for the mission key performance parameters. Then, the first generation of UASs with a camera and payload onboard are designed. Each design is simulated in MATLAB and in the terrain based visualized operational environment presented in this work. Based on the obtained sensor and communication performances the overall mission performance is evaluated and assessed in form of MPI. The best designs are taken to the next generation and new designs are generated. This

procedure is fulfilled to each generated UAS design so that at the end a tailored UAS design for the specified mission is obtained.

Each of the parts of the design environment can be separately used from each other and applied on different design stages. The overall multidisciplinary environment is extendable and therefore new modules, functions and methods can and will be implemented. The emphasis of the multidisciplinary UAS design environment is on:

- Creating and using of a visualized operational environment where sensor and communication performance can be simulated, evaluated and included into the UAS design loop;
- Introduction of the Mission Performance Index, which allows to assess the mission success and to compare different UAS designs.

The presented visualized operational environment outmarks the first step towards this novel design process. Owing to the high resolution and elevation based terrain data, geometry representation of the UAS elements and its interaction with the environment, the sensor and communication performances are simulated. During the UAS mission simulation in the visualization environment the sensor performance is assessed based on the obtained sensor ground swath width, actual GSD values, presence time of objects of interest in the sensor FOV and the presence of uncovered areas. Some of the data, such as area coverage or sensor field of view limitations may be calculated mathematically, but in that case the elevation of the terrain as well as the tilt angle of the sensor are not taken into account. The communication performance is assessed based on the derived information whether the LOS between the UAV and the ground station was interrupted by the terrain and for how long. In addition, simulation of the sensor FOV in the visualization environment allows also to detect whether the field of view of the camera is limited by the aircraft body.

In the presented approach it is shown that the mission flight planning influences the sensor and communication performances and the overall mission success. The flight path planning is implemented into the mission simulation model for several flight patterns. In order to improve the flight path for mission areas with high elevation gradients, a flight path optimization algorithm was implemented. It reduces climbing and descending between the waypoints during the mission, which requires increased UAV flight performance. For the mission performance evaluation it also assessed if the designed UAV can fulfil the required flight path, which is considered in the MPI as well.

In order to validate the feasibility of the presented multidisciplinary UAS mission simulation and evaluation environment for the design of civil UAS, two application studies are presented. The first one is presented by the agricultural study, where several runs of the optimization process prove the overall feasibility of the UAS design and evaluation environment. The influence of mission requirements such as required GSD, side and forward overlaps on the sensor and communication performances as well as on the overall UAS design were investigated.

The second application study is presented by a search and rescue mission in the area with high elevation gradient emphasizing the usage of the operational environment for mission success evaluation. By simulating the mission in the visualized operational environment it was possible to indicate gaps in the coverage area, obstacles in line of sight, communication losses and limitations of different flight patterns. The results of the study have shown that sensor ground swath width and ground footprint are uneven during the mission, which lead to gaps in the coverage area. In order to avoid them, the camera characteristics, size of overlaps, flight altitude and type of flight pattern have to be investigated and optimized together.

The modeling of application studies has shown that depending on the parameter with the greatest weight in the MPI, the designed system changes its configuration including sensor onboard and mission performance results. In case of probability and detection priority, the camera with the highest resolution and smallest FOV was chosen. In terms of mission performance, it brings the best results in form of full coverage area within the shortest possible period of time and high detection probabilities. However, at the same time the camera has the biggest weight, which leads to an enlarged UAV, propulsion system and overall weight of the system. In contrast, for the case when energy has the highest priority, an UAS was designed with the lightest camera onboard leading to a lighter and smaller UAV. However, during the mission simulation, the results of mission success have not been as good as in the previous example, as there have been gaps in the coverage area and one of the search locations turned out to be in one of these gaps.

The simulated FOV of the camera in the visualized operational environment allows to see “what the camera sees” and therefore to derive the time when the object of interest is in the FOV. In the simulations it was shown, that according to Johnson criteria the objects detection probability was 99%, but taking into account the time being in the FOV of the sensor obtained from the mission simulation in the visualized environment the object was in one of the gaps of the coverage area and was not in the camera FOV.

Thus, it was shown that in order to obtain an effective UAS solution for specific mission requirements, the performance of all system elements, especially sensor and communication systems, have to be investigated already at the conceptual UAS design stage, which requires a multidisciplinary design approach. The presented in the thesis UAS mission simulation and evaluation environment allows exploring UAS tradeoffs for civil applications and not only for flat mission areas, but for areas with high elevation differences as well. Owing to the visualized operational environment, the performances of sensor and communication systems are simulated, evaluated and included into the UAS design loop for the first time.

5.2 Outlook

The presented multidisciplinary approach for UAS design covers a wide range of technologies and methods across the aircraft design discipline. However, some simplifications and assumptions have been done in order to focus on the overall UAS design approach presentation and methods of mission performance evaluation for civil applications using the visualized operational environment. Further

areas of potential work and modelling improvements are introduced in this section and can be divided into 4 groups: UAV design, mission modelling, visualized operational environment and evaluation & optimization.

UAV design

In the presented mission based UAS design environment a modular approach is used. That means that each part of the overall design process can be extended by new functions or exchanged completely by another design process.

In the topic of UAV design the propulsion system is the area of potential improvements. For small UAVs operating at low altitudes the propulsion system is mostly presented by propellers, which can be powered by a combustion engine or by an electric motor. In the presented UAV design approach the propulsion system is calculated by a model for a simple combustion engine. However, for small fixed-wing UAVs depending on mission requirements other types of propulsion systems can be used such as electrically driven propulsion or hybrid electric propulsion. Electric motors are much simpler to design and integrate, they have little maintenance, can be custom designed and build with minimal costs compared to other propulsion types. The short endurance is the biggest limitation of this propulsion type. Hybrid electric propulsion systems combine traditional power plants with battery-electric propulsion. According to (Gundlach 2012) it offers improved reliability of a power plant through battery backup, increased electrical power available for payloads, improved fuel efficiency and low acoustic flight, which can improve sensor performance. The downside of this propulsion system is additional weight due to additional generators, motors, batteries and electronics, which makes the systems also more complex. Therefore, implementation of electric and hybrid power plants models will increase the UAS design area.

Furthermore, an improved and enlarged data base for various sensors and communication systems, with weight, power consumption, size and performance values will increase the UAS design space and mission evaluation analysis.

Mission modelling

At the current stage the simulation time of the presented environment can take up to 24 hours. It depends on the mission area size, type of flight pattern, number of individuals and generations. Of course, this time is also influenced by computer calculation and graphic card power. In order to reduce the simulation time, an elevation map of the mission area in MATLAB for flight path waypoints definition should be developed. The available terrain data base in the visualized operational environment contains elevation data as well, however it is only used during the mission simulation and evaluation stage when the flight path is already defined. The usage of this data base for the mission elevation map in MATLAB will make the software independent from the Google Earth service, as it requires internet connection and not all versions of it support the “get elevation data” function and will allow a MATLAB function to access elevation data much faster compared to the current way of using the Google Earth software (version 7.1.2.2041).

Visualized operational environment

The visualized operational environment presented in this thesis is based on the open source toolkit osgVisual and can be expanded with additional functions based on needs. For example, a rendering function depicting a mission area on the terrain might be useful for further data assessment. By calculating intersections between the mission area and the ground swath trail of the sensor it can give a percentage of the area covered by the sensor.

Evaluation & Optimization

The UAS mission performance evaluation model can be enhanced by additional communication analysis. At the current stage communication losses during the mission simulation are taken into account in the MPI. The analysis concerning band width, transmission rate influenced by design speed, flight path overlaps and camera resolution is performed only for already optimized UAS. Therefore, its implementation into the MPI and into the optimization loop will enhance the UAS design process.

The potential improvement in the optimization process concerns the number of design variables. At the moment wing area, aspect ratio, design speed and camera index are used as design variables. More potential design variables for an UAS are presented in (Gundlach 2012, p.722), for example such as number of engines, propulsion type and fuel weight or battery weight.

All these improvements will expand the UAS design space for civil missions, improve accuracy of some parameters and give the user more data for mission assessment.

In mid-2020 MathWorks released a new toolbox, specifically for UAV simulation (MathWorks 2020). It allows designing, simulating, and deploying UAV applications in a visual environment. This is the best proof of the importance and relevance of the topic UAS and its early mission simulation. UAS simulations are an important key point to further develop this technology and thus to establish and include further markets and applications. It confirms the correctness of the approach presented in this thesis optimizing and designing UASs with the help of a visualization environment and taking sensor and communication performances into account during the design loop, already.

6 Publication bibliography

Aber, James S.; Marzolff, Irene; Ries, Johannes B.: Small-format aerial photography. Principles, techniques and geoscience applications. 1. ed. Available online at http://site.ebrary.com/lib/alltitles/docDetail.action?docID=10411924.

Aber, James S.; Marzolff, Irene; Ries, Johannes B.; Aber, Susan E.W. (2019): Small-Format Aerial Photography and UAS Imagery: Elsevier.

Austin, Reg (2010): Unmanned air vehicles. UAV design, development, and deployment. Chichester, West Sussex, U.K, Hoboken, NJ: Wiley.

Bertuccelli, Luca; Choi, Han-Lim; Cho, Peter; How, Jonathan. (Eds.) (2009): Real-Time Multi-UAV Task Assignment in Dynamic and Uncertain Environments. AIAA Guidance, Navigation, and Control Conference. Chicago, Illinois, 10-13 August. American Institute of Aeronautics and Astronautics (AIAA-2009-5776).

Buckley, John (2006): Air Power in the Age of Total War. 1st ed. London: Taylor and Francis (Warfare and History).

Buede, Dennis M. (2016): The Engineering Design of Systems: Models and Methods, 3rd Edition: John Wiley & Sons.

Dannhauer, Torben (2009): osgVisual. Institute of Flight Dynamics, Technical University of Munich. Available online at https://www.osgvisual.org, checked on 2020 April.

de Serpa Marques e Braga Barbosa, Bernardo (2019): Development of a MATLAB Module for Flight Pattern Planning for Various Types of Civil UAS Missions. Semester Thesis. Technical University of Munich, Munich. Institut of Aircraft Design.

European Aviation Safety Agency (2009): Airworthiness certification of unmanned aircraft systems (UAS). Policy Statement. E.Y013-01.

Fahlstrom, Paul Gerin; Gleason, Thomas James (2012): Introduction to UAV systems. 4. ed. Chichester, West Sussex: Wiley (Aerospace Series).

Feger, Jens (Ed.) (2015): Simulationsmodell zur Bewertung der Missionserfüllung unbemannter Fluggeräte im Vorentwurfsstadium. 64. Deutschen Luft- und Raumfahrtkongress. Rostock, Germany, 22-24 September. Deutsche Gesellschaft für Luft-und Raumfahrt.

Feger, Jens; Fokina, Ekaterina; Hornung, Mirko (Eds.) (2018): An integrated design process for mission optimized design of unmanned aerial vehicles. AIAA Aerospace Sciences Meeting. Kissimmee, Florida, USA, 8-12 January. American Institute of Aeronautics and Astronautics (AIAA 2018-1007).

Fokina, Ekaterina; Feger, Jens; Hornung, Mirko (2018a): A Mission Performance Evaluation Approach for Civil UAS Applications. In *MATEC Web Conf.* 221 (2). DOI: 10.1051/matecconf/201822105006.

Fokina, Ekaterina; Feger, Jens; Hornung, Mirko (Eds.) (2018b): An integrated UAS Design Optimization based on Mission Assessment and Evaluation. 67. Deutscher Luft- und Raumfahrtkongress. Friedrichshafen, Germany, 4-6 September. Deutsche Gesellschaft für Luft-und Raumfahrt. Available online at https://www.dglr.de/publikationen/2019/480148.pdf.

Fokina, Ekaterina; Feger, Jens; Hornung, Mirko (Eds.) (2018c): UAV, sensor and mission matching approach using the visualization environment. Aviation Technology, Integration, and Operations Conference. Atlanta, Georgia, USA, 25-29 June. American Institute of Aeronautics and Astronautics. Available online at https://arc.aiaa.org/doi/abs/10.2514/6.2018-3204.

Fokina, Ekaterina.; Feger, Jens.; Hornung, Mirko (2019): Application of a visualization environment for the mission performance evaluation of civilian UAS. In *CEAS Aeronaut J* 10 (3), pp. 817–825. DOI: 10.1007/s13272-018-0350-z.

Fonseca, Carlos M.; Fleming, Peter (Eds.) (1993): Genetic algorithms for multiobjective optimization: Formulation, discussion and generalization. 5th International Conference on Genetic Algorithms. San Mateo, CA, USA.

Göktogan, Ali Haydar; Sukkarieh, Salah; Cole, David; Thompson, Paul (2005): Airborne Vision Sensor Detection Performance Simulation.

Gomez, Mario; Preece, Alun; Johnson, Matthew; Mel, Geeth de: An Ontology-Centric Approach to Sensor-Mission Assignment. In : Lecture Notes in Computer Science, vol. 5268, pp. 347–363.

Gundlach, Jay (2012): Designing Unmanned Aircraft Systems. Reston, VA, USA: American Institute of Aeronautics and Astronautics.

Gundlach, Jay (2016): Civil and commercial unmanned aircraft systems: American Institute of Aeronautics and Astronautics.

Hochstrasser, Markus (2012): Erweiterung einer Hardware-in-the-Loop-Simulation um eine Flugzeug-Visualisierungsumgebung basierend auf Open GL und Matlab/Simulink. Semester Thesis. Technical University of Munich, Munich. Institut of Flight System Dynamics.

Holzapfel, Florian (2017): Flight System Dynamics I. Institute of Flight System Dynamics. Technical University of Munich, 2017.

Hornung, Mirko (2020): Fundamentals of Aircraft Operations. Institute of Aircraft Design. Technical University of Munich, 2020.

Hutton Barron, F. (1992): Selecting a best multiattribute alternative with partial information about attribute weights. In *Acta Psychologica* 80 (1-3), pp. 91–103. DOI: 10.1016/0001-6918(92)90042-C.

Jain, Aditya; Bansal, Ramta; Kumar, Avnish; Singh, K. D. (2015): A comparative study of visual and auditory reaction times on the basis of gender and physical activity levels of medical first year students. In *International journal of applied & basic medical research* 5 (2), pp. 124–127. DOI: 10.4103/2229-516X.157168.

Johnson, John (Ed.) (1958): Analysis of image forming systems. Image Intensifier Symposium. Warfare Electrical Engineering Department, U.S. Army Research and Development Laboratories, Ft. Belvoir, Va.

Kingston, Derek; Rasmussen, Steven; Humphrey, Laura (Eds.) (2016): Automated UAV tasks for search and surveillance. IEEE Conference on Control Applications (CCA). Buenos Aires, Argentina, 19-22 September. IEEE.

Langer, Harald (2005): Extended evolutionary algorithms for multiobjective and discrete design optimization of structures. Dissertation. Technical University of Munich, Munich, Germany. Available online at http://mediatum2.ub.tum.de/doc/601979/document.pdf.

Matarazzo, Benedetto (1986): Multicriterion analysis of preferences by means of pairwise actions and criterion comparisons (MAPPACC). In *Applied Mathematics and Computation* 18 (2), pp. 119–141. DOI: 10.1016/0096-3003(86)90020-2.

MathWorks (2020): UAV Toolbox: MathWorks. Available online at https://de.mathworks.com/products/uav.html.

Mavris, Dimitri; DeLaurentis, Daniel (Eds.) (1995): An integrated approach to military aircraft selection and concept evaluation. Aircraft Engineering, Technology, and Operations Congress. Los Angeles, CA, USA, 19-21 September. American Institute of Aeronautics and Astronautics (AIAA-95-3921).

Morawietz, Sten; Strohal, Michael; Stütz, Peter (Eds.) (2018): A Decision Support System for the Mission-Based Evaluation of Aerial Platforms: Advancements and Final Validation Results. Aviation Technology, Integration, and Operations Conference. Atlanta, Georgia, USA, 25-29 June. American Institute of Aeronautics and Astronautics (AIAA 2018-3975).

Morawietz, Sten; Strohal, Michael; Stütz, Peter (Eds.) (2019): A Mission-Based Approach for the Holistic Evaluation of Aerial Platforms: Implementation and Proof of Concept. 18th AIAA/ISSMO Multidisciplinary Analysis and Optimization Conference. Denver, Colorado, USA, 5-9 June. American Institute of Aeronautics and Astronautics (AIAA 2017-4152).

OpenSceneGraph (2020): OpenSceneGraph. Available online at http://www.openscenegraph.org, checked on Mai 2020.

Perez, Daniel; Maza, Ivan; Caballero, Fernando; Scarlatti, David; Casado, Enrique; Ollero, Anibal (2013): A Ground Control Station for a Multi-UAV Surveillance System. In *J Intell Robot Syst* 69 (1-4), pp. 119–130. DOI: 10.1007/s10846-012-9759-5.

Preece, Alun; Gomez, Mario; Mel, Geeth de; Vasconcelos, Wamberto; Sleeman, Derek; Colley, Stuart et al. (Eds.) (2008): Matching sensors to missions using a knowledge-based approach. SPIE Defence and Security Symposium. Orlando, Florida, USA, 16-20 March (Defense Transformation and Net-Centric Systems 2008, 6981).

Qassim A. Abdullah: Geospatial Applications of Unmanned Aerial Systems (UAS). UAS Mission Planning and Control. The Pennsylvania State University, College of Earth and Mineral Sciences. Available online at https://www.e-education.psu.edu/geog892/node/658, checked on Mai 2020.

Rößler, Christian Ottmar (2012): Conceptual design of unmanned aircraft with fuel cell propulsion system. Disseration. Technical University of Munich, Munich, Germany.

Saaty, Thomas L. (1990): How to make a decision. The analytic hierarchy process. In *European Journal of Operational Reseaarch* 48 (1), pp. 9–26.

SPH Engineering (2020): UgCS. Available online at https://www.ugcs.com, checked on Mai 2020.

Sundog Software LLC: SilverLining and Trition by Sundog Software. 3D Cloud, Sky, Ocean, and Water Visual Simulation. Available online at https://sundog-soft.com/, checked on Mai 2020.

Torenbeek, Egbert (2013): Advanced aircraft design. Conceptual design, analysis and optimization of subsonic civil airplanes. Chichester: Wiley (Aerospace Series).

Valavanis, Kimon P.; Vachtsevanos, George J.: Handbook of unmanned aerial vehicles. Available online at http://dx.doi.org/10.1007/978-90-481-9707-1.

Wolf, Paul R.; Dewitt, Bon A.; Wilkinson, Benjamin E. (2014): Elements of photogrammetry with applications in GIS. 4th ed.: McGraw-Hill Education.

Appendix A UAS simulation environment

A.1 Visualized operational environment: Example of XML file configuration file

```
<?xml version="1.0" encoding="utf-8"?>
<config>
   <module enabled="true" name="sky_silverlining">
      <udp/>
   </module>
   <module name="dataio">
      <udp filename="..\AC-Design\06_Configs\LARUS\VisualConfig\UDPSettings.xml" socket="vcl"/>
   </module>
   <window bgColor="#c0c0c0" fullScreen="false" samples="4" screen="0" windowDecoration="true" windowName="SAR" x="100" y="100">
      <view>
         <perspective aspectRatio="*" fovy="70" zFar="12500" zNear="1"/>
      </view>
   </window>
   <overlay aspectRatio="0.8889" mask="KEY_F1|KEY_F5" objectName="Configuration No.5" type="debugModel"/>
   <overlay aspectRatio="0.8889" mask="KEY_F1|KEY_F5" type="debugVCL"/>
   <overlay aspectRatio="0.8889" mask="KEY_F1" type="debugCamera" viewName="viewport1"/>
   <overlay aspectRatio="0.8889" mask="KEY_F2" type="DetectionTargetOverlay"/>
   <scenery mask="">
      <terrain filename="..\terrain.osgb"/>
      <model dynamic="yes" label="" mask="KEY_F1|KEY_F5" objectName="Configuration No.5">
         <attitude rot_x="0" rot_y="0" rot_z="0"/>
         <updater>
            <position alt="UAV_POS_ALT" lat="UAV_POS_LAT" lon="UAV_POS_LON"/>
            <attitude rot_x="UAV_ROT_X" rot_y="UAV_ROT_Y" rot_z="UAV_ROT_Z"/>
            <label text="Configuration No.5"/>
         </updater>
         <camera key="KEY_F1" type="LookAt">
            <position alt="571.209099418058" lat="48.27535" lon="11.822642"/>
         </camera>
         <camera freeAzimut="false" freeBank="true" freePith="true" key="KEY_F2" type="Mounted">
            ...
         </camera>
         <camera freeAzimut="false" freeBank="false" freePitch="false" key="KEY_F3" type="Uavcam">
            ...
         <camera freeAzimut="true" freeBank="true" freePith="true" key="KEY_F4" type="Mounted">
            ...
         <camera bodyFixedUp="true" distance="5" key="KEY_F5" minDistance="0.022" step="2" stepZoom="0.2" type="Movable">
            ...
         <geometry filename="..\AC-Design\06_Configs\LARUS\Configuration No.5_Geometry.stl">
            <offset rot_x="180" rot_y="0" rot_z="180"/>
            <scalefactor scale_x="1" scale_y="1" scale_z="1"/>
         </geometry>
         <coordinatesystem enabled="false" mask="KEY_F5" orientation="body" thickness="0.01" xLength="2" yLength="2" zLenght="2"/>
         <SensorCone HFOV="59" VFOV="33.1875" enabled="true" height="660.426629172127" mask="KEY_F1|KEY_F5" type="pyramid"/>
         <VisualTrail Width="3" enabled="false" mask="KEY_F1|KEY_F5" numPoints="100000">
            <position alt="471.209099418058" lat="48.27535" lon="11.822642"/>
         </VisualTrail>
         <DataLink enabled="true" linkwidth="1" mask="KEY_F1|KEY_F5">
            <position alt="521.209099418058" lat="48.27535" lon="11.822642"/>
         </DataLink>
         <GroundTrail Width="7" enabled="true" mask="KEY_F1|KEY_F5" numPoints="100000">
            <position alt="471.209099418058" lat="48.27535" lon="11.822642"/>
         </GroundTrail>
         <Communication enabled="false" linkwidth="1" mask="KEY_F1|KEY_F5">
            <position alt="471.209099418058" lat="48.27535" lon="11.822642"/>
         </Communication>
         <position alt="471.209099418058" lat="48.27535" lon="11.822642"/>
         <MissionDefinition enabled="false" linewidth="14" mask="KEY_F1|KEY_F5">
            <position alt1="471.209099418058" alt2="560.426629172127" ... lat1="48.27535" ... lon1="11.822642" .../>
         </MissionDefinition>
         <SearchMission enabled="true" linkwidth="1" mask="KEY_F5">
            <position alt1="476" alt2="473" alt3="475" lat1="48.268282" ... />
         </SearchMission>
      </model>
      <atmosphere mask="">
         <datetime day="7" hour="7" minute="30" month="4" timeZone="CET" useSystemTime="false" year="2020"/>
         <visibility range="20000" turbidity="1"/>
         <clouds/>
         <windlayer bottom="500" direction="90" speed="0" top="1100"/>
      </atmosphere>
   </scenery>
</config>
```

Figure A.1: Example of XML file configuration for visualized operational environment

A.2 Visualized operational environment: Example of UDP configuration file

```
<?xml version="1.0" encoding="utf-8"?>
<CONFIGURATION>
   <CHANNEL multicast_freq="10" multicast_in_group="10.162..." multicast_in_port="25000" name="CHANNEL_MULTICAST_OSG_IN">
      <ENTRY attrib="NONE" expression="" max="10" min="0" name="UAV_POS_LAT" type="DOUBLE" unit="m" value="0"/>
      <ENTRY attrib="NONE" expression="" max="10" min="0" name="UAV_POS_LON" type="DOUBLE" unit="m" value="0"/>
      <ENTRY attrib="NONE" expression="" max="10" min="0" name="UAV_POS_ALT" type="DOUBLE" unit="m" value="0"/>
      <ENTRY attrib="NONE" expression="" max="10" min="0" name="UAV_ROT_X" type="DOUBLE" unit="m" value="0"/>
      <ENTRY attrib="NONE" expression="" max="10" min="0" name="UAV_ROT_Y" type="DOUBLE" unit="m" value="0"/>
      <ENTRY attrib="NONE" expression="" max="10" min="0" name="UAV_ROT_Z" type="DOUBLE" unit="m" value="0"/>
      <ENTRY attrib="NONE" expression="" max="10" min="0" name="UAV_CAM_ROT_X" type="DOUBLE" unit="m" value="0"/>
      <ENTRY attrib="NONE" expression="" max="10" min="0" name="UAV_CAM_ROT_Y" type="DOUBLE" unit="m" value="0"/>
      <ENTRY attrib="NONE" expression="" max="10" min="0" name="UAV_CAM_ROT_Z" type="DOUBLE" unit="m" value="0"/>
   </CHANNEL>
   <CHANNEL multicast_out_group="10.162..." multicast_out_port="25001" name="CHANNEL_MULTICAST_OSG_OUT">
      <ENTRY attrib="NONE" expression="" max="10" min="0" name="ELEV" type="DOUBLE" unit="m" value="0"/>
      <ENTRY attrib="NONE" expression="" max="10" min="0" name="ALT_GND" type="DOUBLE" unit="m" value="0"/>
      <ENTRY attrib="NONE" expression="" max="10" min="0" name="UAV_SENSOR_WIDTH" type="DOUBLE" unit="m" value="0"/>
      <ENTRY attrib="NONE" expression="" max="10" min="0" name="UAV_Obj1_SlRange" type="DOUBLE" unit="m" value="0"/>
      <ENTRY attrib="NONE" expression="" max="10" min="0" name="Theta1" type="DOUBLE" unit="m" value="0"/>
      <ENTRY attrib="NONE" expression="" max="10" min="0" name="Obj_det1" type="DOUBLE" unit="m" value="0"/>
      <ENTRY attrib="NONE" expression="" max="10" min="0" name="UAV_Obj2_SlRange" type="DOUBLE" unit="m" value="0"/>
      <ENTRY attrib="NONE" expression="" max="10" min="0" name="Theta2" type="DOUBLE" unit="m" value="0"/>
      <ENTRY attrib="NONE" expression="" max="10" min="0" name="Obj_det2" type="DOUBLE" unit="m" value="0"/>
      <ENTRY attrib="NONE" expression="" max="10" min="0" name="UAV_Obj3_SlRange" type="DOUBLE" unit="m" value="0"/>
      <ENTRY attrib="NONE" expression="" max="10" min="0" name="Theta3" type="DOUBLE" unit="m" value="0"/>
      <ENTRY attrib="NONE" expression="" max="10" min="0" name="Obj_det3" type="DOUBLE" unit="m" value="0"/>
      <ENTRY attrib="NONE" expression="" max="10" min="0" name="Comm_loss" type="DOUBLE" unit="-" value="0"/>
      <ENTRY attrib="NONE" expression="" max="10" min="0" name="SlantRangeMid" type="DOUBLE" unit="-" value="0"/>
      <ENTRY attrib="NONE" expression="" max="10" min="0" name="ThetaMid" type="DOUBLE" unit="-" value="0"/>
   </CHANNEL>
</CONFIGURATION>
```

Figure A.2: Example of UDP configuration for visualized operational environment

A.3 Visualized operational environment: Example of a camera FOV simulation settings in the main configuration settings file

```
<window bgColor="#c0c0c0" fullScreen="false" samples="4" screen="0" windowDecoration="true" windowName="..." x="0" y="0" width="1920" height="1200">
   <view width="1920" height="1200">
      <perspective aspectRatio="*" fovy="70" zFar="12500" zNear="1"/>
   </view>
</window>

<model dynamic="no" label="Object 1" mask="" objectName="..">
   <position alt="476" lat="48.275" lon="11.799"/>
   <attitude rot_x="0" rot_y="180" rot_z="0"/>
   <geometry filename="..\..\cow.osg">
      <offset rot_x="0" rot_y="0" rot_z="0"/>
      <scalefactor scale_x="1.0" scale_y="1.0" scale_z="1.0"/>
   </geometry>
</model>
```

Figure A.3: Camera FOV simulation settings in the main osgVisual configuration file

In order to set this option in the visualized operational environment, one needs to use the window view of the visual camera called “Mounted” under key F4, see Figure 3.8. Furthermore, the resolution of the view window on the screen needs to be specified according to the resolution of the real camera installed onboard the UAV, see an example of the code lines in A.3.

Appendix B Simulation results for SAR application

B.1 Mission simulation for SAR application with not optimized lane pattern

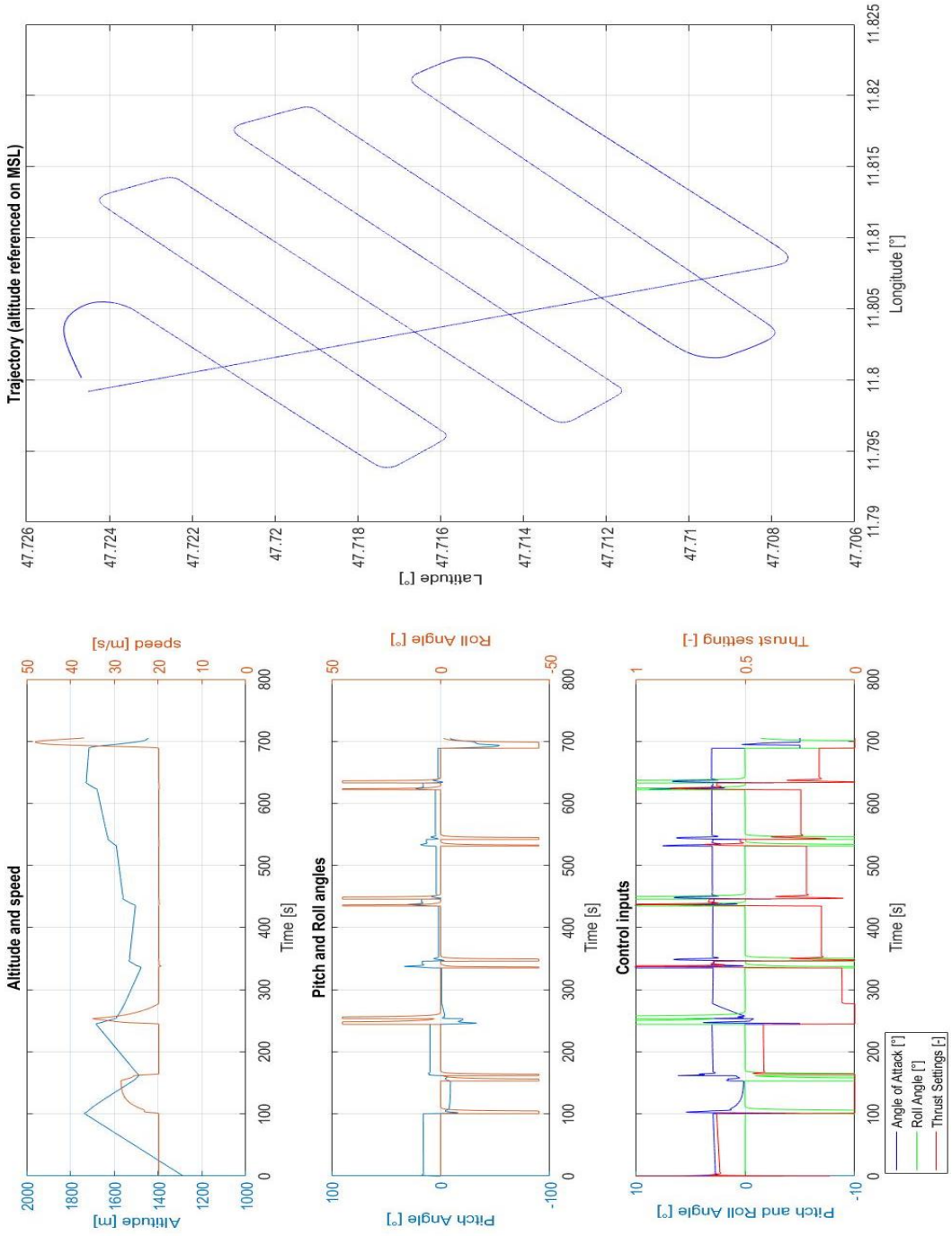

Figure B.1: Mission simulation results for SAR application with not optimized lane search pattern

B.2 Mission simulation for SAR application with UAS optimized for the case with E and ACR priorities and with the lane search pattern

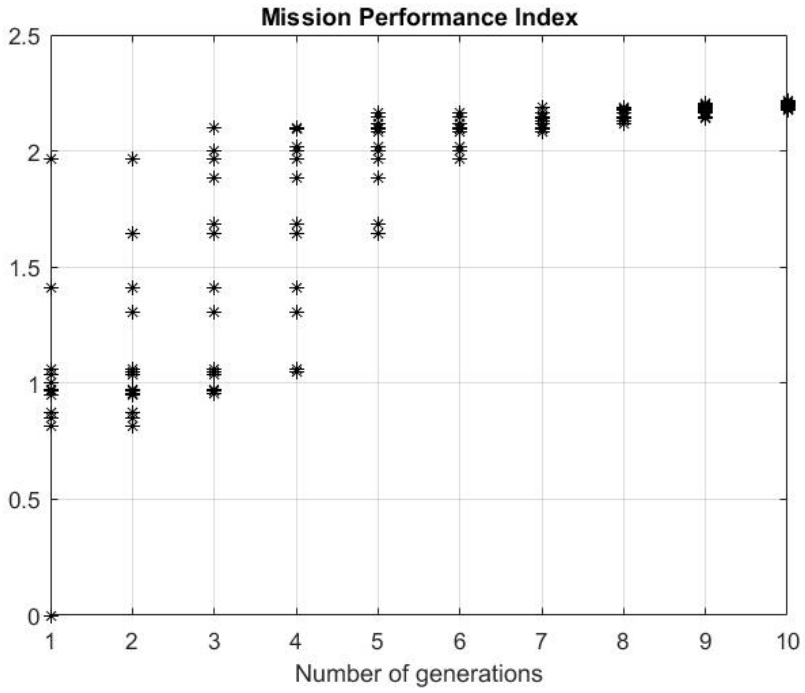

Figure B.2.1: Progress of MPI during the UAS design for the case with E and ACR priorities and with the lane search pattern

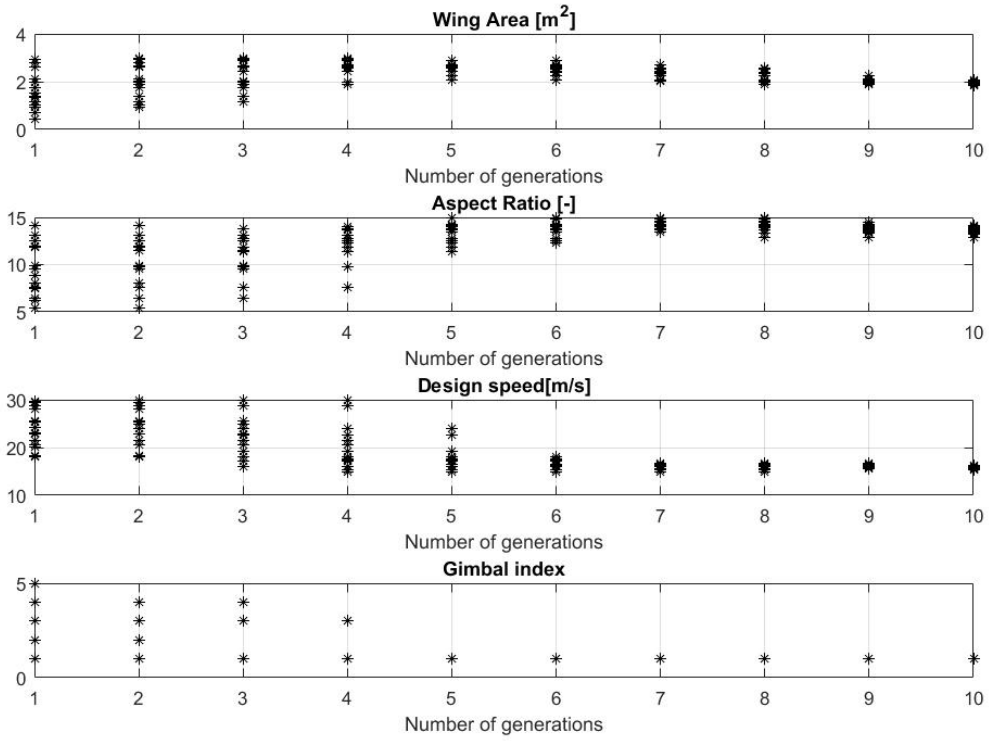

Figure B.2.2: Progress of design variables during the UAS design for the case with E and ACR priorities and with the lane search pattern

B.3 Mission simulation for SAR application with not optimized spiral pattern

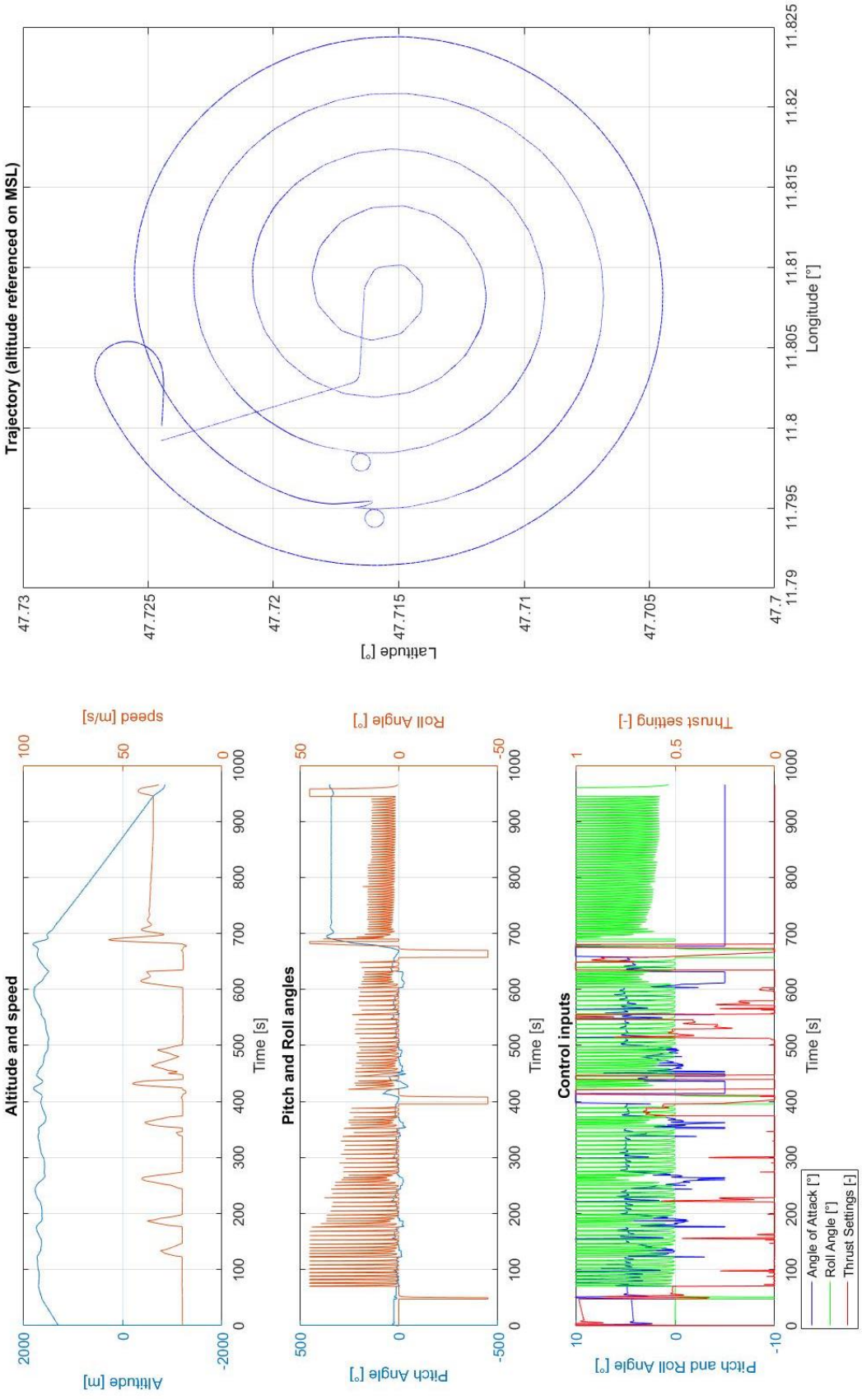

Figure B.3: Mission simulation results for SAR application with not optimized spiral search pattern

B.4 Mission simulation results for the UAS designed with E and ACR priorities, spiral pattern

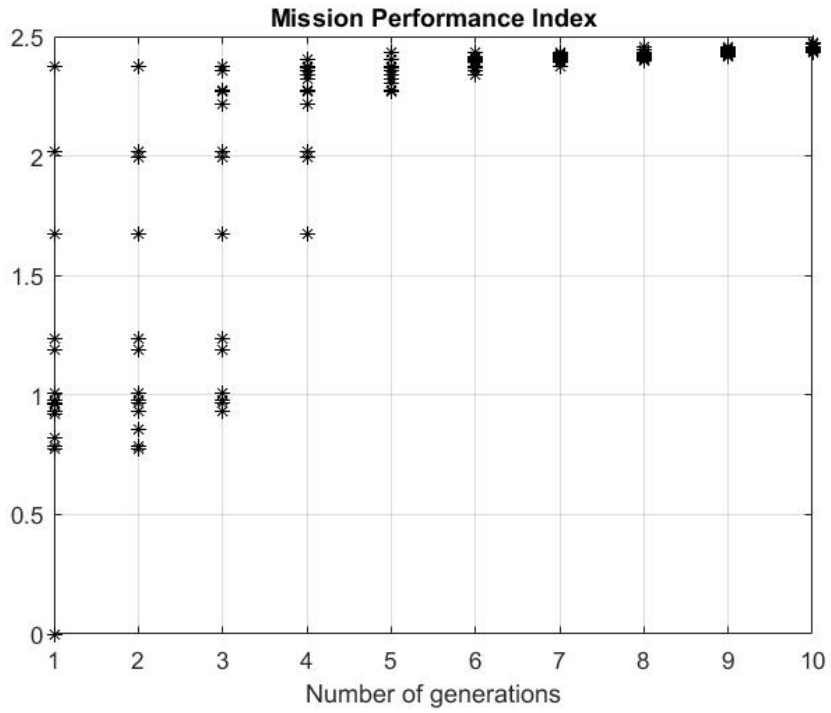

Figure B.4.1: MPI variation of the UAS optimization for the case with E and ACR priorities and spiral pattern

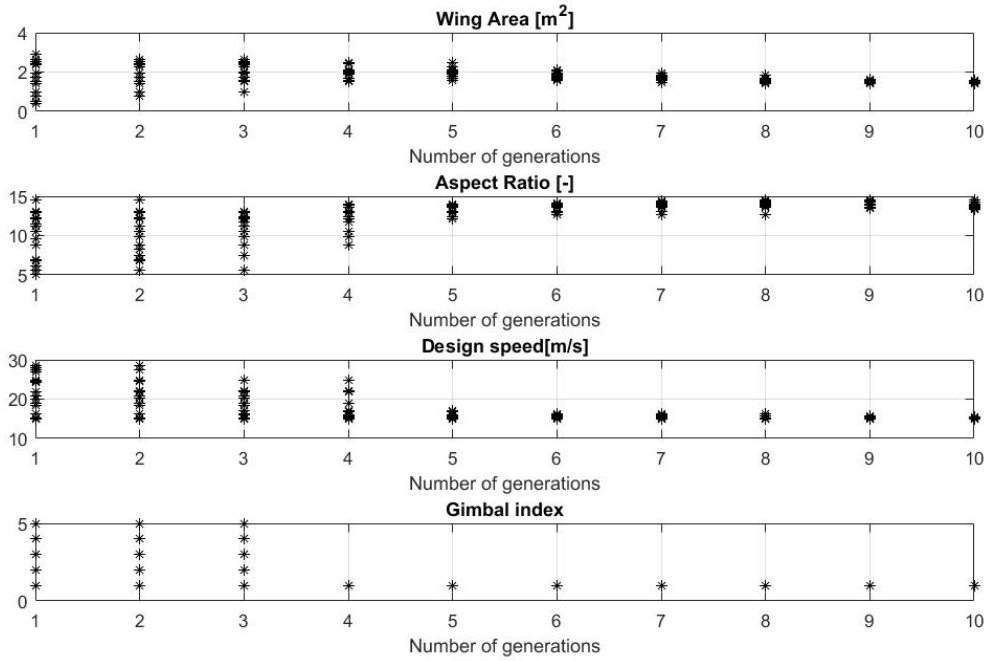

Figure B.4.2: Design variables variation of the UAS optimization for the case with E and ACR priorities and spiral pattern

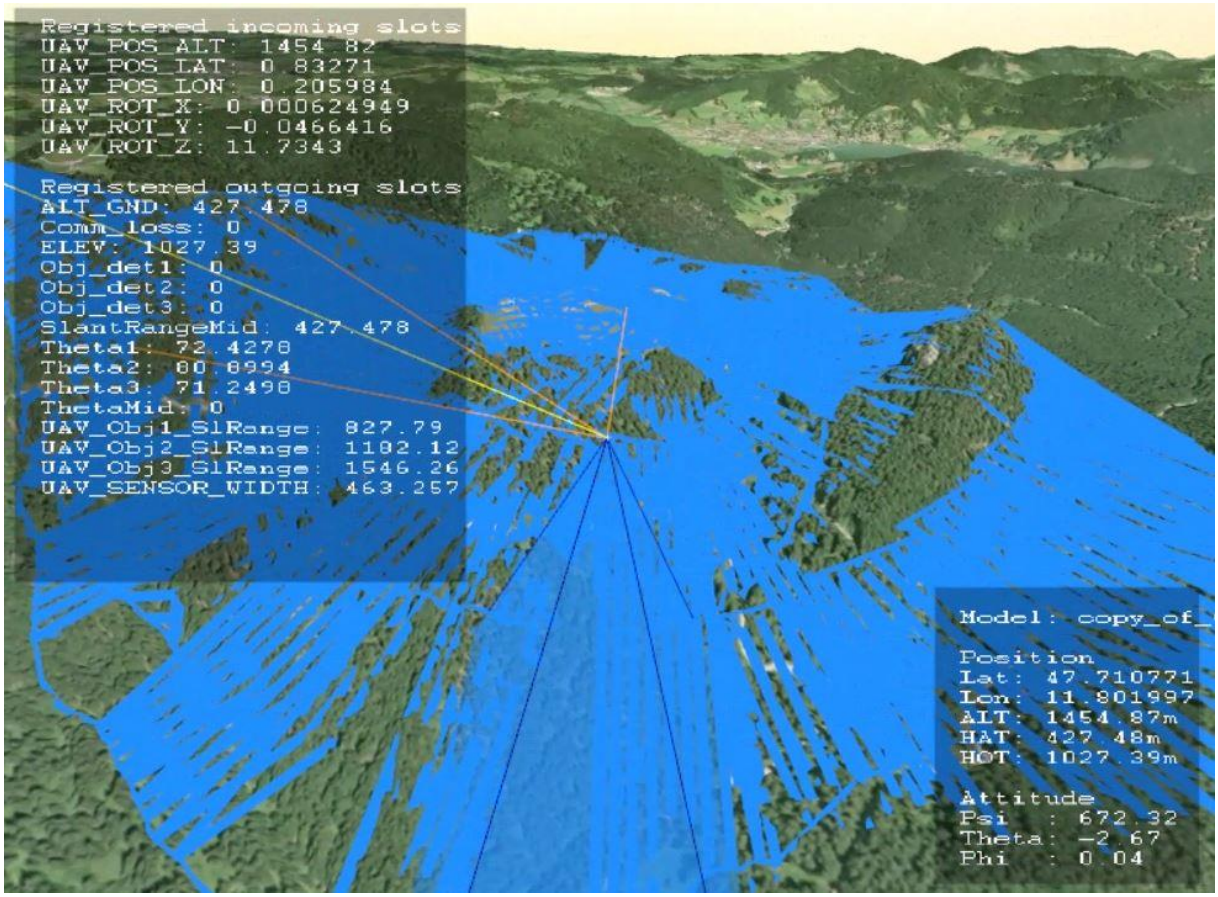

Figure B.4.3: Mission simulation of designed UAS for the case of E and ACR priorities, spiral pattern. Full coverage area with no gaps.